The University Of Sheffield.

THE SYNTHESIS OF GLYCEROL CARBONATE FROM GLYCEROL AND CARBON DIOXIDE OVER HETEROGENEOUS CATALYSTS

Glycerol upgrading

By:

Nurul Razali

Project Supervisor:

Dr James McGregor

A Thesis Submitted

For the Degree of Doctor of Philosophy

Department of Chemical and Biological Engineering

University of Sheffield

AUGUST 2017

ABSTRACT

The aim of this work is to synthesise glycerol carbonate from carbon dioxide (CO_2) and glycerol. Two key challenges that were investigated in this work including: (1) thermodynamic limitation of this work and (2) desirability of using crude glycerol as a feedstock. In this work, carboxylation of glycerol is carried out over La_2O_3 (commercial) and $La_2O_2CO_3$ catalysts prepared *via* co-precipitation, sol-gel and hydrothermal methods. These catalysts are characterised using BET, ATR-FTIR, SEM, XRD, TPD-CO_2 and TPD-NH_3.

The carboxylation reaction is thermodynamically limited, therefore a range of dehydrating agents were introduced to improve the glycerol conversion by shifting the reaction equilibrium to the product side. The impact of dehydrating agents on glycerol conversion and glycerol carbonate formation were therefore studied. Reaction conditions were as follows: 6 wt.% La_2O_3, relative to glycerol, glycerol to dehydrating agent ratio of 22.5:50 mmol, 160 °C and reaction pressure, 45 bar CO_2 and reaction time, 18 hours. High selectivity to glycerol carbonate is observed upon the introduction of adiponitrile (17%), followed by benzonitrile (5%), acetonitrile (4%), and no glycerol carbonate was detected upon the introduction of acetic anhydride.

Additionally this work demonstrated for the first time the efficacy of lanthanum-based catalysts to synthesise glycerol carbonate *via* the direct carboxylation of crude glycerol. Crude glycerol employed herein comprises 74% glycerol, 20% of fatty acid methyl esters, 5 wt.% water, 1% methanol, and 7 g/L of sodium methoxide. It was analysed by GG-MS, ICP-MS and Karl Fisher titration technique. The impact of single and multiple impurities are the aspects investigated in this work. The addition of 10 wt.% water inhibited the formation of glycerol carbonate while blending of glycerol and methanol (80:20 mol%) increased the selectivity to glycerol carbonate to 22%. Only 4% selectivity to glycerol carbonate over La_2O_3-C was observed in the presence of multiple impurities including methanol, fatty acid methyl ester and sodium methoxide. As a result, modification of La_2O_3-C catalyst is crucial. Introduction of ZrO_2/$La_2O_2CO_3$/Ga_2O_3 greatly improved the selectivity to glycerol carbonate (21%); while a selectivity of 5% to glycerol carbonate observed for the direct carboxylation of crude glycerol.

To my parents and Dr. James McGregor,

Who always taught me to dream big and aim high.

TABLE OF CONTENTS

ABBREVIATIONS

4HMO	4-(hydroxymethyl)oxazolidin-2-one
BET	Brunauer- Emmett- Teller
FAME	Fatty acid methyl ester
FTIR	Fourier transform infrared spectrometry
GC-MS	Gas chromatography mass spectroscopy
GlyC	Glycerol carbonate
ICP-MS	Inductively coupled plasma mass spectrometry
MeOH	Methanol
NaOMe	Sodium methoxide
NMR	Nuclear magnetic resonance
SEM	Scanning electron microscope
TPD-CO_2	Temperature programme desorption - carbon dioxide
TPD-NH_3	Temperature programme desorption - ammonia
XRD	X-ray diffraction (powder)

1 INTRODUCTION

This chapter presents an overview of heterogeneous catalysis in general and an introduction to the potential application of carbon dioxide in catalytic reactions and also the potential of glycerol upgrading. This project explores the possibility to utilise both waste carbon dioxide and glycerol produced from the manufacture of biodiesel. Several possibilities are currently being investigated and glycerol carbonate has been considered as a key synthetic target due to its high market value and its wide-ranging reactivity that can be applied in many applications.

1.1 Aim of the work

The aim of this work is to convert carbon dioxide (CO_2) into valuable products, focusing at present on simultaneously upgrading glycerol. The concentration of CO_2 has continuously increased from 315 ppm in 1958 to ~ 408 ppm in July 2017 (CO_2now, 2017). Increased efforts towards carbon capture mean that CO_2 is likely to become a readily available feedstock. Glycerol is a by-product from biodiesel synthesis (Rastegari and Ghaziaskar, 2015). The reaction between glycerol and CO_2 into glycerol carbonate (GlyC) therefore utilises two types of undesired by-products. Additionally, GlyC has a variety of uses including as an electrolyte in lithium ion batteries (Ishak et al., 2016; Sonnati et al., 2013).

1.2 Introduction to catalysis

Catalysts can be defined as 'the substance that change the rate of chemical reactions without itself appearing in the products (Figueiredo, 2008). Catalysis describes the properties of the substances that increase the rate of reaction, by lowering the activation energy, without being consumed in the reaction (Fogler, 2006). The term 'catalyst' was coined by Berzelious in 1835 in his renowned review of the research of Edmund Davy, J. W. Dobereiner and others (Thomas and Thomas, 1967). Catalytic reactions take place when the chemical bonds are broken and transform into new chemical bonds. However, the reactions are too slow or in some cases do not occur in the absence of catalyst. Catalysts and catalytic technology are considered as a highly

important part of the chemicals and petroleum refining industry; contributing to ~ 90% of chemical manufacturing processes around the world (Thomas and Thomas, 2015). In 2007, over $3.5 billion of catalysts were sold in the United State thus contributing to the global economic growth (Fogler, 2006). Table 1.1 shows a summary of different reactions and common catalysts used in these reactions (Fogler, 2006).

Table 1.1. Types of catalysts used in different catalytic reactions (Fogler, 2006).

Reaction	Catalysts
Halogenation/Dehalogenation	$CuCl_2$, AgCl, Pd
Hydration/Dehydration	Al_2O_3, MgO
Alkylation/Dealkylation	$AlCl_3$, Pd, zeolites
Hydrogenation/Dehydrogenation	Co, Pt, Cr_2O_3, Ni
Oxidation	Cu, Ag, Ni, V_2O_5
Isomerisation	$AlCl_3$, Pt/Al_2O_3, zeolites

Homogeneous and heterogeneous catalysis are the two main categories of catalytic processes. Homogeneous catalysis is the process whereby the substrate and catalyst are present in a single phase during this reaction. Heterogeneous catalysis is where the catalyst and reactant are in different phases (Baiker, 1999; Wijngaarden et al., 1998). Phase combinations for heterogeneous catalysis are summarised in Table 1.2.

Table 1.2. Phase combinations for heterogeneous catalysis (Bond, 1974).

Catalyst	Reactant	Example
Liquid	Gas	Polymerisation of alkenes catalysed by phosphoric acid
Solid	Liquid	Decomposition of hydrogen peroxide catalysed by gold
Solid	Gas	Ammonia synthesis catalysed by iron
Solid	Liquid and gas	Hydrogenation of nitrobenzene to aniline catalysed by palladium

In most examples of heterogeneous catalysis, reactants are in liquid or gas form while the catalyst is in solid form. Solid catalysts used in heterogeneous catalysis can be prepared *via* co-precipitation, impregnation, slurry precipitation method among other methods (Jagadeeswaraiah et al., 2014). The surface area and porosity of the catalyst that is accessible to the reactant plays an important role in any reaction. The greater the surface area of the catalyst in contact with the reactant, the higher the conversion of reactant (Bowker, 1998). However, it is not totally dependent on the surface area of a catalyst; active site composition and catalyst structure also play important roles for the efficiency of a reaction (Bowker, 1998). The successful transfer of reactants and products from the outer to the inner catalyst surface is dependent upon the pore size and the pore size distribution (Wijngaarden, Westerterp and Kronberg, 1998). The adsorption and desorption processes of reactant onto the catalyst are illustrated in Figure 1.1 (Bowker, 1998). The performance of a catalyst relates to the rate of reaction, stability, separation process, *etc*. (Centi and Perathoner, 2004).

The mechanisms in heterogeneous catalytic reaction are as follows:

1. Mass transfer (diffusion) of reactant (A) from the bulk fluid to the external catalyst surface. Diffusion of species A through the porous network of the catalyst to the internal catalytic surface.
2. Adsorption of species A onto the catalyst surface (S); $A+S \rightleftharpoons AS$.

3. Surface reaction at the site AS to BS. In the catalytic reaction, the surface reaction step is considered as the rate-determining step.
4. Desorption of B molecules from the surface; BS ⇌ B+S.
5. Diffusion of species B through the porous network to the pore mouth at the external surface.
6. Mass transfer of the products B from the external catalyst surface to the bulk fluid (Fogler, 2006; Rodrigues, 2008).

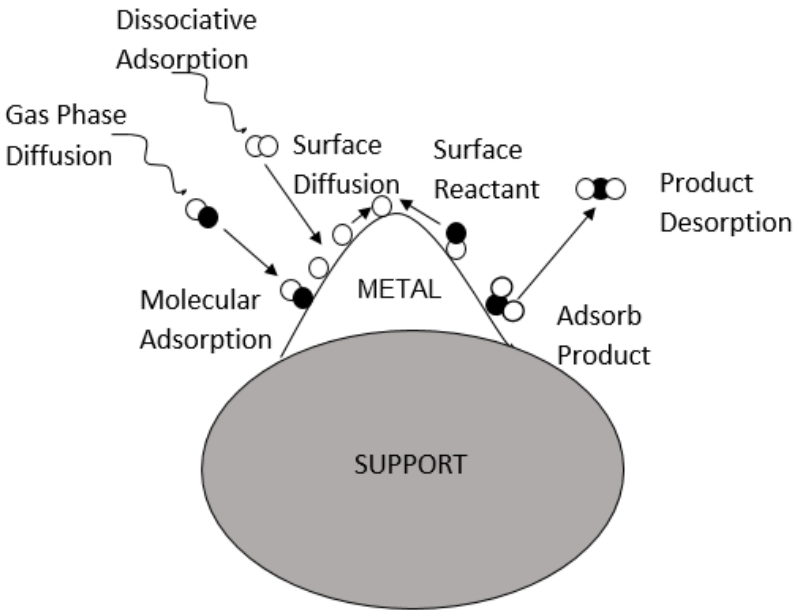

Figure 1.1. The processes taking place in heterogeneous catalysis (Bowker, 1998).

Three main components in designing the catalyst are: active catalyst site, support and in some cases, promoter (Wijngaarden, Westerterp and Kronberg, 1998). The active catalyst are usually metals and oxides; while titania, alumina and zeolite are often used as the support for a catalyst. Titania, alumina, silica (SiO_2) and zeolite provide the active component with a high surface area for dispersion and also improve the mechanical strength of the catalyst. Promoters are the species which are not active by themselves but help in increasing the activity and/or selectivity of a reaction (Figueiredo, 2008). Small amounts of promoter may be added to the catalyst. In some cases, a support is not necessarily needed in designing a catalyst. For example, Pt-Rh

gauze (woven from fine wires) catalysts are widely used in the oxidation of ammonia to nitric acid (Wijngaarden, Westerterp and Kronberg, 1998). Solid catalysts can be classified into four groups including metals, non-stoichiometric oxides and sulphides, stoichiometric oxides and acid catalysts as summarised in Table 1.3 (Bond, 1974).

Table 1.3. Four main groups of solid catalysts (Bond, 1974; Figueiredo, 2008).

Class	Functions	Examples	Description
Metals	Hydrogenation Dehydrogenation Hydrogenolysis (oxidation)	Fe, Ni, Pd, Pt, Ag	Good catalysts for the reaction involving H_2 and hydrocarbons H_2 and hydrocarbons easily adsorb onto the catalyst surface
Non-stoichiometric oxides and sulphides	Oxidation Dehydrogenation Desulphurisation Hydrogenation	NiO, ZnO, MnO_2, Cr_2O_3, Bi_2O_3-MoO_3, WS_2	Good oxidation catalysts Only oxides which are stable under hydrogen can be used as hydrogenation and dehydrogenation catalysts
Stoichiometric oxides	Dehydration	Al_2O_3, SiO_2, MgO	Poor oxidation catalysts Easily absorb water and used as dehydration catalysts
Acids	Polymerisation Isomerisation Cracking Alkylation	H_3PO_4, H_2SO_4, SiO_2-Al_2O_3, Zeolites	Some stoichiometric oxides present acid site on their surfaces and promote carbocations, thus can be used as alkylation, polymerisation, cracking and isomerisation.

1.3 Introduction to CO_2 catalysis

CO_2 is abundant but also a major environmental concerns as ~ 35 gigatonnes (Gt) of CO_2 was emitted from fossil fuel and cement manufacture in 2014 (CO_2earth, 2016). The chemical transformation of CO_2 is a major challenge for CO_2 research due to the unfavourable thermodynamics; therefore the high energy cost associated with CO_2 utilisation must be taken into consideration. CO_2 can be transformed into: (i) chemical building blocks (ii) synthetic fuel and (iii) mineralisation (Wilson *et al.*, 2015).

1.3.1 Physical properties of CO_2

Temperature and pressure affect the physical state of CO_2 (Figure 1.2). CO_2 is in solid state at low pressure and the melting point is - 56 °C. As the temperature and pressure increase up to 5 bar, sublimation occurs. Vaporisation process occur when liquid CO_2 vaporises into vapour or supercritical phase (*CO_2 thermodynamics*, 2017). A supercritical fluid exists when a substance has a temperature and pressure greater than its critical temperature and critical pressure. CO_2 is in supercritical state when the CO_2 is above the critical point (31.1 ^{o}C, 73.9 bar) and behaves like gas (*Gas Encyclopedia*, 2016).

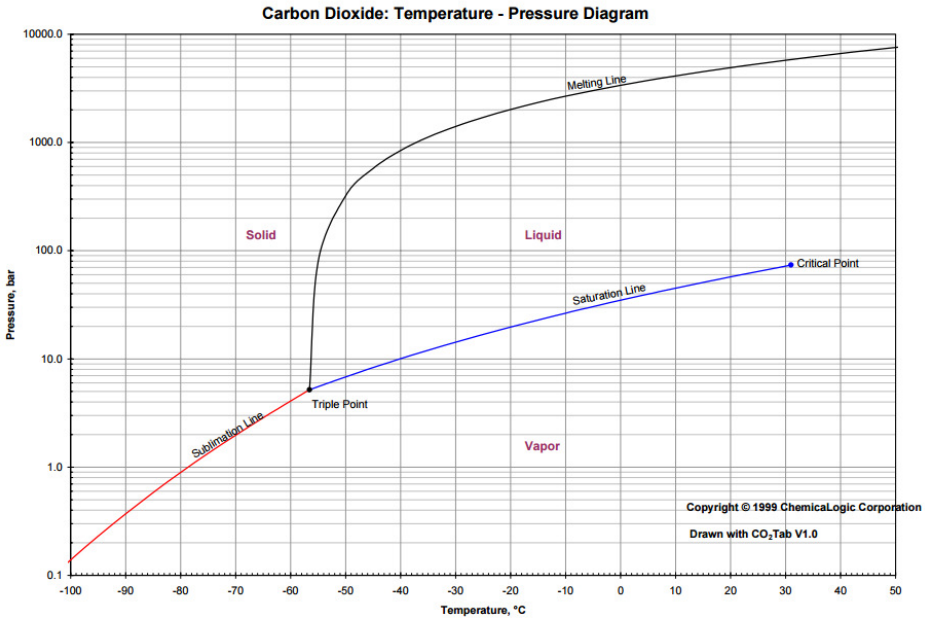

Figure 1.2. The phase diagram of CO_2 (*CO2 thermodynamics*, 2017).

1.3.2 **Sources of carbon dioxide**

Table 1.4 shows characteristics CO_2 produced from several sectors. In general, if the CO_2 is to be captured and utilised from this listed source, there are several factors that should be taken into consideration including:

1- CO_2 emitted from the sources in Table 1.4 are difficult to capture. Retrofitting of post combustion capture units to power generation plants is an available method to capture the emitted CO_2.

2- High cost for CO_2 purification process.

3- The impurities and contaminants may poison or deactivate the catalyst.

Table 1.4. Concentration range of CO_2 (as volume percentage) from a variety of sources and possible contaminants (Styring et al., 2015).

Source	CO_2 concentration (%)	Typical impurities
Power generation (post-combustion)	10-15	N_2, H_2O, SO_X, NO_X
Steel making (blast furnace gas)	18-20	N_2, SO_X, NO_X, O_2
Cement production	c.100	N_2, O_2
Fermentation	c.100	H_2O, H_2S
Natural gas stream	0-8	N_2, H_2S, O_2, C_1-C_4 hydrocarbon
Natural deposits	90-100	N_2, O_2, He
Atmosphere	0.04	N_2, SO_X, NO_X, O_2, particulates

1.3.3 **Carbon capture and storage**

A number of methods are highlighted by Razali *et al*. with regard to controlling carbon emissions (Razali et al., 2012):

(i) Reduce the total energy consumption by improving efficiency.

(ii) Substitute the use of fossil fuels with carbon neutral and/or renewable energy sources.

(iii) Carbon capture and storage of CO_2.

(iv) CO_2 utilisation into a range of useful chemicals.

Carbon capture (point iii) is an attractive method to deal with the abundance of CO_2 in the atmosphere and is already applied in several industrial applications as shown in Figure 1.3.

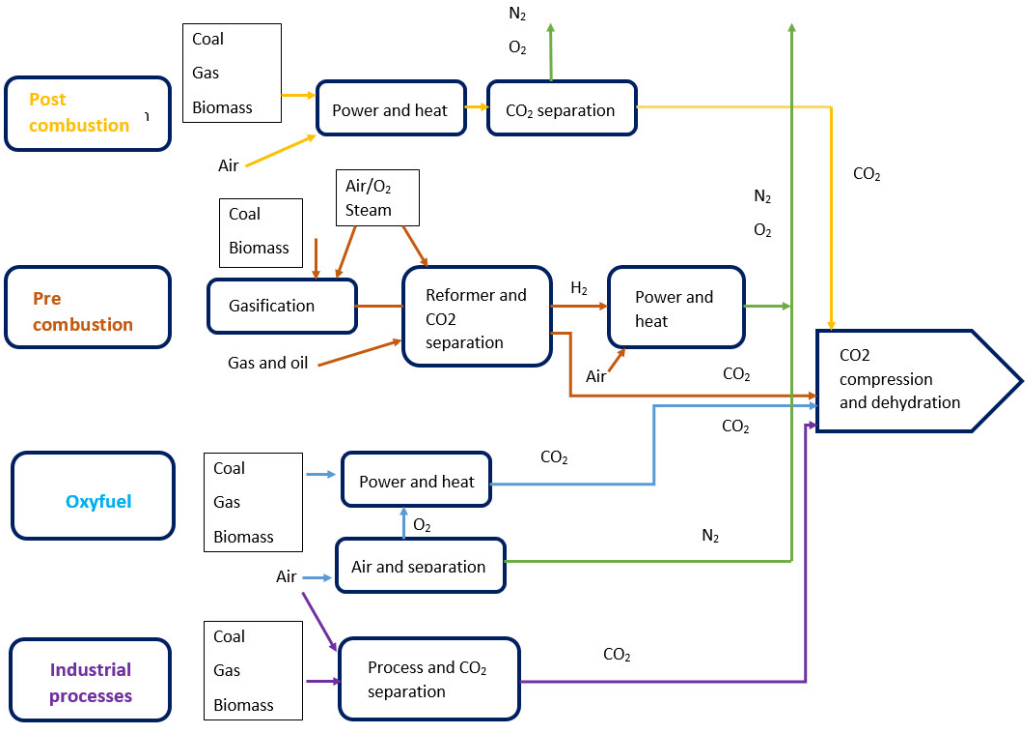

Figure 1.3. Overview of CO_2 capture processes and systems (Metz et al., 2005).

A number of carbon capture techniques have been employed including adsorption onto the surface of sorbent material, physisorption and chemisorption. Amine capture agents including monoethanolamine and diethanolamine have been widely used in industry (Puxty *et al.*, 2009; Boot-Handford *et al.*, 2014; Mumford *et al.*, 2015). The advantages of amines as the CO_2 capture agent are high CO_2 absorption capacity and they can readily react with CO_2 under normal conditions (Supasitmongkol and Styring, 2010). However, the usage of amines are not ideal because they are not used in their pure form; 30:70 (wt/wt.%) of amine to water mixture (Styring *et al.*, 2011). Chilled ammonia is also used and studied (Mumford *et al.*, 2015). This process is also known as the Alstom process, where chilled ammonia is reacted with CO_2 to form carbamic acid. This process is relatively cheap because ammonia is widely available and it has high capture capacity, however, chilled aqueous ammonia is hazardous and toxic in nature.

A number of other technologies are currently being explored for CO_2 capture including zeolites (Vujic and Lyubartsev, 2016) and ionic liquids (Zhang et al., 2014). The ionic liquids have a low vapour pressure at ambient temperature and have a high CO_2 uptake capacity (Supasitmongkol and Styring, 2010). In general, zeolites also have a relatively high CO_2 capacity at low pressures and are very effective for CO_2 separation from flue gas (Boot-Handford *et al.*, 2014). However, the adsorption performance of zeolites is strongly affected in the presence of water because of the hydrophilic property of zeolites (Boot-Handford *et al.*, 2014). Increased efforts towards carbon capture mean that CO_2 is likely to become a readily available feedstock. Thus, an efficient step should be taken into consideration in order to deal with the large amount of CO_2 such CO_2 utilisation (CDU).

1.3.4 **Routes to carbon dioxide utilisation**

CO_2 is abundant, nontoxic, cheap and readily available (due to increase effort toward carbon capture and storage). It has a potential to be utilised into valuable products; CO_2 is an alternative carbon source, rather than a waste. There are two different options of utilising the CO_2 source as shown in Figure 1.4:

1- CO_2 is directly fed into the CO_2 utilisation plant; where CO_2 capture and conversion take place. The costs are dependent on the capturing techniques employed such as pre-combustion, post-combustion and oxyfuel carbon capturing techniques (Ibrahim, Ghazali and Rahman, 2016). Mineralisation and tri-reforming processes are examples for direct conversion of CO_2 into beneficial products.

2- CO_2 is first captured and utilised at the same site or if the CO_2 utilisation is located away from the CO_2 capture plant, the transportation cost and safety requirement to transport gas must be taken into consideration (Styring, Quadrelli and Amstrong, 2015; Ibrahim, Ghazali and Rahman, 2016).

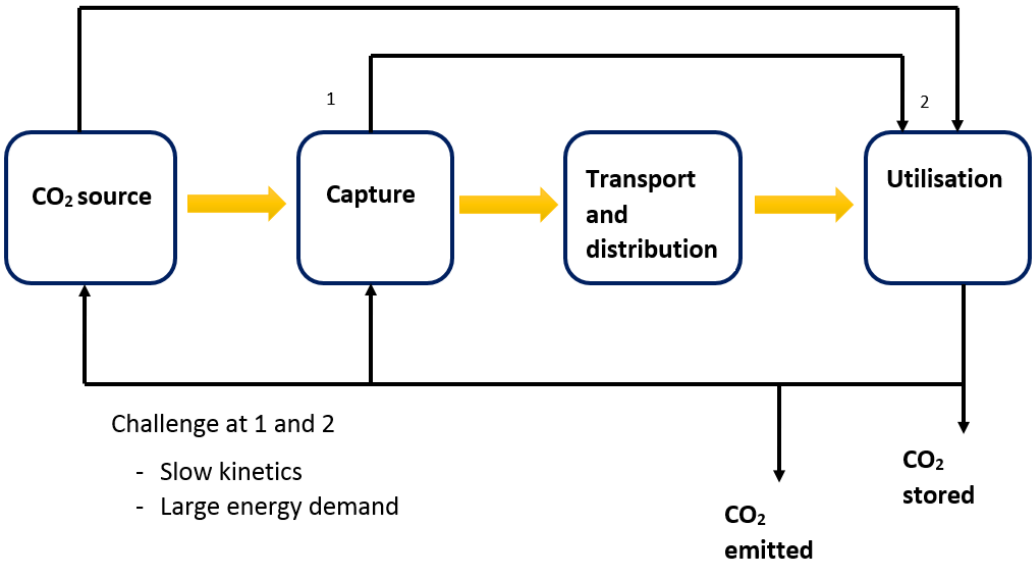

Figure 1.4. Possible routes for CO_2 capture and utilisation (Styring, Quadrelli and Amstrong, 2015).

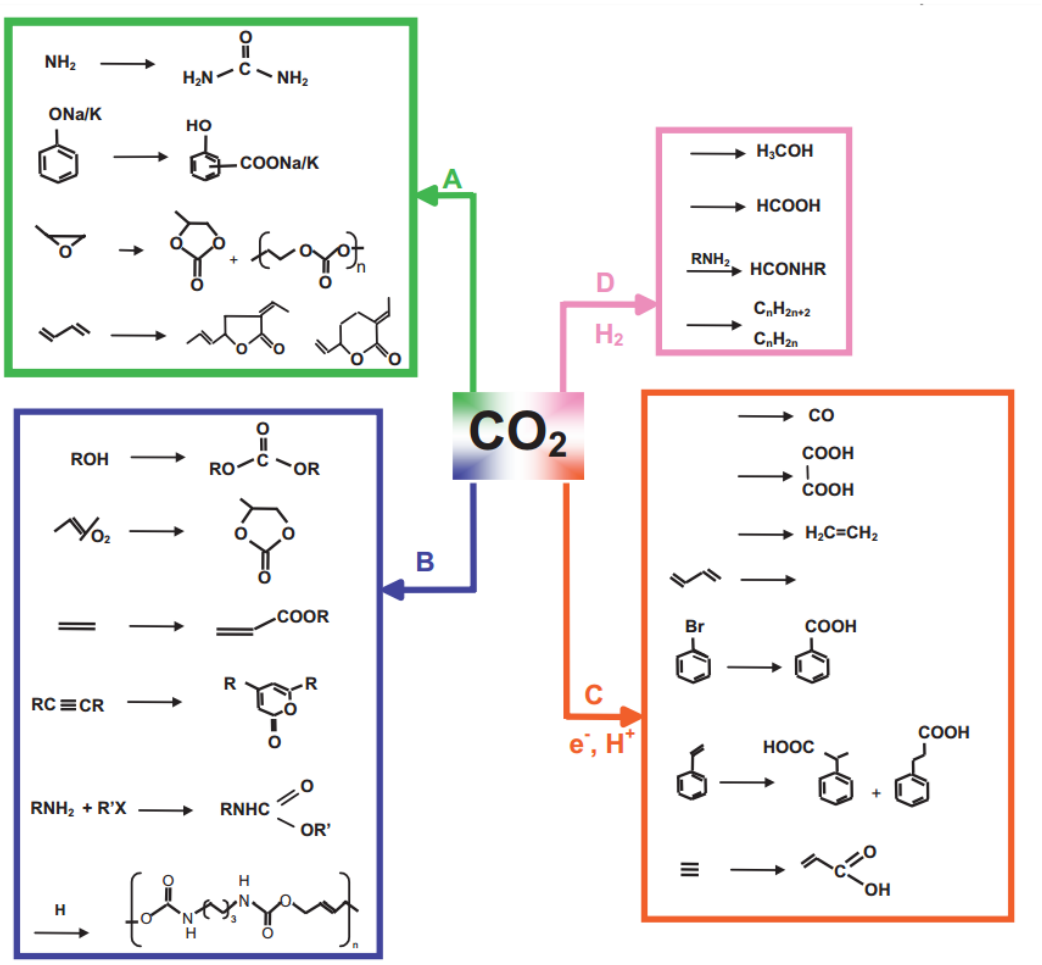

Figure 1.5. Carbon dioxide utilisation into useful chemicals (Aresta, 2010).

Figure 1.5 summarises the potential ways to transform CO_2 into valuable chemicals. Routes A and B incorporate with CO_2 insertion, where carboxylates, carbonates, and carbamates are obtained by incorporation of the entire CO_2 molecule. In contrast, routes C and D involve CO_2 reduction into C_1 or C_n molecules (Aresta, 2010). Photocatalytic reduction and electrochemical reduction of CO_2 are usually employed to synthesise valuable chemicals such as CO, formic acid, formaldehyde, methanol, oxalic acid and methane (Yuan *et al.*, 2017).

Research has been carried out in order to utilise CO_2 and thus improve the chances of CO_2 being commercialised and reused in industrial scale production as shown in Figure 1.6 (Ampelli et al., 2015; Mikkelsen et al., 2010). There are three stages of CO_2 utilisation development including (i) mature (full industrial production),

(ii) developing stages (emerging) and (iii) future applications (laboratory and pilot plant scale) (Alper and Orhan, 2017). Urea (100 million tonnes per year), methanol (2.5 million tonnes per year) and cyclic carbonates (0.05 million tonnes per year) are examples of utilisation of CO_2 at industrial scale (Aresta and Dibenedetto, 2007). A number of emerging technologies such as the production of dimethyl ether, formic acid and polymers are on the threshold to industrial realisation, while the synthesis of organic carbonates, lactones and carboxylic acids from CO_2 are still far from the industrial application (Alper and Orhan, 2017).

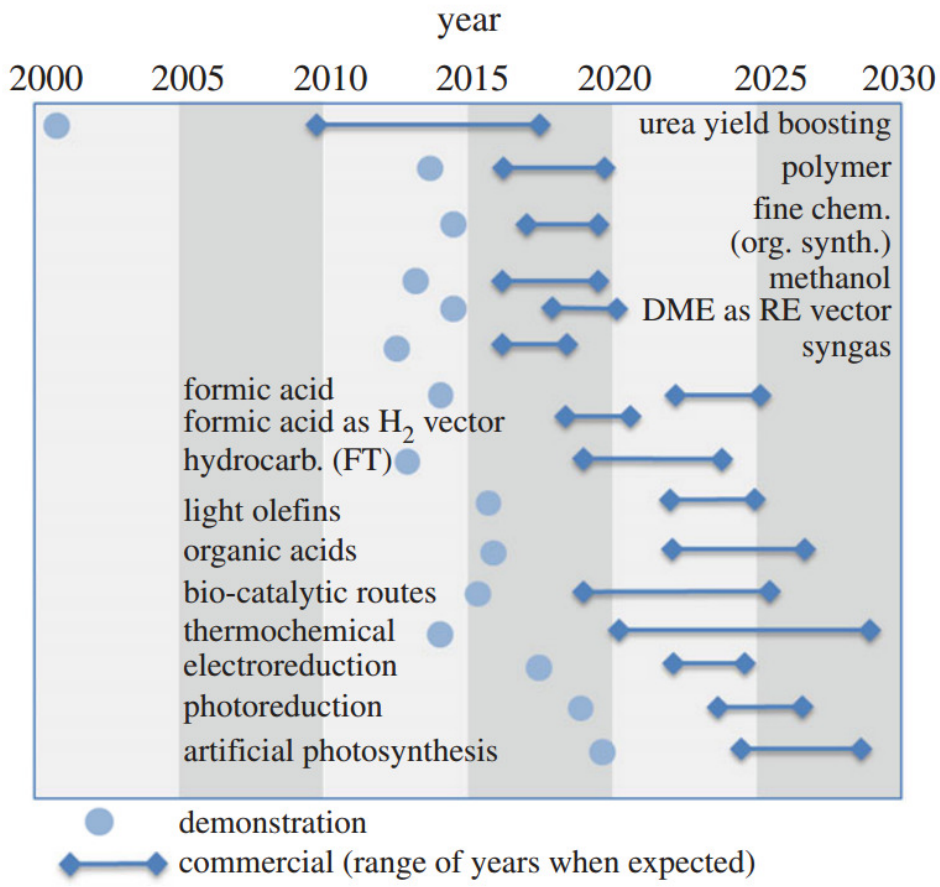

Figure 1.6. Estimated 'technology roadmap' from preliminary demonstration to CO_2 commercialisation paths (Ampelli et al., 2015). The blue circle represents technology at the pilot/demonstration scale, while the bar represents the expected timeframe when commercial operation of the technology is likely.

1.4 Glycerol upgrading

Total energy consumption from fossil fuel source has decreased by 1% from 2003 to 2014, as shown in Figure 1.7. These data show the lack of success of energy policies that aimed for CO_2 emissions reduction (*Global Energy Trends – BP Statistical Review 2014*, 2014). However, the use of renewable energy including wind, solar, geothermal and biofuels has increased from 1 to 3% within 10 years.

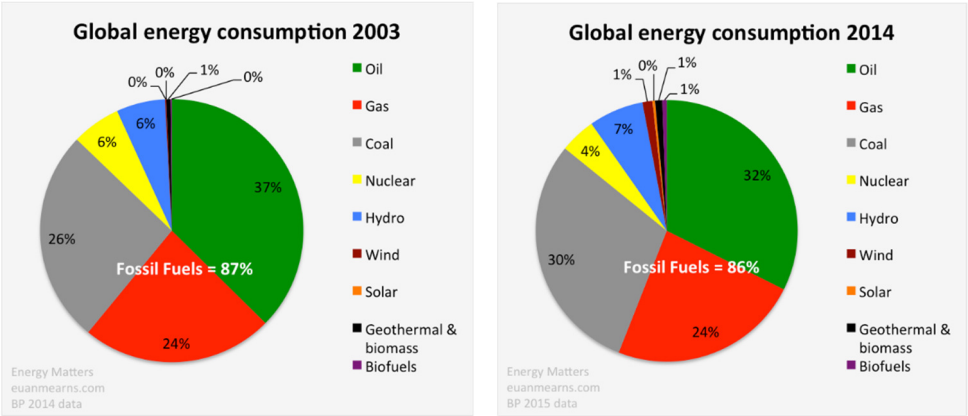

Figure 1.7. The global energy consumption in 2003 and 2014 (*Global Energy Trends – BP Statistical Review 2014*, 2014).

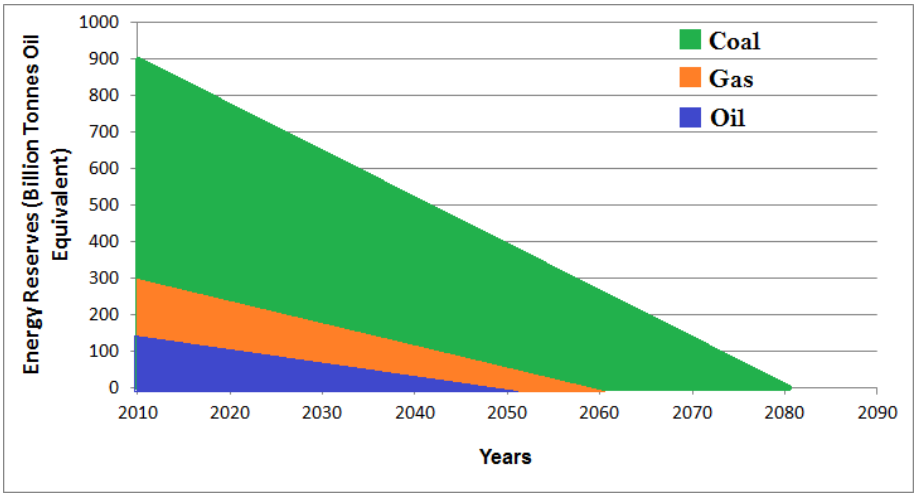

Figure 1.8. The amount of energy reserves (*The end of fossil fuels*, 2016).

The amount of fossil energy including oil, gas and coal reserves is going to be depleted over the coming years and is expected to be fully consumed within a few decades as shown in Figure 1.8. Combustion of fossil fuel releases CO_2 as a by-product and leads to global warming. Concern over global warming and the adverse economic effect of accessing fuel reserves has driven the commercial action of the transesterification reaction of triglyceride with methanol to synthesise biodiesel (Lee et al., 2015). Biofuel production is also in part of substituting oil as source of energy and an alternative approach to produce sustainable transportation fuels. The efforts toward biofuel commercialisation helped to reduce the oil consumption from 37% (2003) to 32% in 2014 respectively (*Global Energy Trends – BP Statistical Review 2014*, 2014). 10 wt.% of glycerol waste is produced along with the production of biodiesel. Purified glycerol has several applications such as personal care, pharmaceutical industry, triacetin production and food industry (Tan et al., 2013). Despite large numbers of glycerol applications, the production capacity of glycerol is far exceeding the market requirements. Crude glycerol waste is expected to reach 2.7 billion kg in 2020 (Ayoub & Abdullah, 2012).

Current work regarding glycerol upgrading into valuable products includes the following processes: hydrogen production by steam reforming (Adhikari et al., 2008; Mitran et al., 2016; Schwengber et al., 2016); etherification, acetylation (Konwar *et al.*, 2015); dehydration (Dalil *et al.*, 2016); hydrogenolysis (Sun et al., 2016); selective oxidation and carboxylation of glycerol. In this thesis, the carboxylation of both pure and crude glycerol are discussed in Chapter 4 and 5. Only a few examples of the direct use of crude glycerol have been reported because the presence of impurities in the crude glycerol reduces the product selectivity and yield. The utilisation of crude glycerol is crucial due to the high cost of crude glycerol purification and refining (Isahak et al., 2015). However, the inconsistency of crude glycerol composition is the major drawback for crude glycerol upgrading (Nanda et al., 2014). The composition of crude glycerol strongly depends on the feedstock used, process/method employed and post treatment involve in biodiesel production (Hu et al., 2012).

1.5 The importance of glycerol carbonate production

Sonnati and Teng in their reviews outlined the potential uses of GlyC, including electrolyte in lithium ion battery, cosmetic, as chemical intermediate and as the solvent (Sonnati et al., 2013; Teng et al., 2014). However, the use of GlyC is currently low due limited GlyC production; consequently contributing to its high market value, > €6/kg (CyclicCO_2R, 2013). GlyC has low toxicity, low odour, low flammability and moisturizing ability; therefore the Huntsman Corporation has suggested that the GlyC can be used in the cosmetic industry including in make-up and nail polish removal, perfumes, hair care products and lipsticks (Huntsman, 2016).

2 LITERATURE REVIEW

This literature review were focused on two main topics including the potential of carbon dioxide utilisation into valuable products in the presence of heterogeneous catalysts which is related to the proposed research topic. The second topic outlines previous work done in synthesising glycerol carbonate and mono-, di- and triacetin, particularly focusing on the synthesis of glycerol carbonate from glycerol and CO_2. There are several routes to synthesise GlyC and these have been discussed in section 2.3: (i) glycerol and CO_2; (ii) glycerol and phosgene; (iii) glycerol and dimethyl carbonate; and (iv) glycerol and urea

2.1 Carbon dioxide as a building block for chemical synthesis

Carbon dioxide (CO_2) is an incombustible and non-toxic renewable carbon resource that plays an important role in the natural carbon cycle; a dynamic carbon exchange between atmospheric, terrestrial and aquatic environments (Aresta and Dibenedetto, 2007). It is produced from the combustion of coal, oil and gas; and CO_2 concentration in the atmosphere has been significantly increasing and contributes ~ 60% of global warming (Huang, 2014). Since 1958, the concentration of CO_2 has continuously increased from 315 to 408 ppm in July 2017 (CO_2now, 2017).

CO_2 emissions arise from many sectors: stationary, mobile and natural sources (Song, 2006). An important aspect of CO_2 utilisation is exploring new methods and developing new catalysts are crucial for this. The evolution of new routes for CO_2 utilisation and the amount of CO_2 used per amount of product formation have been summarised in Table 2.1. By far the production of urea has utilised the largest amount of CO_2; where the formation of urea from CO_2 has been commercialised since 1922 (Styring, Quadrelli and Amstrong, 2015). Although the sources of CO_2 are abundant, CO_2 utilisation at large scale is relatively low and very limited because the CO_2 molecule is thermodynamically stable and unreactive.

Table 2.1. Summary of potential CO_2 utilisation (Styring et al., 2011).

Chemical product and application	Annual market (Mt/year)	Mt CO_2 used per Mt product	Lifetime
Urea	100	70	6 months
Methanol	40	14	6 months
Inorganic carbonates	80	30	Decades to centuries
Organic carbonates	2.6	0.2	Decades to centuries
Poly(urethane)s	10	< 10	Decades to centuries
Technological	10	10	Decades to years
Food	8	8	Months to years

2.1.1 Challenges

CO_2 is thermodynamically and kinetically stable (Sakakura, Choi and Yasuda, 2007). CO_2 is in oxidised form ($G_{\Delta f0}$ = - 394 kJ/mol) which has to be taken into account when considering CO_2 utilisation as chemical feedstock (Dibenedetto et al., 2014; Patil et al., 2009; Song, 2006). The carbon-oxygen bond must be activated, requiring a large input of energy, the use of novel catalysts and effective catalytic processes (Razali et al., 2012). Sakakura highlighted the four important keys to transform CO_2 into valuable chemicals (Sakakura, Choi and Yasuda, 2007):

- Use high-energy starting materials such as hydrogen, unsaturated compounds, small-membered ring compounds, and organometallics.
- Choose oxidized low-energy synthetic targets such as organic carbonates.
- Shift the equilibrium to the product side by removing a particular compound.

- Supply physical energy such as light or electricity (electricity from renewable source is better such as wind energy).

2.2 Potential carbon dioxide utilisation

The combustion of fossil fuels augments CO_2 concentration in the atmosphere; ~ 3.5 tonnes of CO_2 is produced for every tonne of fossil fuel carbon combustion (Jiang et al., 2010). Resultant studies have investigated the transformation of CO_2 into useful and valuable products. CO_2 can be transformed *via* two major approaches: (i) as a chemical feedstock such as carboxylates, carbamate and polymers and (ii) as storage medium includes syngas, methanol and methane. The use of CO_2 as feedstock in synthesising methanol, urea and carbamates has been reviewed by many researchers (Sankaranarayanan and Srinivasan, 2012; Olajire, 2013; Dibenedetto, Angelini and Stufano, 2014).

2.2.1 Syngas production *via* reverse water gas shift reaction

The reverse water gas shift (RWGS) has been proposed as one of the most favourable processes for CO_2 conversion: carbon monoxide (CO) and water (H_2O) are the main products formed from this reaction (Razali *et al.*, 2012; Olajire, 2013; Owen *et al.*, 2016). RWGS is a technology to synthesise CO from CO_2, in which the CO produced will be converted into liquid fuels including diesel, gasoline and alcohols (Daza and Kuhn, 2016). This reaction occurs in many processes where H_2 and CO_2 are present and methane is produced as the by-product as shown in equation 2.1 to 2.3 (Daza and Kuhn, 2016).

$$CO_2 + H_2 \rightleftharpoons CO + H_2O \quad (2.1)$$

Additional side reaction

$$CO + 3H_2 \rightleftharpoons CH_4 + H_2O \quad (2.2)$$

And the Sabatier reaction

$$CO_2 + 4H_2 \rightleftharpoons CH_4 + 2H_2O \quad (2.3)$$

A number of researchers have reported the activity and the reaction mechanism for water gas shift and RWGS reactions in the presence of copper (Cu), ceria (Ce) and alumina (Al) based catalysts (Chen, 2004; Chen et al., 2001; Joo et al., 1999; Kharaji et al., 2013). Gold (Au), nickel (Ni) or Cu deposited on titanium carbide (TiC) successfully catalyse the reaction (Rodriguez *et al.*, 2013). Cu-based catalysts are selective to the production of CO. Au/TiC favours methanol production while large amounts of methanol and methane formed in presence of Ni/TiC.

Chen *et al.* studied the influence of potassium (K) and iron (Fe) as the promoter on Cu supported on silicon dioxide (SiO_2) (C.-S. Chen, 2003, 2014). Sintering of Cu is prevented by the formation of Fe species around the Cu particles (W. Wang et al., 2011). K_2O deposited on Cu/SiO_2 provides the active site for formate formation (a reaction intermediate), thus improving the adsorption of CO_2. Palladium (Pd), platinum (Pt), rhenium (Rh), cobalt (Co) and Ni are frequently used in heterogeneous catalytic hydrogenation (Nerozzi, 2012); Porosoff in his review lists the work done in presence of these catalysts (Porosoff et al., 2016). Pt is found active for H_2 dissociation.

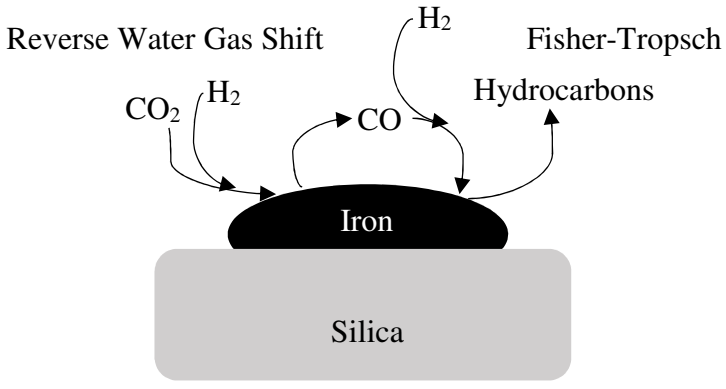

Figure 2.1 CO is synthesised *via* RWGS can be transformed into hydrocarbons *via* Fischer-Tropsch (Owen *et al.*, 2013).

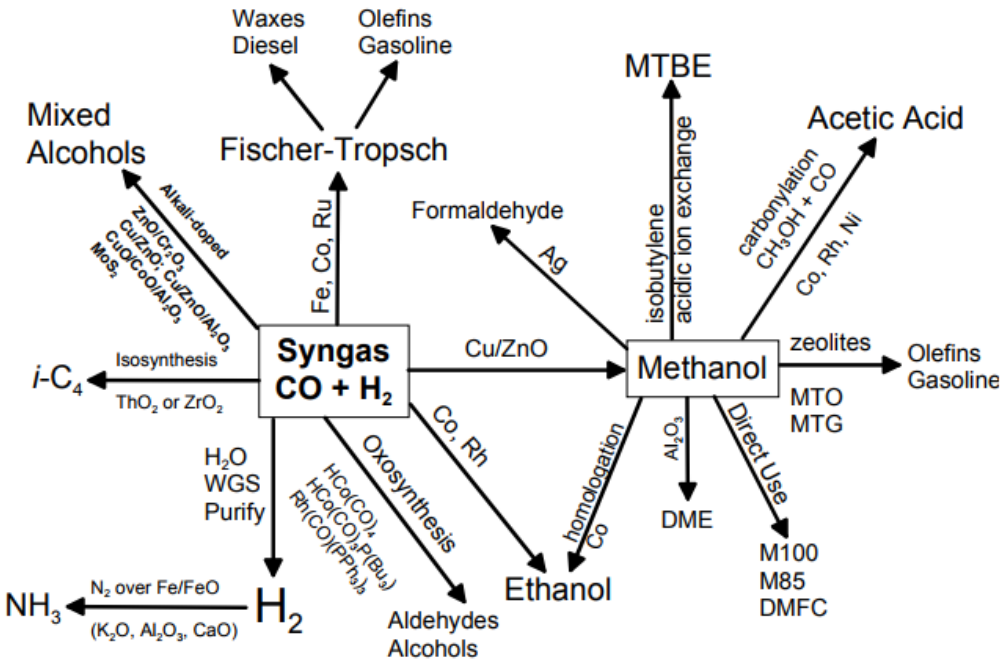

Figure 2.2 Valuable chemicals that can be synthesised from syngas (CO and H_2) (Spath and Dayton, 2003).

Figure 2.1 shows the CO synthesised *via* RWGS; followed by the conversion of CO to hydrocarbons *via* the Fischer-Tropsch mechanism, with direct hydrogenation of CO_2 (Owen *et al.*, 2013). CO formed from this reaction can be utilised as a building block to synthesise valuable chemicals and synthetic fuels and as summarised in Figure 2.2 (Spath and Dayton, 2003; Daza and Kuhn, 2016).

2.2.2 **Hydrogenation of CO_2 to methanol**

Methanol is the smallest alcohol and has been commercially produced at industrial scale since 1960 over Cu-based catalysts supported on ZnO and using CO_2, CO and H_2 as the feed gas (Behrens, 2016). Synthesis of methanol *via* homogeneous (Li et al., 2014) and heterogeneous catalysts (Joo *et al.*, 1999) is successfully applied in CO_2 utilisation. CO_2 is directly used as the reactant in methanol production (equation 2.4). Therefore, preliminary reduction to CO (equation 2.5 and 2.6) can be eliminated. Also, catalytic CO_2 hydrogenation is an alternative approach to synthesise methanol, thus

replacing fossil fuel, natural gas and coal as the raw material (Olah et al., 2009). In general, heterogeneous catalysts used for this reaction are shown in Table 2.2.

$$CO_2 + 3H_2 \rightleftharpoons CH_3OH + H_2O \quad (2.4)$$

$$CO_2 + H_2 \rightleftharpoons CO + H_2O \quad (2.5)$$

$$CO + 2H_2 \rightleftharpoons CH_3OH \quad (2.6)$$

Table 2.2. Methanol synthesis from hydrogenation of CO_2 over a range of transition metal catalysis.

Catalyst	Preparation method	P/ MPa	Temp/ °C	CO_2 conv.%	Methanol selectivity	Ref.
Cu/ZnO/ Al_2O_3/ZrO_2	Co-precipitation	5	230	18	68.4	(Gao *et al.*, 2016)
Pd/ZnO	Impregnation	2	250	10.7	60	(Bahruji *et al.*, 2016)
CuO/MgO/ TiO_2	Impregnation	3	220	5.2	37.9	(C. Liu *et al.*, 2016)
Cu/ZnO/ ZrO_2	Precipitation-reduction	5	230	15.4	66.8	(Donga *et al.*, 2016)
In_2O_3	commercial catalyst	4	270	1.1	54.9	(Sun *et al.*, 2015)
Cu/Ga_2O_3/ ZrO_2	Impregnation	3	250	0.84	90	(Sanguineti et al., 2015)

$CuO/ZnO/Al_2O_3$ catalyst is commercially used for methanol synthesis. Goeppert *et al*., lists supports that are commonly used in Cu-based catalysts such as ZrO_2, SiO_2 and CeO_2 (Goeppert et al., 2014). The advantages of ZnO presence in Cu-based catalysts include (Homs et al., 2013):

- ZnO results in improved Cu dispersion by improving the precursor formation.
- Inevitable agglomeration of Cu particles occurs during long operating periods but can be restricted by adding Al_2O_3 and ZnO.
- Impurities including sulphides and chlorides are poisons for the Cu particles; the presence of ZnO reduces the chances of Cu poisoning.

Advanced research has been done in order to improve the catalytic system such as finding a new synthesis method, studying the system computationally, employing model catalysts, kinetic experiments and advanced catalyst characterisation methods (Behrens, 2016). Xiao *et al*. investigates the catalytic performance of a modified Cu/ZnO catalyst with zirconia dioxide (ZrO_2), titania dioxide (TiO_2) and combination of both as promoter (Xiao et al., 2015). ZrO_2 enhances the catalytic activity for CO_2 hydrogenation and inhibits the impact of H_2O formed from this reaction, thus limiting catalyst deactivation (Li et al., 2014). Addition of TiO_2 and ZrO_2 enhance the basic sites of the catalyst and improved the adsorption of CO_2; consequently increasing methanol selectivity from 36.5 to 43.8%. $Cu/ZnO/Al_2O_3$ modified by adding ZrO_2 shows improvement in terms of CO_2 conversion from 18 to 23%, as well as increasing the methanol selectivity from 43 to 60% (Li et al., 2014).

Fujitani *et al.* reports that the activity and selectivity of CO_2 and methanol over Pd/Ga_2O_3 is higher as compared to the Cu/ZnO catalyst (Fujitani *et al.*, 1995). The influence of the preparation method of Pd/Ga_2O_3 supported on SiO_2 and how it influences this reaction is discussed by Collins *et al*. (2005). Another attempt has been made to improve the selectivity to methanol and the conversion of CO_2 by depositing PdO onto Cu/ZnO catalyst. However, addition of 2 wt.% of PdO only increased the

CO_2 conversion by 2% from 5 to 7% when compared with the unmodified catalyst (Cu/ZnO); while the methanol selectivity is increased only from 71 to 76% (Melian-Cabrera et al., 2002).

Research shows that Cu/ZnO is readily susceptible to sulfur poisoning. Therefore, a series of Pd catalysts supported on MCM-41 have been employed for methanol synthesis. CO_2 conversion of 12.1% and 65.2% selectivity to methanol are recorded in the presence of Pd/CaO/MCM-41 (Song et al., 2015). More research is needed to understand the influence of transition metal oxides on the reaction mechanism and how they affect the formation of products.

2.2.3 **Hydrogenation of CO_2 to methane**

CO_2 methanation or the Sabatier process, shown in equation 2.3, involves the reaction of CO_2 and H_2. CO_2 methanation is a highly exothermic reaction and is thermodynamically favourable. However, the reduction of fully oxidised carbon is difficult to achieve due to the significant kinetic barrier (eight-electron reduction process) (Su *et al.*, 2016). In general, methane is synthesised from this reaction at 350 °C at 30 to 50 bar (Garbarino et al., 2014). CO_2 methanation can be employed in chemical and petrochemical industries (Jacquemin et al., 2010), thus reducing the use of natural gas (Du *et al.*, 2007). Reforming of methane produces syngas; which can be used in production of higher alkanes and oxygenates. However, this section will be focused on the hydrogenation of CO_2 to methane.

A number of attempts have been made to synthesise methane using Ni based catalysts; (i) Ni support on SiO_2 (Falconer, 1980), (ii) Ni supported on Al_2O_3 (Fujita et al., 1993, Lim *et al.*, 2016) and Ni supported on MCM-41 (Du *et al.*, 2007). Ni, Co, Cu and Zn supported on MCM-41 are developed and tested (Lu and Kawamoto, 2014). Ni-based catalysts are considered cheap and widely used in industrial processes. The drawbacks of Ni catalysts are (i) catalyst deactivation due to sintering of catalyst, (ii) formation of carbon deposits and (iii) the formation of mobile nickel sub-carbonyls (Su *et al.*,

2016). Therefore, the development of effective catalysts through, *e.g*, adding a catalyst support and improving the catalyst preparation method is very important.

The role of the support has to be taken into consideration. A range of Ni catalysts supported on SiO_2, Al_2O_3 and ZrO_2 have been prepared using incipient wetness impregnation and employed for CO_2 methanation (Zhu et al., 2014). The yield of methane is highest with $Ni/SiO_2/ZrO_2$ followed by the catalyst supported on Al_2O_3, SiO_2 and unsupported catalyst. The advantages of employing ZrO_2 and Al_2O_3 as catalyst support are that they have high surface area and basicity (Cai et al., 2011), while CeO_2/ZrO_2 catalyst has high thermal stability and limits the catalyst sintering (Ocampo, Louis and Roger, 2009).

This reaction was also been carried out at atmospheric pressure in presence of Ni/Al_2O_3. The reaction is carried out at 500 °C successfully producing a methane selectivity of 100% and 75% CO_2 conversion (Garbarino *et al.*, 2014). The influence of alkaline earth metals as structural promoters has also been investigated. $Ni/MO/SiO_2$ (MO = MgO, CaO, SrO and BaO) have been tested and MgO inhibited the catalytic reaction (Guo and Lu, 2014). The influence of CaO on CO_2 methanation is insignificant. Addition of SrO and BaO improved the conversion of CO_2 and CH_4 selectivity, but only SrO enhance the catalyst stability and inhibit metallic Ni sintering (Guo and Lu, 2014).

In general, transition metals from groups VIII, IX, X and XI such as Ni, Ru, Rh, Cu, Pd and Pt have been widely discussed in several publications due to their ability to synthesise methane with high selectivity and yield (Toemen et al., 2016; Wang & Gong, 2011; G. Zhou et al., 2016). Ru, Rh, Pd and Pt are costly, therefore, such metals are unsuitable to be commercialised in industrial scale. Ni and Ru based catalysts are selective in synthesising methane, while Cu and Ag favour the formation of methanol and CO (Wambach et al., 1999). Active metal catalysts provide the sites for CO_2 and H_2 to adsorb and dissociate into H, CO and O atoms (Wang et al., 2011). Park and Farland reported the conversion CO_2 to CO as 60% and 40% in the presence of $Pd\text{-}MgO/SiO_2$ and Pd/SiO_2 respectively. However, < 1% of CO_2 conversion is

recorded in the presence of MgO/SiO_2; therefore, Mg itself is considered as inactive for CO_2 activation thus inactive for CO_2 methanation (Park and McFarland, 2009).

2.2.4 **Synthesis of dimethyl ether**

The production of dimethyl ether (DME) in the early 1990s was only about 100000 tonnes/year worldwide because of limited commercial application, it being mainly used to substitute the use of chlorofluorocarbon in the aerosol industry (Fleish et al., 1995). Haldor Topsøe in collaboration with Amoco and Navistar International Corp. developed a low cost and single step DME production method, thus allowing a large scale of DME production (Fleish et al., 1995). Then, production of DME gained much interest because it was employed as a liquid petroleum gas (LPG) substitute, acting as clean fuel when burned in engines that are properly optimised and helping to reduce the exhaust emission problems of diesel engine (Zha *et al.*, 2012; Homs, Toyir and Piscana, 2013).

DME is the simplest ether compound and is formed from the dehydration of methanol under high pressure (Huang, 2014). DME can be produced directly *via* hydrogenation of CO_2 and also indirectly *via* conversion of syngas (equation 2.7 to 2.9). Methanol produced in equation 2.7 is transformed into DME by methanol dehydration, equation 2.8, with H_2O as the only by-product. Then, water gas shift reaction removes H_2O produced during the methanol dehydration process (Takeguchi et al., 2000). The drawback of DME synthesised *via* methanol dehydration (equation 2.8) is the high production cost dependent on the market price of methanol (Dadgar et al., 2016). Dehydration of DME favours the formation of ethylene (olefin) (equation 2.10) (Zhokh, Trypolskyi and Strizhak, 2017). Direct DME synthesis is therefore attractive because methanol separation and purification is unnecessary.

$$2CO + 4H_2 \rightleftharpoons 2CH_3OH \quad (2.7)$$

$$2CH_3OH \rightleftharpoons CH_3OCH_3 + H_2O \quad (2.8)$$

$$2CO_2 + 6H_2 \rightleftharpoons CH_3OCH_3 + 3H_2O \quad (2.9)$$

$$CH_3OCH_3 \rightleftharpoons C_2H_4 + H_2O \quad (2.10)$$

Direct synthesis of DME is also reported by Aguayo *et al*. (2005) and An *et al*. (2008). Conversion of syngas to DME over a hybrid catalyst is investigated by combining methanol-synthesis catalysts and solid acid catalysts for methanol dehydration (*e.g*., H-ZSM-5 and ɣ-Al_2O_3) and treated with base (Abu-Dahrieh et al., 2012). The function of the base is to reduce the strength of acid sites, thus inhibiting hydrocarbon formation (equation 2.10) by poisoning the strong acid sites on the catalysts (Kulawska and Madej-Lachowska, 2013).

The most important aspect to take into consideration in preparing the highly active hybrid catalyst is the optimisation of composition of two catalysts components (Sun et al., 2014). Highly acidic catalysts lead to the secondary reaction in which DME will be converted into hydrocarbon while strongly basic catalysts favour the formation of methanol (Takeguchi *et al.*, 2000; Mao *et al.*, 2005). Deposition of 1.25 wt.% of MgO with CuO/ZnO/Al_2O_3-HZSM-5 increased the DME selectivity from 48% to 65% and inhibited the hydrocarbon (C_2 to C_5) formation, from 9.3% to 0.08% respectively (Mao *et al.*, 2005). Ateka *et al.* showed the catalyst with 2:1 composition of SAPO-18 to CuO/ZnO/Al_2O_3 yield a high quantity of DME while further addition of SAPO-18 favours the formation of by-products (Ateka et al., 2016). SAPO-18 has moderate acid site strength, uniform microporous structure and homogeneous acidity. Moderate acid site strength provides a high hydrothermal stability to a catalyst (Ateka et al., 2016). In addition to the composition of acidity and basicity of a catalyst, modification of CuO/ZnO catalyst (by adding metal oxide as the active catalyst) is also important and is summarised in Table 2.3.

Table 2.3. Modification of solid catalyst for the direct dimethyl ether synthesis from syngas.

Catalyst	Temp./ °C	Press./ MPa	Time/ hours	DME (yield)	DME (selectivity)	References
$CuO/ZnO/Al_2O_3/Ta_2O_3$-Al_2O_3	250	3	100	N/A	59.5	(Y. Wang et al., 2016)
$CuO/ZnO/Al_2O_3$/HZSM-5/$SrCO_3$	265	4	150	N/A	94.5	(Zhang et al., 2015)
$CuO/ZnO/ZrO_2$-MFI	240	5	N/A	11.6	N/A	(Frusteri *et al.*, 2015)
$CuO/ZnO/ZrO_2$-SAPO-18	275	3	6	35	94	(Ateka *et al.*, 2016)
CuO/ZnO/MnO-SAPO-18	275	3	6	34	95	(Ateka *et al.*, 2016)
$CuO/ZnO/Al_2O_3$. + 5.9% Nb_2O_5/Al_2O_3	265	5	18	N/A	64.9	(Limaa et al., 2014)
$CuO/ZnO/Al_2O_3/MgO$/HZSM-5	260	4	100	N/A	64.5	(Mao *et al.*, 2005)

Dadgar *et al.* in their work, studied the influence of H_2O on the DME synthesis. CO_2 conversion into methanol is decreased in the presence of H_2O. No methanol is detected when reaction is carried out at < 240 °C (Dadgar *et al.*, 2016). High concentrations of H_2O also lead to the deactivation of the hybrid catalyst. Catalytic activity of Al_2O_3 catalyst decreased due to the high adsorption of H_2O on the acid sites; HZSM-5 zeolite is commonly chosen as one bifunctional catalyst component because it is less sensitive to H_2O (Wang *et al.*, 2011). Addition of promoters , *e.g.*, B_2S_3, SiO_2, Cr_2O_3 and Ga_2O_3 onto $CuO/ZnO/Al_2O_3$ limit the catalyst deactivation problem (Tao et al., 2001).

2.2.5 **Glycerol carbonate synthesis**

Glycerol is a by-product formed from biodiesel synthesis (Sankaranarayanan and Srinivasan, 2012). Due to the large amount of glycerol produced every year, the market value of refined glycerol has reduced from ~ $1750/tonne to ~ $750/tonne since 2005 and crude glycerol is about $100/tonne (Quispe et al., 2013). Therefore, valorisation of both glycerol and crude glycerol is crucial (Sandra *et al.*, 2016).

GlyC synthesis from glycerol and CO_2 attracted much attention for several reasons: this process utilises two types of undesired products and GlyC has wide-ranging reactivity that can be applied in many applications*, e.g.,* electrolyte in lithium ion battery, cosmetic, as chemical intermediate and as the solvent (Sonnati *et al.*, 2013). Sonnati outlines other methods of synthesising the GlyC *via* hydrocarbon chain; which do not involve CO_2 as a reactant. These routes include the reaction of glycerol and (i) urea (ii) dimethyl carbonate and diethyl carbonate (iii) phosgene (iv) ethylene carbonate and propylene carbonate. However, carboxylation of glycerol is proposed as a green route to synthesise GlyC through avoiding the use of phosgene. Cyclic compounds including cyclic carbamates and cyclic carbonates are commonly manufactured from phosgene which is toxic and hazardous in nature (Narkhede and Patel, 2015). The carboxylation of glycerol *via* heterogeneous catalysis produces water as the by-product (Sonnati *et al.*, 2013). A range of solid catalysts have previously been investigated in this reaction: zeolites, basic ion-exchange resins, tin complexes and Ce-based catalysts (Aresta et al., 2006; Vieville et al., 1998). This reaction is further investigated by developing active heterogeneous catalysts such as Al_2O_3 (CeO_2-Al_2O_3) or Nb_2O_5 (CeO_2-Nb_2O_5).

Table 2.4. Comparative study of catalysts with different reaction conditions.

Catalyst	Dehydrating agent	Reaction condition				Gly. Conv. (%)	Selectivity (%)	Yield (%)	Ref.
		Temp (°C)	Time (hr)	P^a (MPa)	P^b (MPa)				
CeO_2	[c]2-cyanopyridine	150	5	3	4	N/A	N/A	20	(J. Liu *et al.*, 2016)
Zn/Al/LaF	Acetonitrile	170	12	4	N/A	30.6	46	14	(Li et al. 2015)
Zn/Al/La-Li	Acetonitrile	170	12	4	N/A	35.7	42.2	15.1	(H. Li, Jiao, *et al.*, 2015)
Cu/La_2O_3	Acetonitrile	150	3	4	7	8.9	29.3	N/A	(Zhang and He, 2014b)
2.3 wt.% Cu/La_2O_3	Acetonitrile	150	12	4	7	33.4	45.4	15.2	(Zhang and He, 2014a)
$La_2O_2CO_3$-ZnO	Acetonitrile	170	12	4	N/A	30.3	47.3	14.3	(Li *et al.*, 2013)

[a]Initial pressure of CO_2 at room temperature

[b]Reaction pressure of CO_2 at reaction temperature.

[c]Reaction was carried out in the presence of dimethyl formamide.

Carboxylation of glycerol in the presence of $La_2O_2CO_3$-ZnO and acetonitrile was first reported by Li *et al.* (2013). Acetonitrile acts as the chemical water trap, consequently shifting the reaction equilibrium to the product side. Cu/La_2O_3 has also been employed to synthesise the GlyC (Zhang & He, 2014a). Further studies have been carried out employing Cu-based catalysts supported on: (i) acid and basic supports (ii) supports with acid sites only (iii) supports with basic sites only and (iv) supports with neither acid nor basic site (Zhang & He, 2014b). Further research employing Zn/Al/La/M (M = Li, Mg and Zr) hydrotalcite as the catalysts for this reaction. Zn/Al/La/Zr,

calcined at 500 °C, resulted in a 14.1% yield of GlyC (43.3%). In order to improve the yield of GlyC at a lower temperature and pressure, 100 °C and 2.5 MPa, the reaction was carried out by reacting 3-chloro-1,2-propanediol and CO_2 in the present of trimethylamine (Ochoa-Gómez *et al.*, 2011). Ozorio and co-worker have studied the mechanism of glycerol carboxylation over metal impregnated zeolites in absence of dehydrating agent; however, the reaction must take place at high pressure, 100 bar. This resulted in a 6% yield of GlyC (Ozorio *et al.*, 2015). Research shows the success of synthesising GlyC from glycerol and CO_2 over heterogeneous catalysts in presence or absence of acetonitrile, however, the yield of products formation is considered low. Recently 2-cynopyrine has been employed; resulting in a 20% yield of GlyC with 2-picolinamide as the by-product (J. Liu *et al.*, 2016; Su *et al.*, 2017). The list of catalysts used for the carboxylation of glycerol are summarised in Table 2.4.

2.3 Conventional routes to glycerol carbonate

2.3.1 Phosgene

Transcarbonation of glycerol using phosgene is shown in Figure 2.3. Table 2.5 shows the examples of linear and cyclic carbonates; in which both linear and cyclic carbonates have an industrial interest and are mainly produced from phosgene (Aresta and Dibenedetto, 2007). The use of phosgene as carbonate source to synthesise glycerol carbonate must be eliminated because it is toxic and highly corrosive. However, Shukla & Srivastava in their review highlight the phosgene-free methods available to synthesise diethyl carbonate (linear carbonate) (2016).

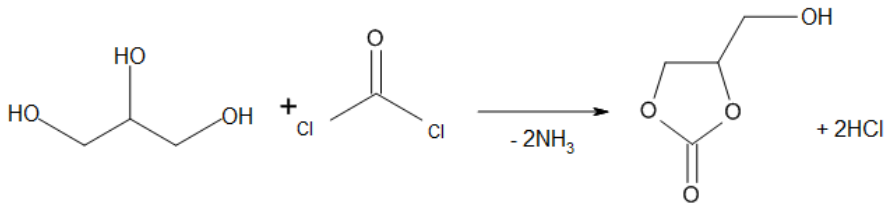

Figure 2.3. Transcarbonation of glycerol using phosgene (Sonnati *et al.*, 2013).

Table 2.5. Examples of linear and cyclic carbonate and their uses (Aresta and Dibenedetto, 2007).

Carbonates		Market	Uses
Linear	Dimethyl carbonate	18 Mt per year	Solvents, reagents, additives for gasoline
	Diallyl carbonate		
	Diethyl carbonate		Monomers for polymers, synthesis for hydroxyesters and hydroxyamines component
	Diphenyl carbonate		
Cyclic	Ethylene carbonate		
	Propylene carbonate		
	Cyclohexene carbonate		
	Styrene carbonate		

2.3.2 **Glycerol and urea**

Synthesis of GlyC from urea and glycerol in the presence of homogeneous and heterogeneous catalysts represents an interesting field. This phosgene-free route utilising the easily available, low cost and less toxic materials which releases ammonia gas as by-product (Figure 2.4) is carried out in the absence of solvent. A number of heterogeneous catalysts have been reported for this reaction such as Au (Ab Rahim *et al.*, 2012), Pd (Hammond *et al.*, 2011), silicotungstates supported on MCM-41 (Narkhede and Patel, 2015), metal ion exchange zeolite (Marakatti et al., 2014) and hydrotalcite (Climent *et al.*, 2010). Sonnati in his review listed the potential catalysts for the reaction of glycerol and urea including metal oxides (CaO, La_2O_3, MgO, ZrO_2, ZnO and Al_2O_3), hydrotalcite, Co_3O_4/ZnO nanodispersion and gold-supported on ZSM-5 (Sonnati *et al.*, 2013).

Introduction of 2.5 wt.% of Au to MgO yields 56% GlyC. Au-MgO prepared *via* impregnation have a high stability and yield 55% GlyC after 10^{th} cycle of experiments

(Hammond *et al.*, 2011). 2:1 Sn and tungsten catalyst prepared from co-precipitation method also show a good performance yielding a selectivity toward GlyC of 95% (Jagadeeswaraiah et al., 2014). Indran et al. and Zuhaimi et al. studied the use of waste materials such as ash/char and gypsum as the catalyst resulting in 90% conversion of glycerol with a yield > 75% of GlyC (Indran *et al.*, 2014; Zuhaimi *et al.*, 2015). It is clear that waste material can be used as an active catalyst to synthesise GlyC from glycerol and urea.

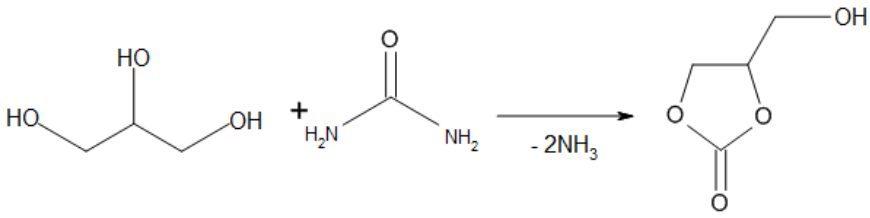

Figure 2.4. Synthesis of glycerol carbonate by glycerolysis of urea where 2,3-dihydroxypropyl carbamate is formed as the reaction intermediate (Ab Rahim *et al.*, 2012).

2.3.3 **Glycerol and dimethyl carbonate**

As shown in Figure 2.5, transesterification of glycerol and dimethyl carbonate to GlyC produces methanol as the by-product. Heterogeneous catalysis is an alternative method to replace the use of enzymatic and homogeneous catalysts. Okeye and Hameed reviewed the possible catalysts that are successful catalysed this reaction such as MgO, Na_2O, CaO, hydrotalcite, K-zeolite, ZnO and La_2O_3 (Okoye and Hameed, 2016).

A range of Na-based zeolites have been employed in transesterification of glycerol and dimethyl carbonate (Saiyong *et al.*, 2012). High glycerol conversion, 80%, and 100% selectivity to GlyC is recorded in the presence of NaY; while low selectivity to GlyC is observed upon the introduction of Naβ and NaZSM-5 catalysts. In this case, the influence of the pore size and the basicity of catalysts are very important and must be taken into consideration. Zeolite-based catalysts suffer from knocking and

deactivation problems due to poorly structured channels within the zeolites and addition of solvent is crucial in order to drive the reaction processes (Algoufi and Hameed, 2014; Okoye and Hameed, 2016)

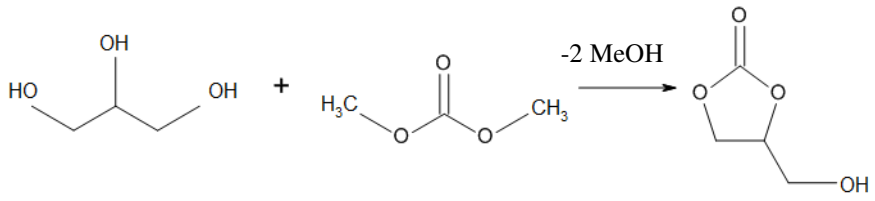

Figure 2.5. The stoichiometric equation of glycerol carbonate synthesis *via* glycerol esterification with dimethyl carbonate (Okoye and Hameed, 2016).

$Mg_4AlO_{5.5}$ hydrotalcite (80:20 mol ratio) is prepared *via* the co-precipitation method (Liu *et al.*, 2015). 1 to 15 wt.% of $LiNO_3$ is introduced to the $Mg_4AlO_{5.5}$ hydrotalcite in order to study the impact of number of basic sites of a catalyst. The selectivity to GlyC decreased in the presence of strong basic catalyst because it is promotes the decomposition of GlyC to glycidol (Okoye et al., 2017). Malyaadri *et al.* studied the impact of catalyst morphology by calcining the $MgO/Al_2O_3/ZrO_2$ at different temperatures. Only 8% GlyC yield is observed in the presence of uncalcined catalyst while 68 to 94% yield of GlyC are observed in the presence catalysts that have been calcined from 450 to 750 °C (Malyaadri et al., 2011).

2.4 **Conventional routes to acetins**

The interest in glycerol acetylation in the presence of acid catalyst has increased exponentially due to the increase of the quantity of biodiesel production; thus contributes to the production valuable chemicals, *e.g.*, mono-, di- and triacetin. In general, acetylation of glycerol takes place in the presence of acetyl source including acetic acid, ethyl acetate or acetic anhydride. Monoacetin is a starting material for the production of explosives while diacetin is widely use as solvent and plasticiser (Reddy et al., 2010). Triacetin is commonly use as the fuel additive and act as anti-knocking agent (Mufrodi et al., 2014; Okoye & Hameed, 2016; Sandesh et al., 2015). General

product applications of glycerol derived bio-additives are summarised in Table 2.6 (Kong *et al.*, 2016).

Table 2.6. General starting material and application of mono-, di- and triacetin and bio-additives (Kong *et al.*, 2016).

Bio additive	Starting material	Product application
Monoacetin	Acetic acid, glycerol	- Excellence solvency - Raw material for the production of biodegradable polyesters
Diacetin		- Plasticiser for cellulose acetate, nitrocellulose and ethyl cellulose - Plasticiser for cellulosic polymers and cigarette filter
Triacetin		- As an antiknock additive for gasoline - Improve cold low and viscosity properties of biodiesel
Glycerol tertiary butyl ether (GTBE) and Glycerol di-tert butyl ether (GDBE)	Isobutylene (gas phase); glycerol or tert-butyl alcohol (liquid phase); glycerol	- Used in diesel and biodiesel reformulation - Oxygenated additives for diesel fuel - Decreasing cloud point of biodiesel fuel - To reduce fumes, particulate matters, carbon oxides and carbonyl compounds in exhausts
Glycerol di-ethyl ether (di-GEE) and Glycerol tri-ethyl ether (tri-GEE)	Ethanol; glycerol	- Used for fuel formulation - Important intermediate for various chemicals
Glycerol mono-ethyl ether (Mono-GEE)		
Polyglycerol	Glycerol	- Excellent lubricity and used as additive in lubricant

Figure 2.6 shows the reaction scheme of mono-, di- and triacetin synthesised from glycerol and acetic acid, which involves a three step reversible equilibrium reaction. Mineral acids such as sulfuric acid, paratoluene sulphonic acid, hydrofluoric acid have been employed in glycerol acetylation reaction (Ferreira et al., 2009; Kale et al., 2013). Due to the high toxicity, corrosive and hazardous nature of those acids, multi-step catalysts and products recovery is needed (Okoye and Hameed, 2016); the heterogeneous catalysts employed are listed in Table 2.7.

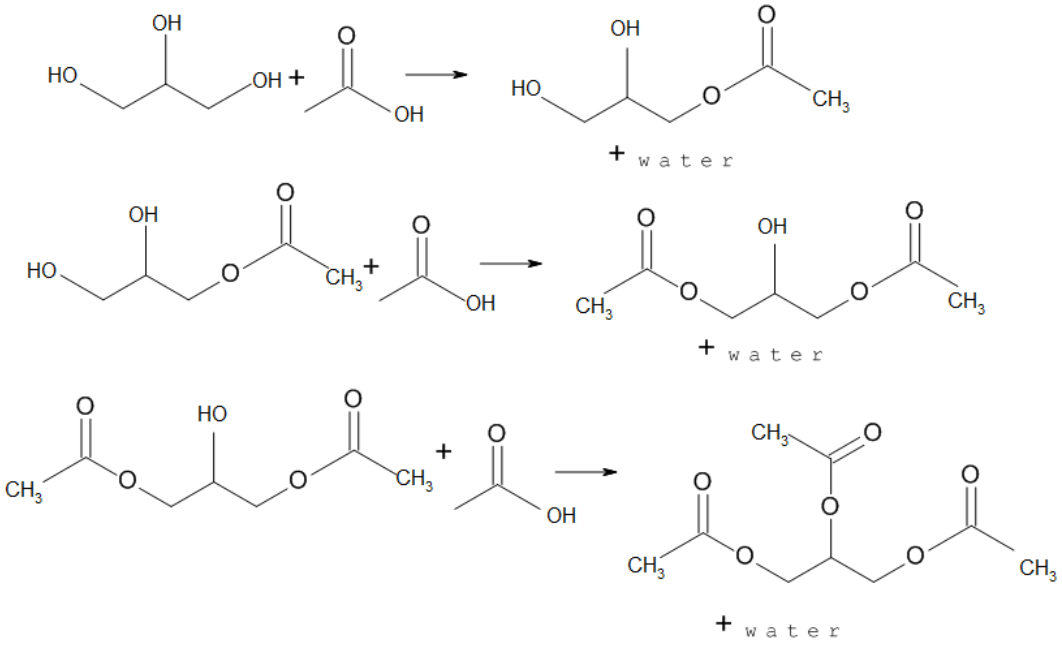

Figure 2.6. Glycerol acetylation scheme to synthesise mono-, di- and triacetin (Hu *et al.*, 2015). Acetylation of glycerol to mono-, di- and triacetin can be carried out in the presence of acetic acid or acetic anhydride at atmospheric pressure and is summarised in Table 2.7.

Table 2.7. Glycerol esterification in presence of acetic acid and acetic anhydride over heterogeneous catalyst. All reactions have been carried out at atmospheric pressure.

Catalyst	Glycerol conversion (%)	Reaction conditions		Selectivity to products (%)			Reference
		Temp. (℃)	Time (hr)	Mono-	Di-	Tri-	
Acetic acid							
7 wt.% CsPWA	98	85	2	25	59	16	(Sandesh *et al.*, 2015)
TPA /MCM-41	87	100	6	25	60	15	(Patel and Singh, 2014)
TPA/ZrO_2	80	100	6	60	36	4	(Patel and Singh, 2014)
Amberlyst 15	100	80	8	21	63	15	(Kim, Kim and Lee, 2014)
Amberlyst 15	97	110	4.5	9	47	44	(Zhou et al., 2013)
HZSM-5	85	110	4.5	68	25	7	(Zhou, Al-Zaini and Adesina, 2013)
HUSY	78	110	4.5	2	78	20	(Zhou, Al-Zaini and Adesina, 2013)
H-beta	94	120	2	48	39	4	(Silva et al., 2010)
PMo /NaUSY	68	-	3	37	59	2	(Ferreira et al., 2009)

Catalyst	Glycerol conversion (%)	Reaction condition		Selectivity (%)			References
		Temp (°C)	Time (hr)	Mono-	Di-	Tri-	
Acetic anhydride							
4 wt.% CsPWA	100	30	2	0	20	80	(Sandesh *et al.*, 2015)
H-Y	100	120	2	0	0	100	(Konwar *et al.*, 2015)
H-beta	100	120	2	0	0	100	(Silva, Goncalves and Mota, 2010)

Konwar and co-worker in their research concluded that a high density of surface acid site and the large pore size of H-Y zeolite (mesoporous) facilitated triacetin formation (Konwar *et al.*, 2015). H-beta (microporous) was also employed produces a high selectivity to triacetin of 100% (Silva et al., 2010). However, excess acetic anhydride to glycerol (4:1) has been employed. The reaction temperature also affects the products formed from this reaction. The selectivity to triacetin increases from 3 to 10% with increasing the reaction temperature from 50 °C to 110 °C; consequently, a drop in the selectivity to monoacetin to 78 to 30% is observed (Ghoreishi and Yarmo, 2013). Addition of acetic anhydride favours the production of triacetin. Despite high selectivity to triacetin, acetic anhydride is more expensive (0.98 USD/kg), than acetic acid, 0.5 USD/kg (Kong *et al.*, 2016). It is demonstrated that both acetic acid and acetic anhydride can be successful in synthesising acetins; but acetic anhydride is hazardous in nature (Redasani *et al.*, 2010). Moreover, the use of acetic anhydride is highly restricted in laboratories for research and also restricted by law in many countries. It is widely use for the production of morphine (Yadav and Joshi, 2002; Okoye and Hameed, 2016). Therefore, efforts towards the development of acidic heterogeneous catalysts are crucial.

3 EXPERIMENTAL WORK

This chapter describes the catalysts employed, apparatus, procedures and experimental reaction conditions used in this work. Section 3.1 explains the theory of catalyst preparation methods. The heterogeneous catalysts studied within this thesis are prepared via (i) co-precipitation (ii) hydrothermal and (iii) sol-gel methods as described in section 3.2. The carboxylation of glycerol is carried out in the presence of dehydrating agents and heterogeneous catalysts; and tested with pure, model crude glycerol and crude glycerol and will be discussed briefly in this chapter. The general procedure for catalytic testing and details of GC-MS analysis methods are described in section 3.3 and 3.4. Section 3.5 and 3.6 will focus on the catalyst and crude glycerol characterisation techniques employed within this thesis. All experimental work done to synthesise glycerol carbonate are explained in section 3.7.

3.1 Theory of catalyst preparation methods

3.1.1 Impregnation method

The impregnation method involves three steps: (1) contacting the support with the impregnating solution, (2) drying and evaporating the liquid solvent and (3) catalyst activation, *i.e,* calcination and reduction of prepared catalysts (Perego and Villa, 1997). Impregnation is commonly used in industry because of its simple execution and low waste streams (Munnik, Jongh and Jong, 2015). Its simplicity enables large quantities of catalysts to be prepared. It works with any porous material and metal salt combination as long as the solvent is compatible with both materials (Rioux, 2006). One of the drawbacks associated with impregnation is poor distribution of metal in the pores (metal loading), > 30% (Lok, 2009). Activation steps such as drying (evaporation of solvent) must be taken into consideration because it generally causes the agglomeration of metal precursors; thus leading to the formation of large particles after the reduction step (Rioux, 2006).

3.1.2 **Bulk method**

Co-precipitation: This is the most common method used to prepare catalyst; which is comprised of three major step: (1) liquid mixing, (2) nucleation and (3) crystal growth to form primary particles and aggregation of primary particles (Lok, 2009). The size of the crystallites formed is dependent on the relative rate of nucleation compared to crystal growth (Hutchings and Vedrine, 2004); where high rate of nucleation compared to crystal growth leads to the formation of small crystallites. The advantages of employing this method are high attainable metal loading, up to 60% to 80% and has relatively high metal dispersion (Lok, 2009). However, co-precipitation processes generate a large quantities of waste, *i.e,* salt solution is filtered after the aging process. In addition, there are several factors that affected the properties of the precipitate such as pH of the mixture, aging time, temperature, precipitating agent *etc.*(Schuth and Ugner, 1999). This method is not suitable for large scale because it is difficult to control the pH and homogeneity of the mixture during the aging process.

Sol-gel: A sol is defined as the suspension of solids in a liquid as colloidal particles (in range of nm to μm) and is coagulated to form gel (Hutchings and Vedrine, 2004). Catalysts prepared from this method have several advantages over precipitation because they have better surface area, pore volume, pore size distribution and high porosity (Perego and Villa, 1997; Hutchings and Vedrine, 2004). For example, amorphous gels of silica and alumina are used to synthesise zeolites and molecular sieves (Hutchings and Vedrine, 2004).

Hydrothermal: Hydrothermal treatments of precipitates are commonly carried out at low temperature (> 300 ℃) and aging in the presence of the mother liquor (Campanati, Fornasari and Vaccari, 2003). The advantages of this method are shown in Table 3.1; where they involve the textural and/or structural modification of the solid particles (Fonseca, 2008).

Table 3.1 Main hydrothermal transformation (Campanati, Fornasari and Vaccari, 2003; Fonseca, 2008).

From	To
Amorphous solid	Crystalline solid
Small crystal	Large crystal
Small amorphous particles	Large amorphous particle
Kinetically favoured phase	Thermodynamically favoured phased
Highly porous gel	Low porosity gel

3.2 **Preparation of catalyst**

The initial work on carboxylation of glycerol to synthesise GlyC described herein focused on the use of commercial La_2O_3 purchased from Sigma Aldrich with 99.9% purity and denoted as La_2O_3-C. The morphology of lanthanum-based catalysts were modified by manipulating the catalyst synthesis methods. The catalytic activity of ZnO catalyst (Sigma Aldrich, 99%) was also tested. One of the main reasons for employing ZnO as a catalyst is the ability of ZnO to activate glycerol and the success of this catalyst in synthesising GlyC has been reported in recent research (Li et al., 2013, Li et al., 2014 & Li et al., 2015). ZnO and $La_2O_2CO_3$ with a composition of 9:1 and 7.5:2.5 were also prepared *via* co-precipitation and wet impregnation methods. ZrO_2, with both acidic and basic sites, was introduced as catalyst support. ZrO_2, $ZrO_2/La_2O_2CO_3$ (7:3), and $ZrO_2/La_2O_2CO_3/Ga_2O_3$ (65:30:5) were prepared and tested over the carboxylation of pure glycerol, model crude glycerol and crude glycerol reactions.

3.2.1 $La_2O_2CO_3$ preparation methods

Co-precipitation: $La_2O_2CO_3$-CP was prepared *via* co-precipitation technique similar to that employed by Liu *et al* (2016) and Unnikrishnan & Darbha (2016). $La_2O_2CO_3$-CP was prepared from $La(NO_3)_3.6H_2O$ (Acros Organics, 99%); the salt was dissolved in 50 ml of deionised water and stirred. Precipitation of 0.5 M of $La(NO_3)_3.6H_2O$ was carried out by dropwise addition of 2 M of NaOH (Sigma Aldrich, 97%) with a constant pH of 11. The catalyst synthesis took place in a round-bottom flask fitted with a glass water condenser. The catalyst was aged for 4 hours at 60 °C and washing step was crucial to remove residual nitrates. Nitrates can cause particle sintering and agglomeration during thermal treatment, thus lead to a loss of surface area (Munnik, Jongh and Jong, 2015). The wet catalyst was centrifuged, washed with deionised water (until it reach pH 6 to 7) and dried for 13 hours at 110 °C. The catalyst was then calcined at 400 °C for 5 hours. The prepared catalyst was denoted as $La_2O_2CO_3$-CP.

Hydrothermal: 30 ml of 6 M of NaOH and 15 ml of 0.5 M of $La_2(NO_3)_2.6H_2O$ were prepared by dissolving the salts with deionised water. The salt mixture was stirred vigorously for 30 minutes. The mixture was placed in a 45 ml stainless steel autoclave equipped with magnetic stirrer and sealed tightly (J. Liu *et al.*, 2016). The hydrothermal treatment took place over 22 hours under constant mixing. The prepared catalyst was centrifuged at 6000 rpm and washed with deionised water to remove the residual nitrates (until it reach pH 6 to 7). Finally, it was dried at 110 °C for 13 hours and calcined at 400 °C for 5 hours. The prepared catalyst was denoted as $La_2O_2CO_3$-HT.

Citrate sol gel: 50 ml of 0.5 M of $La_2(NO_3)_2.6H_2O$ and 0.5 M of citric acid (Alfa Aesar, 99%) was dissolved in 25 ml of ethanol (Fisher Scientific, HPLC grade) and 25 ml of water (J. Liu *et al.*, 2016). The mixture was added into a 500 ml round bottom flask. The mixture was stirred, the temperature was set at 90 °C and placed in a silicon oil bath (Alfa Aesar, usable range from - 40 to 200°C). The salt mixture was stirred vigorously and evaporated to form transparent sol. The sol prepared was dried at

60 °C for 13 hours and calcined at 400 °C for 5 hours. The prepared catalyst was denoted as $La_2O_2CO_3$-SG.

3.2.2 Catalyst and support preparation methods

Co-precipitation: ZnO/$La_2O_2CO_3$-CP (90:10) was prepared from $Zn(NO_3)_2.6H_2O$ (Sigma Aldrich, 98%) and $La(NO_3)_3.6H_2O$ as reported by Li et al. (2013). Both salts were dissolved in 50 ml of deionised water and stirred. Precipitation of $Zn(NO_3)_2.6H_2O$ and $La(NO_3)_3.6H_2O$ was carried out by dropwise addition of 2 M of NaOH until it reached pH 11. The catalyst was aged for 4 hours at 60 °C. The mixture was then filtered by vacuum filtration. The catalyst washed with deionised water and dried overnight at 100 °C. Then, it was calcined for 5 hours at 400 °C. ZrO_2, $ZrO_2/La_2O_2CO_3$ and $La_2O_2CO_3/ZrO_2/Ga_2O_3$ were prepared using the same method and $ZrO(NO_3)_2 \cdot xH_2O$ (Sigma Aldrich, 99%) and $Ga(NO_3)_2.xH_2O$ (Alfa Aesar, 99.9%) were employed to synthesise those catalysts (Bienholz *et al.*, 2011). The wet catalyst was centrifuged and washed with deionised water (until it reach pH 6 to 7). The catalysts was dried overnight at 110 °C; then calcined at 400 °C for 5 hours.

Impregnation: ZnO/$La_2O_2CO_3$-I (90:10) was prepared from $Zn(NO_3)_2.6H_2O$ and La_2O_3-C in the manner reported by Zhang and Ozorio with slight modification (Zhang and He, 2014a, 2014b; Ozorio *et al.*, 2015). 16.5 g of $Zn(NO_3)_2.6H_2O$ was dissolved in 100 ml of ethanol. 0.5 g of La_2O_3-C was added into the zinc nitrate solution. The mixture was stirred for 5 hours at room temperature. The catalyst liquid mixture was then filtered by vacuum filtration. The wet catalyst was dried for 13 hours at 110 °C and calcined for 5 hours at 400 °C.

3.3 Apparatus and procedure

3.3.1 The autoclave

All catalytic reactions were carried out in a 45 ml high pressure stainless steel autoclave (Parr Instruments, Model 4714) equipped with a magnetic stir bar and an

external thermocouple. The reactor was heated in silicon oil (usable range from - 40 to + 200 °C) and placed on a heating plate equipped with adjustable heating temperature (maximum temperature, 500 °C) and adjustable stirring speed. The reactor was connected with a CO_2 gas line at the inlet valve. The connection line was examined for gas leakage and any leakage must be avoided. The reaction was carried out at the desired temperature and the pressure and monitored by a pressure gauge. The reaction was designed not to exceed 60 bar at any time as the maximum pressure of experimental work is limited to 100 bar by equipment design. The outlet valve was slowly opened and gas was vented to depressurise the reactor. A pressure relief valve was installed to protect the equipment in the event of over pressure. Due to safety considerations, all of the reactions were performed in a fume cupboard at all times and in the event of pressure build up, the safety valve release pressure.

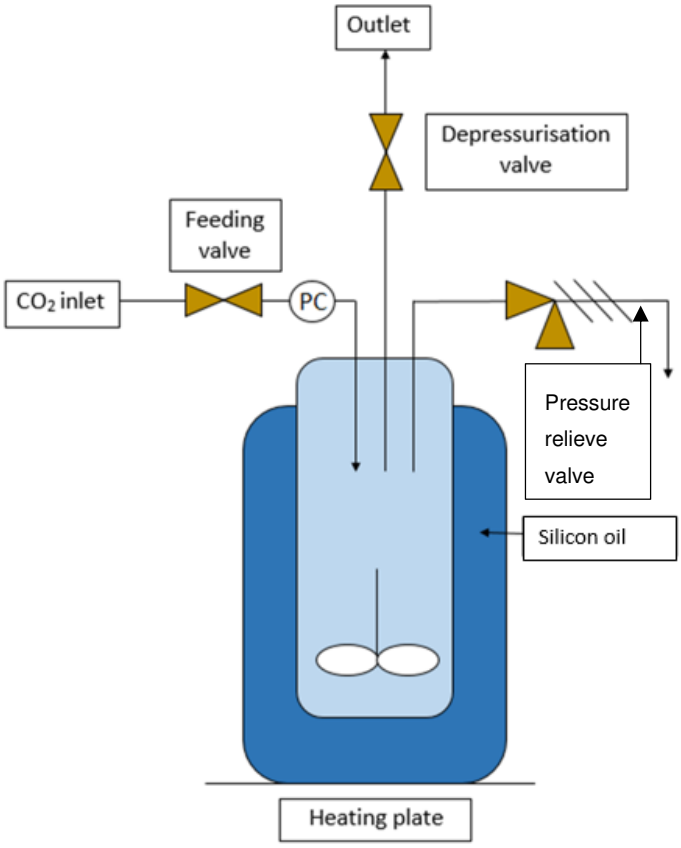

Figure 3.1. Scheme of the experimental configuration employed. PC is the pressure control.

3.3.2 **Operating procedure**

General: Direct carboxylation of glycerol was carried out for 13 to 25 hours in an oil bath-heated high pressure stainless steel autoclave (45 ml). 6 wt.% catalyst, 22.5 mmol glycerol and 45 mmol dehydrating agent were measured and loaded into the reactor. The reactor was purged and cycled with 20 bar of CO_2. This step was very important to remove the air trapped inside the reactor. Then, the reactor was pressurised with 34 bar CO_2 at room temperature. This resulted in initial pressure at reaction temperature of 45 bar. The operating temperature was set at 160 °C and the oil bath was preheated before the autoclave was placed in it (Zhou et al., 2014). Once the temperature had stabilised and reached 160 °C ± 2 °C, the magnetic stirrer was turned on. After the desired reaction time, the reaction was quenched by placing the reactor ice water. The pressure inside the reactor before and after cooling down were recorded and then the reactor was depressurised slowly.

Model crude glycerol: Model crude glycerol were prepared by mixing glycerol and methanol to the ratio of 80:20 (22.5 mmol in total). 1 wt.% NaOMe, 10 wt.% FAME and/or 10 wt.% water were added into the glycerol and methanol mixture. 45 mmol adiponitrile and 6 wt.% catalyst were also loaded into the reactor.

Crude glycerol: 2.1 g crude glycerol (17 mmol glycerol) was loaded into the reactor along with 45 mmol adiponitrile and 6 wt.% catalyst. 1 wt.% NaOMe and 5 wt.% methanol were also added into the crude glycerol.

The sample of crude glycerol was obtained as the by-product of biodiesel synthesis from sunflower oil and methanol and catalysed by NaOMe. The reaction was carried out on a Golden Ray biodiesel processor at Department of Chemical and Biological Engineering, University of Sheffield.

3.4 Sample analysis

3.4.1 Liquid sampling method

50 µL of liquid sample (collected after the reaction) containing glycerol, dehydrating agent, products and catalyst were extracted and diluted in 1000 µL of ethanol (1:20). Then, the sample was shaken well and filtered using a 0.2 µm pore size Captiva Premium Syringe Layered Filter (Agilent). This step was crucial to remove particles of catalyst. The sample was then analysed using GC-MS. Centrifugation is a common method used to separate the liquid products and solid catalysts. In this case, this method cannot be employed due to high viscosity of the reaction samples.

3.4.2 Gas chromatography (liquid phase analysis)

Gas chromatography (GC) equipped with mass spectrometry (MS) are employed to analyse complex samples in form of liquids (Annino and Villalobos, 1992). There are several types of GC detector including MS (mass spectrometry), TCD (thermal conductivity detector), FID (flame ionisation detector) and ECD (electron capture detector) (Levy, 2007). A GC instrument consists of gas inlet, injector, column oven, detector and data system. An inert gas, *e.g.*, helium, nitrogen or hydrogen is commonly used as the carrier gas (Chromacademy, 2013).

The sample is injected into the injection port and the sample is split before it enters the column (is divided according to the split ratio selected). Separation in the GC is based on different affinities between the constituents of the mobile phase to the stationary phase. Chemicals with strong affinity to the stationary phase have longer retention times and those with weak affinity have shorter times (Levy, 2007), leading to separation.

A small amount (µL) of sample is injected into the carrier gas stream. Volatilised sample components flow along the column into the detector. The detector signal is sent to the data signal and a chromatogram is then constructed. The detector signal in form of peak height and area under a peak are analysed (Annino and Villalobos, 1992).

A gas chromatograph equipped with a mass spectrometer detector, (Shimadzu, GCMS QP2012SE), was employed to analyse the composition of the liquid products collected from the reaction. A 30 m HP Innowax capillary column with 0.25 mm internal diameter and 0.25 μm film thickness was used. Helium was used as the carrier gas, the stream split ratio and injection temperature were set at 100 and 250 °C. The sample was analysed with injection volume of 0.5 μL for 32 minutes. Figure 3.2 shows the method developed to analyse glycerol, GlyC and mono-, di- and triacetin. The temperature of the oven was held for 2 minutes at 40 °C and the temperature was increased at a rate of 10 °C/min from 40 to 163 °C and then held isothermally for 1 minute at 163 °C. The temperature was then ramped rapidly from 163 to 190 °C at 50 °C/min and was kept constant for three minutes. This method was important to improve the peak separation. The oven temperature was then increased to 205 °C at a rate of 10 °C/min and held for another 3 minutes. The temperature was increased to 250 °C at a rate of 10 °C/min and kept constant for 5 minutes.

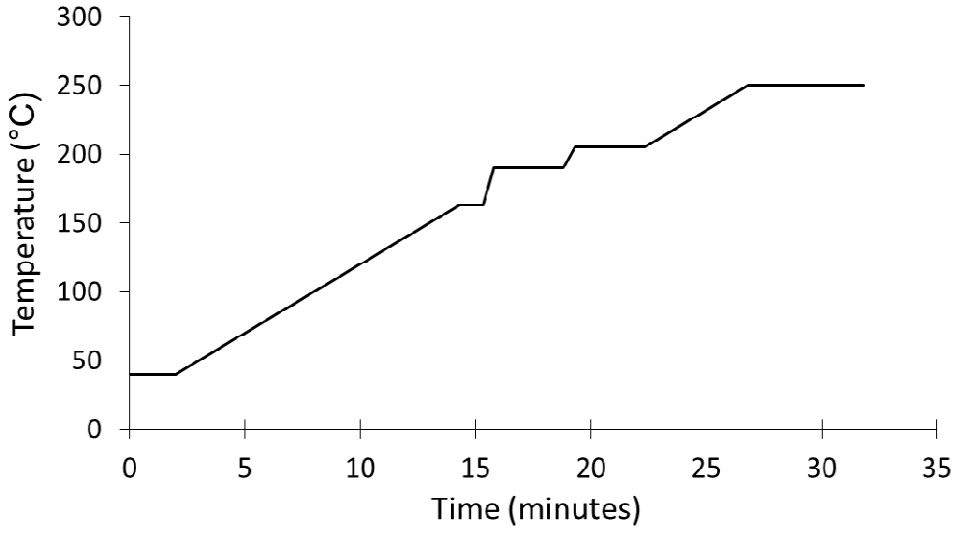

Figure 3.2. GC method developed for glycerol, product and by-products analysis.

3.4.3 **GC Calibration**

The GC-MS system was calibrated using 99.9% purity glycerol and 90% purity of GlyC. The glycerol and GlyC calibration curve are shown in Figure 3.3 and 3.4.

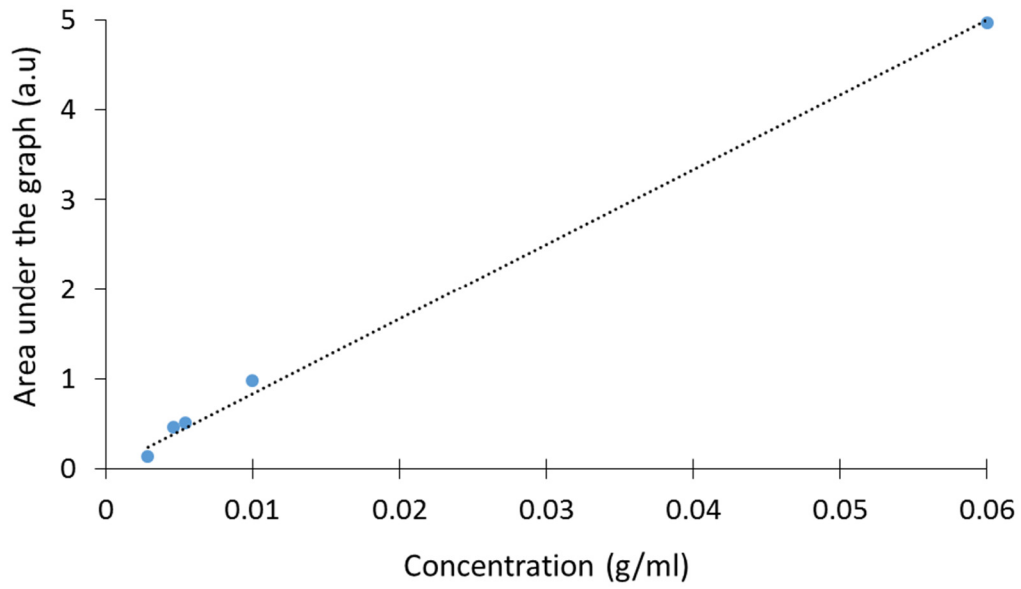

Figure 3.3. Calibration line of glycerol; where y = 81.2 x + 0.11.

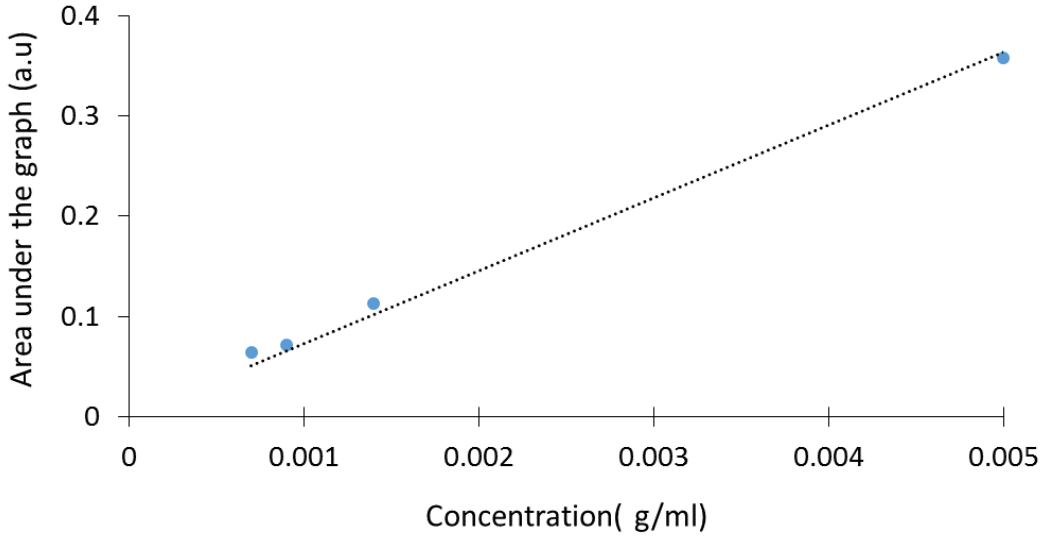

Figure 3.4. Calibration line of glycerol carbonate; where y = 68.8 x + 0.01.

The glycerol concentration was measured as follows:

$$y = mx + c \quad (3.1)$$

$$y = 81.2\ x + 0.11 \quad (3.2)$$

Where

y = area of reactant or products under the peak curve

m = is the gradient of reactant or products calibration curve (m = 81.2)

x = the final reactant or products concentration

c = point at which the line crosses the y-axis

Glycerol conversion, yield and selectivity to the products formed from these reactions were analysed and calculated as follow:

The conversion of glycerol

$$\%\ conversion = 100\ x\ \left(\frac{C_{0_{glycerol}} - C_{glycerol}}{C_{0_{glycerol}}}\right) \quad (3.3)$$

Where

C_0 = initial concentration of glycerol (g/ml)

C = final concentration of glycerol (g/ml)

Selectivity of the products formed

$$\%\ selectivity = 100\ x\ \left(\frac{moles\ of\ product\ formed}{moles\ of\ glycerol\ consumed}\right) \quad (3.4)$$

Yield of product formed

$$\%\ yield = 100\ x\ \left(\frac{moles\ of\ product\ formed}{moles\ of\ glycerol\ introduced}\right) \quad (3.5)$$

3.4.4 **ATR-FTIR (liquid analysis)**

An infrared spectrum represents a sample with absorption peaks which correspond to the frequencies of vibrations between the bonds of the atoms. The wave number is typically measured over the range of 400 to 4000 cm^{-1} (Duckett and Gilbert, 2000; LPD Lab Services, 2017). FTIR is a measurement technique to collect the infrared spectra (IR). This beam passes through an aperture and then enters the interferometer where the "spectral encoding" takes place. Subsequently the beam is transmitted to the surface of the sample and finally to the detector. The detector is used to measure the interferogram signal (Thermo Scientific, 2013).

ATR-FTIR analysis for liquid samples was conducted employing a Shimadzu IRAfiinity-1S. Spectra were collected over the range 400 to 4000 cm^{-1} with a resolution of 4 cm^{-1}. A drop of reaction sample was placed onto the sample holder and analysed.

3.5 **Catalyst characterisation methods**

3.5.1 **BET**

Nitrogen adsorption and desorption at 77 K is a method to determine the range of pore sizes and pore volume distribution of porous materials including micropores, mesopores and macropores (Seaton, Walton and Quirke, 1989; Leofanti *et al.*, 1997). The BET theory provides a simplified model for the adsorption of gas molecules onto a surface, and is used to calculate the surface area of materials. N_2, argon and krypton can be employed for this analysis (Llewellyn, Bloch and Bourrelly, 2012). The BET model improved the model proposed by Langmuir in 1915. The BET model proposed the adsorption of multiple layers of gas (Figure 3.5); while Langmuir adsorption model is based on the assumption of the formation of only one monolayer of strongly adsorbed gas (Llewellyn, Bloch and Bourrelly, 2012). There are four experimental protocols of the BET analysis such as activation (outgassing), dead volume space calibration, adsorption and desorption (Llewellyn, Bloch and Bourrelly, 2012).

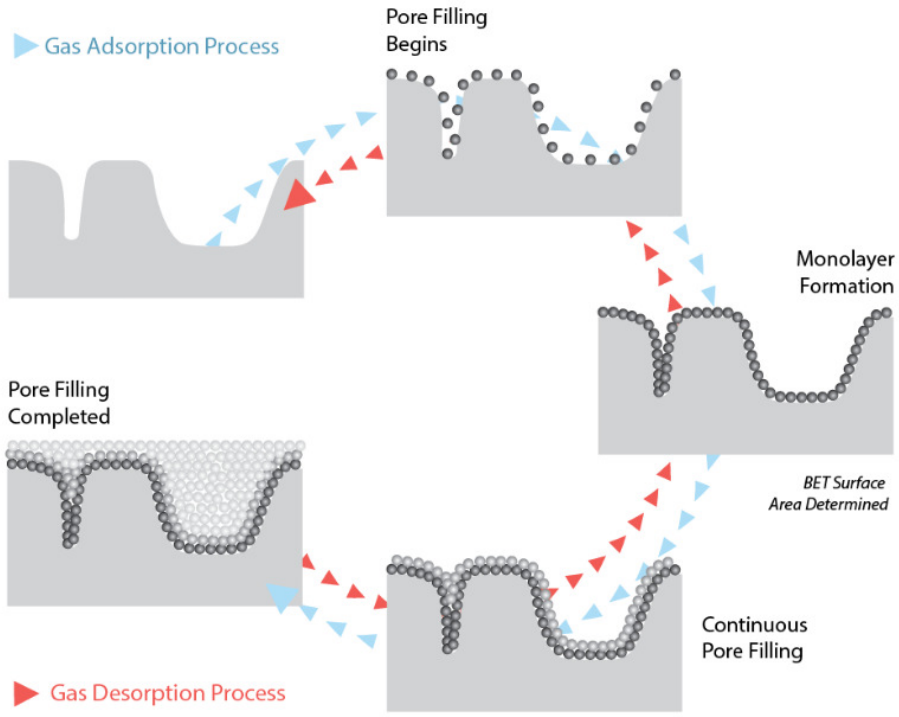

Figure 3.5. BET model of multilayer adsorption and desorption of gas, *e.g,* nitrogen (Particle Technology Lab, 2017).

Brunauer Emmett Teller (BET) measurements (Micrometrics 3-Flex) identified the total surface area of catalyst. Pore volume and pore size were determined from the desorption branch of isotherm *via* the BJH method. 0.5 g catalyst was loaded into the sample tube and degassed at 250 °C for 3 hours prior to analysis using Vac Prep 061. Nitrogen sorption measurement was carried out at 77 K and under vacuum condition.

Thanks to Ben Palmer, Department of Material Science and Engineering at University of Sheffield for technical support whilst using this facility.

3.5.2 **TPD**

TPD is mainly used for the characterisation of the acidic and basic site in gas-solid interaction where a range of the gas probes can be used including NH_3, pyridine, SO_2 and CO_2. NH_3 and pyridine are commonly used to study the acidity of catalyst, while basicity of catalyst can be analysed using SO_2 and CO_2. This experiment consists of

three phases including pre-treatment, adsorption and desorption (Mekki-Berrada and Aurox, 2012).

Pre-treatment: The catalyst sample is treated with inert gas at low pressure and at a temperature to remove impurities from the catalyst surface without degrading the sample structure.

Adsorption: The catalyst sample is treated with CO_2 or NH_3 gas at room or low temperature until the catalyst pores are saturated with the gas.

Desorption: The sample is heated and a flow of inert gas carries the desorbed molecule to the detector. In the desorption method, weakly bonded molecules (physisorption) will desorb first followed by strongly bonded molecules (chemisorption).

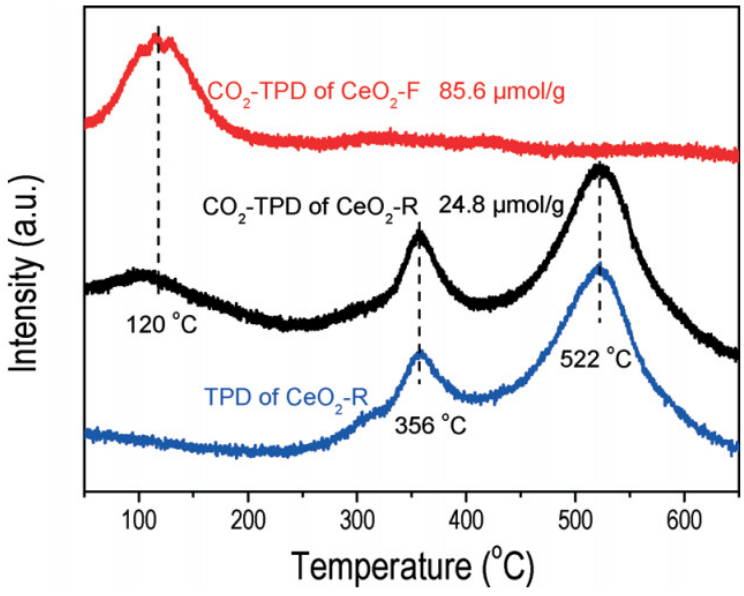

Figure 3.6. CO_2-TPD profile of CeO_2, where peak detected < 250 °C indicates the presence of weak basic, while peak detected from 250 to 400 °C and > 400 °C indicate the presence of medium and strong catalyst basic sites (Z. Zhang *et al.*, 2016).

Peaks detected at < 250 °C indicate the presence of weakly basic sites, while peaks detected from 250 to 400 °C and > 400 °C indicate the presence of medium and strong catalyst basic sites as shown in Figure 3.6.

TPD-CO_2 was performed on a QuantaChrome ChemBet Pulsar/TPR and equipped with thermal conductivity detector. 0.1 g of catalyst was measured and placed in U shape quartz reactor. The catalyst was pre-treated using He at 300 ℃ for 1 hour. The sample was then cooled to room temperature (30 ℃) and was treated with flowing pure CO_2 for 1 hour. The catalyst was then purged with He to remove the physisorbed CO_2. The temperature was increased from 30 to 900 ℃ at a rate of 10 ℃ min^{-1}.

TPD-NH_3 was also performed on a QuantaChrome ChemBet Pulsar/TPR and equipped with thermal conductivity detector. 0.1 g of catalyst was measured and placed in U shape quartz reactor. The catalyst was pre-treated using He at 300 °C for 1 hour. The sample was then cooled to room temperature (30 °C) and was treated with flowing 0.1% NH_3/Ar for 6 hours. The catalyst was then purge with He to remove the physisorbed NH_3. The temperature was increased from 30 to 900 °C at a rate of 10 °C min^{-1}.

Thanks to Prof Chris Hardacre and Dr Sarayute Chansai, School of Chemical Engineering, Manchester University, for the TPD-NH_3 and TPD-CO_2 equipment and technical support.

3.5.3 **SEM**

Scanning electron microscope (SEM) is a surface imaging method that scans a specimen using a high energy beam of electrons to analyse the external morphology (texture) (*Scanning Electron Microscopy (SEM)*, 2016) including properties such as shape, particle size distribution and speciation structure of a sample (catalyst) (Tiede *et al.*, 2008). The sample surface is scanned using the incident electron beam and interacts with the sample to generate signals (Lin *et al.*, 2014). The incident electrons

cause emissions of backscattered electrons (BSE) and low-energy secondary electrons (SE) from the atoms on the sample surface and secondary electron imaging (SEI) is typically used for SEM analysis (Lin *et al.*, 2014; AZO Material, 2017).

The morphology of the catalyst was also studied using SEM (scanning electron microscopy). The solid catalyst was placed on a black carbon stick. The prepared sample underwent gold coating; sample coating required if the catalyst was not electrically conductive. The stub was placed on the coater sample table and the chamber was flushed and pressurised with 0.3 bar of argon. The sample coating took place over 8 seconds. The analysis was carried employing on JEOL JSM-6010LA. The acceleration voltage was at 12 to 20 kV. The images were magnified 100 to 1000 times. The particle size of the catalysts were analysed using Image J software. The diameter of these particles were measured at 100 points across the sample.

Thanks to Dr Alan Dunbar and the ESPRC (4CU Grant, EP/K001329/1) for the SEM images, technical support and training whilst using the SEM facilities at University of Sheffield.

3.5.4 **ATR-FTIR**

The working principle of ATR-FTIR is explained in section 3.4.4. Surface functionalities of the solid catalysts were identified employing a Fourier transform infrared spectroscopy (FTIR) (Shimadzu IRAfiinity-1S). Spectra were collected over the range of 400 to 4000 cm^{-1} with a resolution of 4 cm^{-1}.

3.5.5 **Powder XRD**

X-ray diffraction is a non-destructive method to characterise the crystal structure and determine the chemical phase composition of a catalyst (Satterfield, 1980; Cullity and Stock, 2001). An X-ray diffractometer consist of X-ray tube, a sample holder and X-ray detector (Dutrow and Clark, 2017) as shown in Figure 3.7. The X-rays are

generated by a cathode ray tube by heating a filament to produce and accelerate electron and directed toward the sample. The interaction of the incident rays with the sample produces constructive interference and a diffracted ray. The sample and detector are rotated and intensity of the reflected rays are recorded. Cu, Fe, Co, Cr, Mo are the target material that can be used for crystal diffraction but CuK_{α} radiation = 1.5418 Å is commonly used for single crystal diffraction and data is collected at 2θ from ~ 5° to 70° (Dutrow and Clark, 2017).

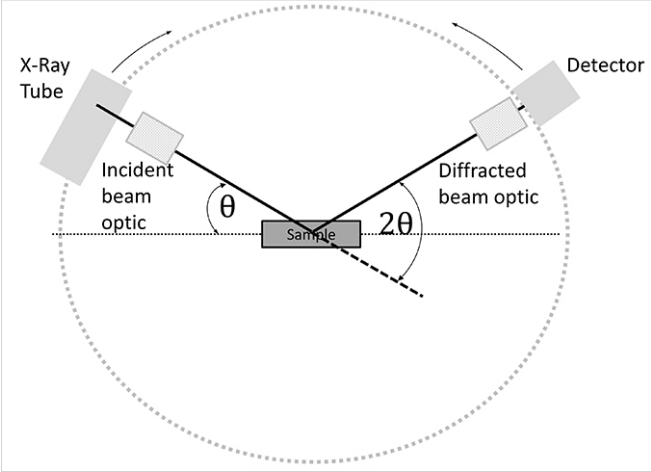

Figure 3.7. Schematic of a diffractometer (AOCS Lipid Library, 2017).

Sir W. H. Bragg and Sir W. L. Bragg explained the relation between the crystalline lattice and scattering beam of an angle. This is described using Braggs's law as shown in equation 3.6.

$$n\lambda = 2d \sin \theta \qquad (3.6)$$

λ = wavelength of the incident beam; it is assumed the λ of incident beam and λ of the reflected beam are equal

n = the order of reflection

d = the interplanar spacing of the crystal

θ = the angle of incidence

The average crystallite size is calculated from XRD peaks using Debye-Scherrer's formula as summarised in equation 3.7. All data analysis were performed using Fityk software.

$$Dp = \frac{0.94*\lambda}{\beta_{\frac{1}{2}}*\cos\theta} \quad (3.7)$$

D_p = the average particle size

λ = the wavelength of the X-ray

$\beta_{\frac{1}{2}}$ = the width (in radians) of the diffraction peaks at half height

θ = the Bragg angle of peak

X-ray diffraction (D2 Phaser Bruker Ltd), with CuKα1 radiation (λ = 1.5406 Å and 2θ range from 10° to 60°) was employed in order to identify the crystalline phase of solid catalyst. A graphite monochromator were analysed at 10 ℃ min^{-1} and maintained at a tube voltage and current of 30 kV and 10 mA. The crystalline phases were identified by comparing the peak detected from the XRD pattern and the Powder Diffraction Files (PDF).

Thanks to Dr Nik Reeves-McLaren for the XRD analysis, technical support and training whilst using the XRD facilities at Department of Materials Science and Engineering, University of Sheffield.

3.6 **Characterisation of crude glycerol**

The industrial grade crude glycerol was analysed and characterised using a range of characterisation techniques. Crude glycerol (Figure 3.9 b) was separated using a 50 ml separating funnel in order to remove the methanol and ash content. GC-MS was employed to analyse the purity of glycerol and to measure the percentage of methanol

content in crude glycerol. The FAME component was identified and compared with the NIST library.

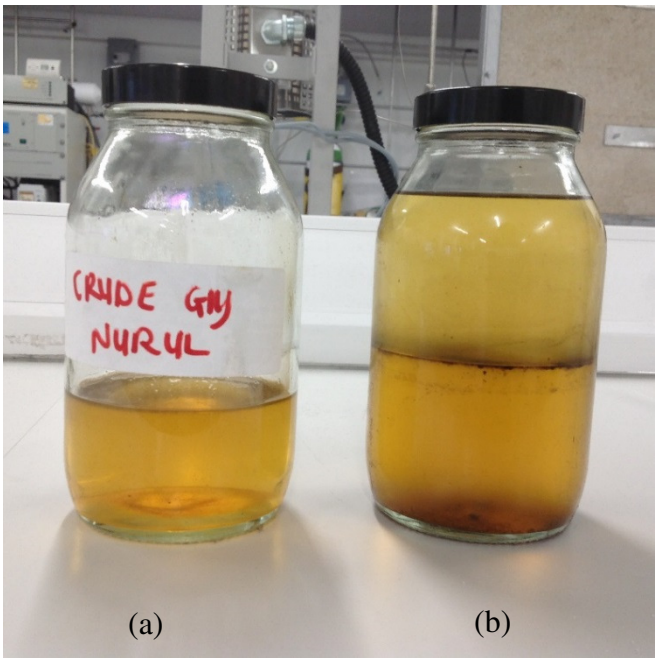

Figure 3.8. Sample of crude glycerol (a) after separation (b) before separation.

The percentage of water content was tested using Karl Fisher titration technique; carried out by Quality Context Limited. There are two methods to perform the Karl Fisher titration tests including volumetric and coulometric; where the coulometric method has the advantage of being able to measure low moisture content (10 µg to 100 mg) (GPS Instrument Ltd., 2017). Karl Fisher reagent consist of iodine (I_2), sulphur dioxide (SO_2), solvent and buffer. Methanol is commonly used as the solvent while imidazole or pyridine is used as the buffer. Water is reacted with iodine until the endpoint of the titration is reached. Water and iodine are consumed in 1:1 mole ratio and the percentage of water content is calculated based on the amount of Karl Fisher Reagent consumed during the reaction. The pH of the crude glycerol was analysed using pH paper, while, the percentage of Na contained in the crude glycerol was detected using ICP-MS technique and was carried out at Dainton Building, Department of Chemistry at University of Sheffield.

Inductively Coupled Plasma (ICP) is a technique used to determine the elemental composition of a sample; an ICP source convert elemental atoms into ions (Wolf, 2005). Samples are introduced into argon plasma as an aerosol; the plasma then dissociates the molecules and then removes an electron from the components. The ions generated from this process is directed into the MS. The ions detected by the MS are then sorted according to their mass to charge ratio (m/z) (Perkin Elmer, 2014). In general, elements that form negative ions such as Cl^{-1}, I^{-1} and F^{-1} are difficult to determine using this technique.

3.7 Catalytic reaction studies

3.7.1 Glycerol carbonate synthesis from the reaction of CO_2 and glycerol (99% purity)

The reaction of glycerol and CO_2 was carried out in the presence of 6 wt.% of catalyst. The methodology of this reaction was discussed in section 3.3.2. In total, four cases were studied and these are summarised in Table 3.2. Preliminary studies were carried out in the absence of a dehydrating agent and/or catalyst. The second case was focused on the catalyst screening, where lanthanum-based catalysts yield a high selectivity to GlyC. In this case, lanthanum was chosen in order to study the influence of catalyst preparation methods and how they are affecting the formation of the products (third case). The reaction was carried out in the presence of $La_2O_2CO_3$ catalysts prepared by (i) co-precipitation (ii) hydrothermal (iii) sol-gel methods. Only La_2O_3-C was introduced into this carboxylation reaction (case four and five) in order to aid reproducibility of this work. The fourth case was focused on the optimisation of reaction conditions. The influence of the amount of catalyst to reactant ratio, the influence of molar ratio of glycerol and dehydrating agents and the influence of reaction temperatures were investigated. The final case focused on the influence of dehydrating agents. Two types of dehydrating agents were then introduced: (1) nitrile based dehydrating agents and (2) acidic dehydrating agents. A green solvent, anisole, was also employed in order to study the ability of green solvents to replace the function of the dehydrating agent in synthesising GlyC.

Table 3.2. Designed case studies for the carboxylation of glycerol of 99% purity.

Case study	Catalysts	Dehydrating agent	Glycerol: DA amount (mmol)
Case 1 (blank reaction)	N/A	N/A	22.5:0
	N/A	Adiponitrile	22.5:45
	La_2O_3-C	N/A	22.5:0
Case 2 (Catalysts screening)	La_2O_3-C	Adiponitrile	22.5:45
	ZnO	Adiponitrile	22.5:45
	ZnO/$La_2O_2CO_3$-CP	Adiponitrile	22.5:45
	ZnO/$La_2O_2CO_3$-I	Adiponitrile	22.5:45
	ZnO/SnO2	Adiponitrile	22.5:45
Case 3 (Effect of La_2O_3-C and $La_2O_2CO_3$ preparation method)	La_2O_3-C $La_2O_2CO_3$-CP $La_2O_2CO_3$-HT $La_2O_2CO_3$-SG	Adiponitrile	22.5:45
Case 4 (Range of reaction parameters)	La_2O_3-C	Adiponitrile	(1) Wt.% of catalyst (2) Mol of dehydrating agent (3) temperature
Case 5 (Influence of dehydrating agents)	La_2O_3-C	Acetonitrile Benzonitrile Adiponitrile Acetic anhydride Anisole	22.5:45

3.7.2 **Carboxylation of crude glycerol or model crude glycerol**

As the impurities in the crude glycerol are likely to interact with one another, the influence of impurities in the crude glycerol including methanol, FAME, water and NaOMe on carboxylation reaction was investigated. First, catalyst screening has been carried out employing pure glycerol and adiponitrile over La_2O_3-C, $La_2O_2CO_3$-CP and Zr-based catalysts (Case 1). High selectivity to GlyC was observed in the presence of La_2O_3-C, $La_2O_2CO_3$-CP and ZrO_2/$La_2O_2CO_3$/Ga_2O_3; thus, only these three catalysts were introduced into the direct carboxylation of both model and crude glycerol.

Case 2 and 3 focused on the individual and multiple impacts of impurities and how they affect glycerol conversion and selectivity to GlyC. These reactions were carried out in the presence of La_2O_3-C to aid reproducibility of this reaction. Addition of methanol to glycerol reduces the concentration of glycerol, therefore it is proposed to improve the mass transfer of the glycerol, adiponitrile, CO_2 and the catalyst itself. Addition of methanol appears to have positive impact on the catalytic system; in which highest selectivity to GlyC, 25%, was achieved in the presence of La_2O_3-C. The carboxylation of glycerol and methanol was also investigated over $La_2O_2CO_3$-CP and yield 42% selectivity to GlyC. Therefore, the optimisation of reaction conditions was carried out in the presence of $La_2O_2CO_3$-CP and is summarised in Table 3.3 (Case 4 and 5). Finally, carboxylation of crude glycerol with added impurities was carried out in the presence of La_2O_3-C, $La_2O_2CO_3$-CP and ZrO_2/$La_2O_2CO_3$/Ga_2O_3 as listed in Table 3.3 (Case 6).

Table 3.3. Experimental works designed for the carboxylation of model crude glycerol and crude glycerol.

Case study	Catalysts	Impurities
Case 1 (Catalyst screening/ Influence of transitional metal)	La_2O_3-C $La_2O_2CO_3$-CP ZrO_2 $ZrO_2/La_2O_2CO_3$ $ZrO_2/La_2O_2CO_3/$ Ga_2O_3	(1) N/A
Case 2 Model crude glycerol 1 (Influence of impurities)	La_2O_3-C	(1) 10 wt.% FAME (2) 10 wt.% water (3) 1 wt.% NaOMe (4) 80:20 mol% glycerol to MeOH
	$La_2O_2CO_3$-CP	(5) 80:20 mol% glycerol to MeOH
Case 3 Model crude glycerol 2 (Influence of methanol and another impurities)	La_2O_3-C	(1) 1 wt.% NaOMe (2) 10 wt.% FAME (3) 10 wt.% FAME +1 wt.% NaOMe
Case 4 Model crude glycerol 3 (Influence of methanol composition)	$La_2O_2CO_3$-CP	(1) 100:0 mol% glycerol to MeOH (2) 80:20 mol% glycerol to MeOH (3) 60:40 mol% glycerol to MeOH
Case 5 Model crude glycerol 4 (Time online analysis)	$La_2O_2CO_3$-CP	(1) 80:20 mol% glycerol to MeOH (reaction sample were measure at 13, 15.5, 18. 23. 25 hours)
Case 6 Crude glycerol	La_2O_3-C	(1) Blank (2) 5 wt.% MeOH (3) 5 wt.% MeOH 1 wt.% NaOMe
	$La_2O_2CO_3$-CP	(1) 5 wt.% MeOH
	$ZrO_2/La_2O_2CO_3/$ Ga_2O_3	(1) 5wt.% MeOH

3.8 **Reproducibility and experimental error**

Methods to reduce the experimental error associated with the calibration of reactant and products using the GC-MS will be discussed here. The calibration of GC-MS was carried out regularly in the way discussed in section 3.4.3. The reaction sample used for GC-MS analysis was prepared repeatedly and injected three times for each sample using the technique proposed in section 3.4.1. The standard deviation were calculated were lower than 5%. In addition, several experiments were selected and re-tested; the results confirmed that the experimental works were repeatable. The standard deviation was calculated as in equation 3.8 and 3.9.

$$S^2 = \left(\frac{\Sigma(x-\mu)^2}{n-1}\right) \tag{3.8}$$

$$S = \sqrt{\left(\frac{\Sigma(x-\mu)^2}{n-1}\right)} \tag{3.9}$$

Where:

S^2 = Sample variance

S = standard deviation

Σ = summation or total

x = sample

μ = mean value of the population

n = number of values in sample - 1

4 EFFECT OF CATALYST PREPARATION METHODS

This chapter results the catalytic performance of ZnO and La_2O_3-C in the carboxylation of glycerol under the same reaction conditions. ZnO/$La_2O_2CO_3$, and $La_2O_2CO_3$ prepared in-house were also tested. ZnO has the ability to activate glycerol and hence was employed as supporting catalyst. $La_2O_2CO_3$ catalysts prepared via co-precipitation, sol-gel and hydrothermal methods were successful in yielding a high selectivity to glycerol carbonate. This reaction was thermodynamically limited and the presence of a dehydrating agent was crucial in order to improve the glycerol conversion by shifting the reaction equilibrium into the product site. Therefore, adiponitrile was employed in order to overcome this limitation.

4.1 Preparation of solid catalysts

All catalysts employed within this work have been prepared using a standard preparation method described in section 3.2. The initial work focused on the use of commercial La_2O_3 (La_2O_3-C) purchased from Sigma Aldrich. Later, modified ZnO/$La_2O_2CO_3$ prepared *via* impregnation and co-precipitation methods were introduced. High yield and selectivity to GlyC synthesised upon the introduction of La_2O_3-C has informed catalyst modification. The performance of $La_2O_2CO_3$ based catalysts prepared *via* co-precipitation, sol-gel and hydrothermal methods was investigated (J. Liu *et al.*, 2016). In general, base catalysts have high activity and selectivity and do not exhibit corrosion problem. High temperature (> 400 ℃) is required to decompose the carbonates deposited on the catalyst surface (Hutchings and Vedrine, 2004). Base catalysts are easily absorb CO_2 from ambient air.

4.2 Solid catalyst characterisation

Solid catalysts were characterised using a range of characterisation techniques including SEM, BET, TPD-CO_2, XRD and ATR-FTIR.

4.2.1 **SEM**

Figure 4.1 shows the SEM micrograph of the lanthanum-based catalysts. The catalyst preparation methods employed have a significant impact on the catalyst morphology. Each catalyst shows an irregular shape and particle size. $La_2O_2CO_3$-CP and $La_2O_2CO_3$-HT catalysts have large particle size, ~ 5 μm and ~ 6 μm in comparison with $La_2O_2CO_3$-SG (~ 3 μm) and La_2O_3-C (~ 1 μm) (Table 4.1) as determined using ImageJ software. In general, small particle size of catalysts have high surface area. It is expected that catalysts with high surface area have better catalytic performance; presumably due its high number of catalytic active sites.

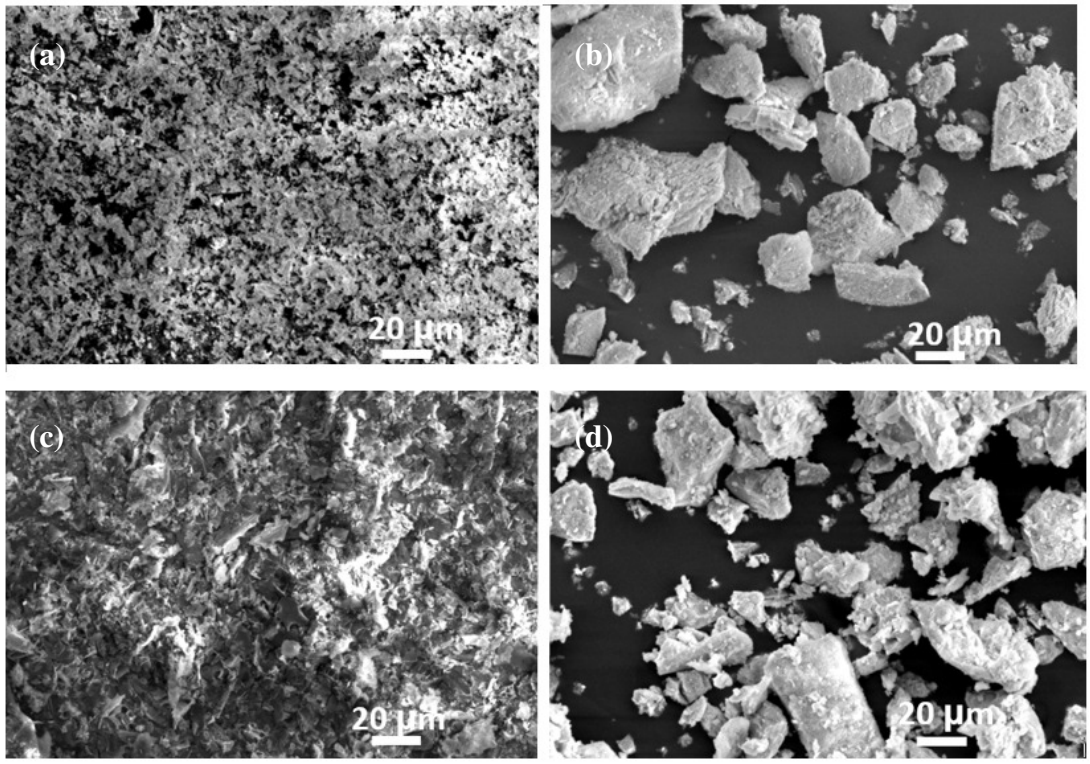

Figure 4.1. The SEM micrograph of (a) La_2O_3-C, (b) $La_2O_2CO_3$-CP, (c) $La_2O_2CO_3$-SG and (d) $La_2O_2CO_3$-HT Magnification is 600x and acceleration voltage is 12 to 20 kV.

Table 4.1. Particle size of the catalysts.

Catalyst	Particle size (μm)
La_2O_3-C	1
$La_2O_2CO_3$-CP	5
$La_2O_2CO_3$-HT	6
$La_2O_2CO_3$-SG	1

4.2.2 **XRD (powder)**

XRD has been employed in order to confirm the crystalline phase of La_2O_3-C, $La_2O_2CO_3$-CP, $La_2O_2CO_3$-HT and $La_2O_2CO_3$-SG as shown in Figure 4.2. It was demonstrated that most of the crystalline fraction of La_2O_3-C is in a hexagonal crystal phase (JCPDS 73-2141) (Abboudi *et al.*, 2011; Zhou *et al.*, 2015); characterised by 2θ peaks at 27.5°, 28.1°, 29.3°, 30.1°, 39.6°, 46.2° 48.9° and 52°. The presence of $La(OH)_3$ was inferred from the peak at 15.9° (Wang *et al.*, 2006; Zhang and He, 2014a). La_2O_3-C is highly sensitive to atmospheric water (Mu and Wang, 2011; Pons *et al.*, 2014), resulting in the formation of $La(OH)_3$ (Mu and Wang, 2011). The monoclinic $La_2O_2CO_3$ (JCPDS 48-1113) was characterised by peaks at 22.5°, 25.4°, 27.0° and 30.4° for the $La_2O_2CO_3$-CP sample while hexagonal $La_2O_2CO_3$ (JCPDS 37-0804) was observed by peaks at 15.7°, 21.4°, 25.8° and 29.4°. Only a few diffraction peaks ascribed to hexagonal $La_2O_2CO_3$ and monoclinic $La_2O_2CO_3$ were found in the $La_2O_2CO_3$-SG catalyst, indicating that $La_2O_2CO_3$-SG may exist in an amorphous state. $La_2O_2CO_3$ catalysts prepared from co-precipitation, hydrothermal and sol-gel methods were calcined at 400 ℃ with no peak detected at 15.9° ($La(OH)_3$) supporting the evidence that dehydration of water was took place at 370 ℃ (Pons *et al.*, 2014); therefore water has been removed from the surface of the catalyst.

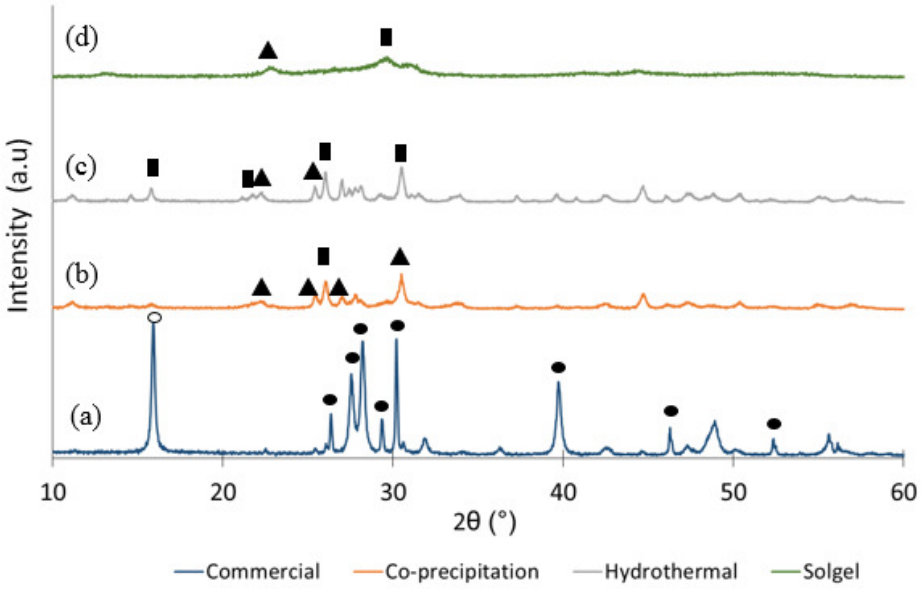

Figure 4.2. XRD patterns of the catalysts prepared from several preparation methods; (a) La_2O_3-C, (b) $La_2O_2CO_3$-CP, (c) $La_2O_2CO_3$-HT and (d) $La_2O_2CO_3$-SG where; (°) $La(OH)_3$, (●) hexagonal La_2O_3, (▲) hexagonal $La_2O_2CO_3$ and (■) monoclinic $La_2O_2CO_3$.

The crystallite size of La_2O_3-C (uncalcined) and $La_2O_2CO_3$ (calcined at 400 ℃) were calculated using Scherrer's equation (Table 4.2). La_2O_3-C has the largest crystallite size, 37 nm, while $La_2O_2CO_3$-HT and $La_2O_2CO_3$-CP have the crystallite sizes of 27 and 31 nm respectively (Table 4.2). $La_2O_2CO_3$ prepared from sol-gel method is in the amorphous state. Liu *et al.* reported that the catalyst prepared from the co-precipitation method yields a higher crystallite size than the catalyst prepared from hydrothermal and sol-gel methods (J. Liu *et al.*, 2016). In general, a decrease in La crystallite size is considered to promote catalytic activity due to an increase in active surface area (Tada and Kikuchi, 2014). Notably, catalyst preparation method has a big impact on the structural properties.

Table 4.2. The crystalline size and surface area of catalysts were determined by XRD using Scherrer equation.

Catalyst	2θ position (degrees)	D_p, crystallite size (nm)	Surface area (m^2/g)
La_2O_3-C	28.2	37	17
$La_2O_2CO_3$-CP	30.5	31	36
$La_2O_2CO_3$-HT	30.5	27	41

4.2.3 **BET**

Table 4.3 summarises the measured BET surface area of ZnO and lanthanum-based catalysts. BET measurements of ZnO yield a surface area of 11 m^2/g; while 9:1 ZnO/$La_2O_2CO_3$-CP and 7.5:2.5 ZnO/$La_2O_2CO_3$-CP have surface area of 47 and 17 m^2/g. In contrast, only 12 m^2/g was calculated for 9:1 ZnO/$La_2O_2CO_3$-I which is similar to that for the unmodified ZnO. However, the composition of all 7.5:2.5 ZnO/$La_2O_2CO_3$-CP, 9:1 ZnO/$La_2O_2CO_3$-CP and 9:1 ZnO/$La_2O_2CO_3$-I catalysts were based on theoretical calculation. ICP-MS analysis must be carried out in order to determine the actual metal oxide composition. A possible explanation for this is the salt precursor may be lost during catalyst washing or/and also poor distribution of metal (Lok, 2009).

The $La_2O_2CO_3$-based catalysts prepared in-house show a large BET surface area: 60, 194 and 28 m^2/g for $La_2O_2CO_3$-CP, $La_2O_2CO_3$-SG and $La_2O_2CO_3$-HT respectively in comparison to La_2O_3-C (14 m^2/g). The high surface area of $La_2O_2CO_3$-CP is hypothesised to enhance the catalytic performances per mass basis through the increasing the area available for adsorption, reaction and enhancing the internal mass transfer. The range of average pore diameter of those catalysts are between 2 nm to 14 nm, while, the molecular diameter of CO_2, glycerol and GlyC are 0.33 nm, 0.52 nm and 0.65 nm (Saiyong *et al.*, 2012; Yang *et al.*, 2012). Therefore, the mass transfer of the reactant within the catalyst pores is expected to be relatively facile, as the

molecular diameter of reactants and product are smaller than the pore diameter of pore of those catalyst. It therefore more likely that mass transfer between the gas-phase (CO_2) and the catalyst surface in the liquid (glycerol) phase is likely to be the dominant transport effect. In all cases, catalyst preparation methods are most likely to affect the catalyst surface areas.

Table 4.3. BET surface area, pore volume and average pore diameter for solid catalysts.

Catalysts	BET surface area (m^2g^{-1})	Pore volume (cm^3g^{-1})[a]	Average pore diameter (nm)
ZnO	11	0.01	3
La_2O_3-C	14	0.02	3
$La_2O_2CO_3$-CP	60	0.34	14
$La_2O_2CO_3$-SG	194	0.15	2
$La_2O_2CO_3$-HT	28	0.09	9
9:1 ZnO/$La_2O_2CO_3$-CP	47	0.07	4
7.5:2.5 ZnO/$La_2O_2CO_3$-CP	17	0.03	4
9:1 ZnO/$La_2O_2CO_3$-I	12	0.01	3
ZnO/SnO_2	63	0.05	2

[a]Measured from the desorption branch according to the BJH method.

4.2.4 **ATR-FTIR**

Surface functionalities of catalysts were analysed using ATR-FTIR (Figure 4.3). La_2O_3-C shows a peak at 3607 cm^{-1} indicating the presence of bulk –OH functionalities. It shows that the La_2O_3-C phase, upon exposure to the atmosphere, has

been transformed into $La(OH)_3$. No peak was detected at 3607 cm^{-1} for the re-calcined La_2O_3-C; this indicates that the chemisorp water adsorbed on the surface of La_2O_3-C has been removed. Peaks at 1508 and 1460 cm^{-1} show that CO_2 and H_2O have reacted on $La_2O_2CO_3$ surface forming the chemisorbed carbonate and bicarbonates (Gangwar et al., 2014). The peaks at 1382 and 844 cm^{-1} were due to the carbonate groups, as per La_2O_3-C, but with greater intensity.

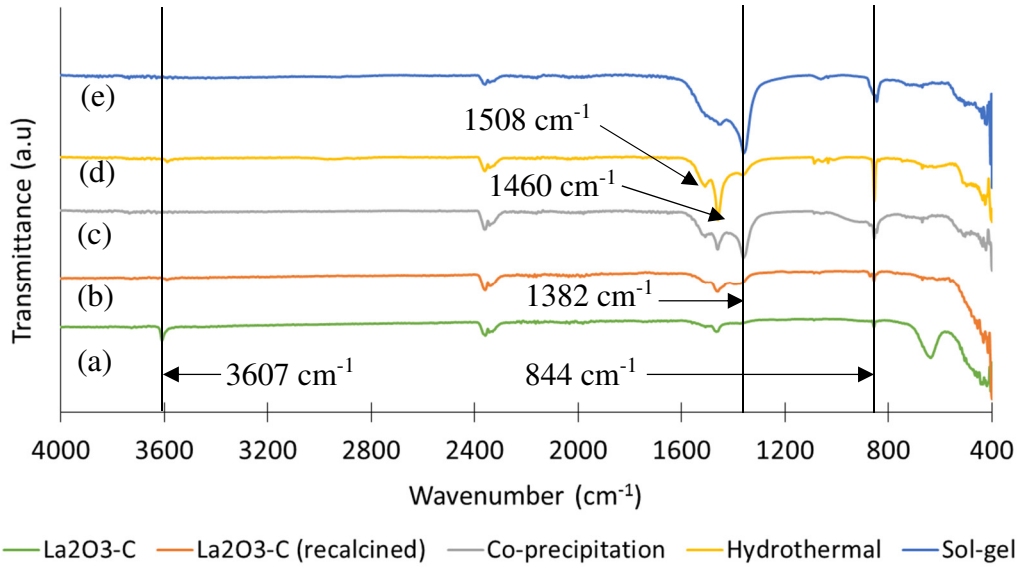

Figure 4.3. ATR-FTIR spectrum of (a) La_2O_3-C (uncalcined), (b) calcined La_2O_3-C, (c) $La_2O_2CO_3$-CP, (d) $La_2O_2CO_3$-HT and $La_2O_2CO_3$-SG.

4.2.5 **TPD-CO_2**

TPD-CO_2 analysis has been employed in order to study the basicity of the catalysts. Hou and co-workers demonstrated that La_2O_3 catalyst has more basic sites than $La_2O_2CO_3$ (Hou *et al.*, 2015). However, in this case, La_2O_3-C presents the lowest concentration of basic sites (0.8 µmol of $CO_2/g_{catalyst}$) as compared with $La_2O_2CO_3$-based catalysts (> 0.9 µmol of $CO_2/g_{catalyst}$). The total number of basic sites was calculated and is summarised in Table 4.4. The total basicity of these catalysts was affected by catalyst preparation methods and the total number of basic sites decreases in the order $La_2O_2CO_3$-HT > $La_2O_2CO_3$-CP > $La_2O_2CO_3$-SG and La_2O_3-C. ZnO has no basic sites.

$La_2O_2CO_3$ is decomposed to La_2O_3 at high temperature (> 720 °C) (Shirsat *et al.*, 2003; Pons *et al.*, 2014) as shown in equation 4.1. TPD analysis has been carried out in the presence of CO_2 from 30 to 900 °C. Therefore, it is expected that the CO_2 measured on the TCD detector was the CO_2 desorbed into the catalyst pores and also the CO_2 produced from the decomposition of $La_2O_2CO_3$. Further investigation was crucial to confirm whether the decomposition of $La_2O_2CO_3$ to La_2O_3 had occurred or not. A test was therefore carried out in the present of inert gas, He. It is calculated that 39% of CO_2 detected from the TPD-CO_2 was formed from decomposition reaction. The data was summarised in Table 4.4.

$$La_2O_2CO_3 \rightleftharpoons La_2O_3 + CO_2 \quad (4.1)$$

Table 4.4. The concentration of basicities for the series of ZnO, La_2O_3-C and $La_2O_2CO_3$ catalysts prepared *via* sol-gel, hydrothermal and co-precipitation methods.

Catalysts	Total basicity (mmol of $CO_2/g_{catalyst}$)	[a]Total basicity (mmol of $CO_2/g_{catalyst}$)
ZnO	0	0
La_2O_3-C	0.8	0.8
$La_2O_2CO_3$-CP	1.5	0.9
$La_2O_2CO_3$-HT	1.6	1.0
$La_2O_2CO_3$-SG	1.4	0.8

[a]TPD analysis has been carried out in the presence of inert gas, He. It was calculated that 39% of CO_2 detected from the TPD-CO_2 was formed from decomposition of $La_2O_3CO_3$ to La_2O_3 and CO_2.

4.3 Catalyst screening

4.3.1 Influence of heterogeneous catalysts

The literature review in Chapter 2 describe the positive impacts upon the introduction of heterogeneous catalysts to catalyse the carboxylation reaction. The direct carboxylation of glycerol would not be successful without the introduction of a dehydrating agent (Vieville *et al.*, 1998). No GlyC was formed in the absence of acetonitrile (Li *et al.*, 2013; Zhang and He, 2014a). This work was also focused on the influence of heterogeneous catalysts in the presence of adiponitrile to synthesise GlyC from glycerol and CO_2. Based on the literature review, base catalysts favour the formation of GlyC while the acidic catalysts favour the formation of by-products. Li *et al.* and Zhang *et al.* studied the impact of alkaline earth metal such as MgO and CaO (Li *et al.*, 2013; Zhang and He, 2014b); however, only < 1% glycerol conversion was observed. In contrast to alkaline earth metal, lanthanoid catalysts including La_2O_3 and CeO_2 were shown high selectivity and yield to GlyC (Zhang and He, 2014a; J. Liu *et al.*, 2016; Su *et al.*, 2017).

In this work, the catalytic performance of ZnO, La_2O_3-C, ZnO/$La_2O_2CO_3$ and ZnO/SnO_2 were tested under the same reaction conditions and testing procedure described in section 3.3.1 and 3.3.2. Glycerol conversion was the highest upon the introduction of ZnO, 64%; however, it exhibited a low selectivity to GlyC (7%) (Table 4.5). 12% of GlyC yield was observed upon the introduction of ZnO (Li *et al.*, 2013) and the reaction conditions were as follows: 5 wt.% La_2O_3, relative to glycerol, glycerol to acetonitrile of 50:190 mmol, 170 °C, 12 hours and initial reaction pressure was 40 bar. 10 wt.% of $La_2O_2CO_3$ supported on ZnO was also employed. Introduction of $La_2O_2CO_3$ helped to increase the number of Lewis basic sites; and thus increased the chances for CO_2 adsorption and activation (Li *et al.*, 2013). A 9:1 ZnO/$La_2O_2CO_3$ catalyst was prepared *via* co-precipitation and impregnation methods. A comparison of these two catalysts showed 26% of glycerol conversion but no GlyC upon the introduction of ZnO/$La_2O_2CO_3$-I; while the selectivity to GlyC was 11% employing ZnO/$La_2O_2CO_3$-CP. In general, ZnO/$La_2O_2CO_3$-I has no impact on the carboxylation of glycerol; with the result obtained almost identical to the blank reaction. The specific surface area of the 9:1 ZnO/$La_2O_2CO_3$-CP (47 m^2/g) was larger than the ZnO

(11 m^2/g), suggesting that the introduction of $La_2O_2CO_3$-CP (60 m^2/g) was beneficial to the increase of the surface area.

Table 4.5. Glycerol conversion and GlyC selectivity and yield formed from the carboxylation of glycerol over heterogeneous catalysts. Reaction conditions: reaction pressure = 40 bar, 6 wt.% catalyst to glycerol ratio, 22.5 mmol glycerol, 45 mmol adiponitrile, 18 h and reaction temperature = 160 ℃.

Catalyst	Glycerol conversion	GlyC selectivity	GlyC yield
Blank	26	0	0
La_2O_3-C	52	15	8
ZnO	64	7	5
ZnO/$La_2O_2CO_3$-CP (90:10)	53	11	6
ZnO/$La_2O_2CO_3$-CP (75:25)	54	8	4
ZnO/$La_2O_2CO_3$-I (90:10)	25	0	0
ZnO/SnO_2 (90:10)	52	12	5

The observed increase in the selectivity to GlyC upon increasing the surface area of catalyst could be attributed to the increased number of the active catalytic sites. BET measurement of ZnO/$La_2O_2CO_3$-I showed a surface area of 12 m^2/g. In this case, the surface area, pore volume and average pore diameter of ZnO/$La_2O_2CO_3$-I were similar to the ZnO catalyst. It is expected only a small amount of $La_2O_2CO_3$ has been impregnated onto the ZnO. This indicates that the co-precipitation method remarkably improves the dispersion of the active components. The composition of prepared

catalysts were based on theoretical calculations. Further investigation using ICP-MS is required to study the composition of this catalyst.

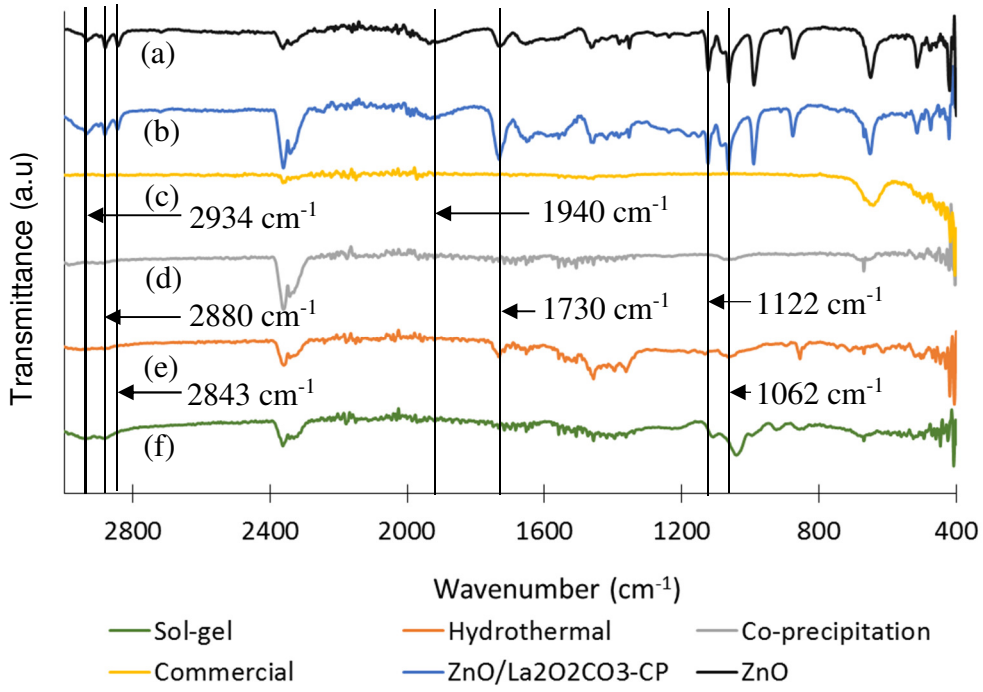

Figure 4.4. ATR - FTIR spectra of spent catalysts where (a) ZnO, (b) ZnO/$La_2O_2CO_3$-CP, (c) La_2O_3-C, (d) $La_2O_2CO_3$-CP, (e) $La_2O_2CO_3$-HT and (f) $La_2O_2CO_3$-SG.

Used catalysts were washed with acetone, filtered and dried for 8 hours at 100 ℃. The FTIR spectra were analysed in order to gain a better understanding of the processes involved in this reaction (Figure 4.4). Peaks identified at 1122 and 1062 cm^{-1} describe the C-O stretching of the glycerol while C-H bonds detected at 2934 and 2880 cm^{-1} indicate the presence of retained hydrocarbonaceous species (Li *et al.*, 2013). The peak at 1940 cm^{-1} was only detected from zinc-based catalysts and indicates the presence of OH···O bending. In this case, zinc glycerolate ($Zn(C_3H_6O_3)$) was formed and no lanthanum glycerolate was detected from this reaction. This finding supports the evidence that ZnO strongly activates glycerol (Li *et al.*, 2013). This conclusion was confirmed through a comparison of the glycerol conversion upon the introduction of ZnO, 64% and La_2O_3-C, 52%.

High selectivity to GlyC (11%) was observed upon the introduction of 9:1 ZnO/$La_2O_2CO_3$-CP. Changing the composition of $La_2O_2CO_3$ from 10 to 25% reduced the selectivity to GlyC from 11 to 8%. Addition of 25 wt.% of $La_2O_2CO_3$ significantly affected the surface area of this catalyst decreasing the value from 47 to 17 m^2/g. Addition of 25 wt.% of $La_2O_2CO_3$ is expected to increase the specific surface area of a catalyst. However, increasing of percentage La resulted in decreased surface area. A possible explanation for this might due to the accumulation of La at the pore (Dewajani *et al.*, 2016) or/and the salt precursor may be lost during catalyst washing.

The reaction was then conducted by employing La_2O_3-C. Zhang and co-worker reported that only 1% of glycerol conversion with 6% selectivity of GlyC was achieved over La_2O_3 catalyst (Zhang and He, 2014a). La_2O_3-C and ZnO have similar values for surface area, pore volume and pore diameter. Comparing the two results, it can be seen that La_2O_3-C has a higher selectivity to GlyC (15%) as compared to ZnO (7%). It is interesting to note that La_2O_3-C has a high number of basic sites (0.8 μmol of $CO_2/g_{catalyst}$) (Table 4.4). Taken together, these results provide an insight into the importance of the number of basic sites to synthesise GlyC. Considering the lewis acidic nature of CO_2, it is expected that the carboxylation process will take place on the basic sites of La_2O_3-C (Fujita, Arai and Bhanage, 2014). ZnO/SnO_2 has a large surface area (63 m^2/g) and was also tested due to its ability to synthesise GlyC from glycerol and urea (Jagadeeswaraiah et al., 2014; Manjunathan et al., 2016). However, only 12% selectivity to GlyC was observed from this reaction. A set of catalysts with a range of surface areas from 13 to 63 m^2/g and pore volumes, 0.01 to 0.07 cm^3/g, have been employed. It was concluded that the glycerol conversion and GlyC formation do not simply correlate with the surface area and pore volume of the catalyst. High yield and selectivity to GlyC achieved by La_2O_3-C, has led it to being manipulated by modifying the catalyst preparation methods. The next section discusses the impact of the basicity and average pore diameter of La_2O_3 and $La_2O_2CO_3$ catalysts on the GlyC and by-products formation.

4.4 Influence of lanthanum-based catalysts and its preparation method on the carboxylation of glycerol

This section focuses on the catalyst preparation methods which directly affect the morphology and number of basic sites of those catalysts; thus affecting its catalytic performance. TPD-CO_2 measurements yield a higher number of basic sites for $La_2O_2CO_3$-CP, 0.9 mmol/$g_{catalyst}$ than the La_2O_3-C (0.8 mmol/$g_{catalyst}$). Therefore, $La_2O_2CO_3$-CP is expected to have better catalytic performance to synthesise GlyC. The selectivities to GlyC of La_2O_3-C and $La_2O_2CO_3$-CP were 17 and 18% respectively (Table 4.6). These findings supported the hypothesis that the basic catalysts favour the formation of GlyC (Zhang and He, 2014a).

Table 4.6. Catalytic performance of $La_2O_2CO_3$ prepared by several methods. Reaction conditions: reaction pressure = 45 bar, 6 wt.% catalyst to glycerol ratio, 22.5 mmol glycerol, 45 mmol adiponitrile, 18 h and reaction temperature = 160 °C.

$La_2O_2CO_3$ (Precipitation method)	Glycerol conversion	GlyC selectivity	GlyC yield
Blank	26	0	0
La_2O_3-C	58	17	10
$La_2O_2CO_3$-CP	57	18	10
$La_2O_2CO_3$ -SG	46	3	1
$La_2O_2CO_3$ -HT	51	11	6

Interestingly, Table 4.7 shows that there has been a sharp increase in the number of 4-hydroxymethyl(oxazolidine)-2-one (4HMO) ($C_4H_7NO_3$) and by-products. It is difficult to interpret the result, but it may be related to basic strength distribution and the average pore diameter of the catalyst. The average pore diameter of $La_2O_2CO_3$-CP (14 nm) is bigger than the La_2O_3-C, 3 nm, therefore it improves the chances for the

formation of by-products with large molecular diameter. $La_2O_2CO_3$-CP (14 nm) and $La_2O_2CO_3$-HT (9 nm) have large average pore diameters and yield a high selectivity to GlyC (18 and 11%) and produce a high quantity of 4HMO and by-products (Table 4.7). In contrast, $La_2O_2CO_3$-SG with small average pore diameter (2 nm) yields a low selectivity to GlyC and 4HMO; in fact, no other by-products have been formed from this catalytic system.

Table 4.7. Influence of the catalyst loading on by-product formation. Reaction conditions: reaction pressure = 45 bar, 6 wt.% catalyst to glycerol ratio, 22.5 mmol glycerol, 45 mmol adiponitrile, 18 h and reaction temperature = 160 °C. The by-products detected from the reaction was measured qualitatively, value shown in the table correspond to chromatogram peak area.

Products	La_2O_3-C	$La_2O_3CO_3$-CP	$La_2O_3CO_3$-HT	$La_2O_3CO_3$-SG
[a]Adiponitrile	390	420	396	695
4HMO	2	5	13	2
Unknown 1 (minute 30.8)	2	10	14	N/A
Unknown 2 (minute 31.3)	4	21	9	N/A
Unknown 3 (minute 33.9)	2	8	17	N/A

[a]Adiponitrile left after the reaction, the area under peak was measured qualitatively.

It was concluded that the basic catalysts favour the formation of GlyC. However, catalysts with large average pore diameters may promote the formation of by-products. Further research should concentrate on investigating the average pore diameter and the influence of the number of basic sites and how they affect the formation of GlyC. This will help in developing an active catalyst with high selectivity to GlyC and eliminate the production of by-products.

4.5 **Influence of reaction conditions**

The optimisation of reaction conditions can significantly affect the carboxylation of glycerol; however, the current investigation was limited to: (a) the influence of reaction temperature; (b) the influence of ratio of catalyst to reactant; and (c) the adiponitrile to reactant ratio. This work focused on the efficacy of La_2O_3-C as a catalyst to synthesise GlyC at low pressure, 45 bar due to the limitation of the experiment set-up.

One of the most significant factors that may affect the selectivity to GlyC is reaction temperature. Conversion of glycerol and selectivity to GlyC were seen to steadily increase from 10 to 61% and 0 to 19% with the increase of reaction temperature from 140 to 160 °C. As expected, further temperature increase to 170 ℃ does not improve the selectivity to GlyC because GlyC decomposes at high temperature (H. Li, Jiao, *et al.*, 2015). GlyC is thermally stable up to 160 °C (Huntsman, 2016). Given the observation that the presence of 4HMO at 170 ℃ was five times higher than at 160 ℃; it seems that high reaction temperatures favour the formation of by-products (F. Li *et al.*, 2015). A high quantity of by-products was observed from the carboxylation reaction at 170 ℃ as shown in Table 4.8. It is suggested that the reaction temperature could be the major factor, if not the only one, causing the decomposition of GlyC to by-products (unknown 1 and 3, Table 4.8). In this case, 160 ℃ was chosen as the optimum temperature due to high selectivity to GlyC, 17%.

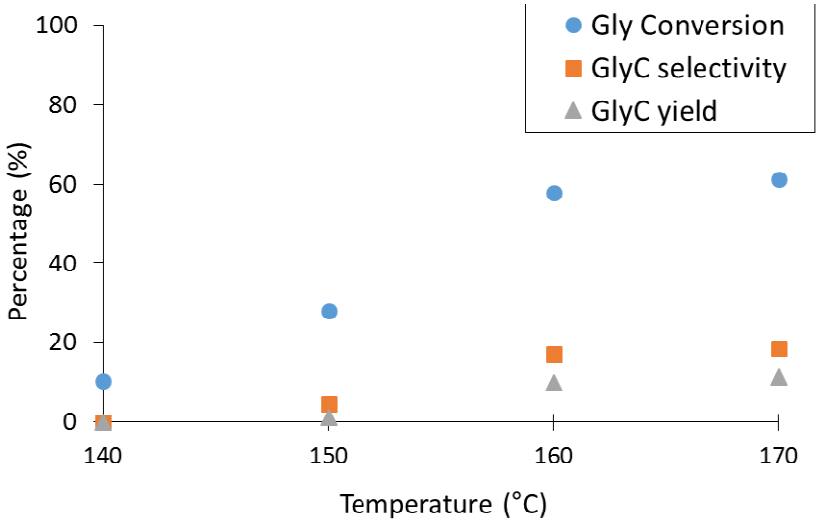

Figure 4.5. Influence of reaction temperature. Reaction conditions: reaction pressure = 45 bar, 6 wt.% La_2O_3-C, 22.5 mmol glycerol, 45 mmol adiponitrile and 18 h.

Table 4.8. By-products formed from the carboxylation of glycerol at different temperatures. Reaction conditions: reaction pressure = 45 bar, 6 wt.% La_2O_3-C to glycerol ratio, 22.5 mmol glycerol, 45 mmol adiponitrile and 18 h. The by-products detected from the reaction was measured qualitatively, value shown in the table correspond to chromatogram peak area.

By-product	140 °C	150 °C	160 °C	170 °C
4HMO	n/a	n/a	2	10
Unknown 1	n/a	n/a	2	19
Unknown 2	n/a	n/a	4	17
Unknown 3	n/a	n/a	2	19

The importance of a catalyst is to increase the rate of reaction and reduce the activation energy; thus enhancing the formation of desired products. However, optimum amount of catalyst must be identified; herein, 0 to 10 wt.% of La_2O_3-C to glycerol ratio was

investigated. As shown in Figure 4.6, glycerol conversion and selectivity to GlyC increase to 58% and 17% in the presence of 6 wt.% of La_2O_3-C to glycerol ratio as compared to 49% and 11% in the presence of 10 wt.% of La_2O_3-C. A glycerol conversion of 26% was observed in the absence of a catalyst but no GlyC was produced. The observed increase in the selectivity to GlyC upon increasing the amount of catalyst could be attributed to the increased number of the active catalytic sites. The amount of catalyst was further increased to 10 wt.% resulting in decreased GlyC selectivity to 11%. There are two likely causes for the reduction in selectivity to GlyC: (1) high number of active catalytic sites enhance the decomposition reaction of GlyC to by-products (Figure 4.7) and (2) another problem arises from the high amount of catalyst loading (above the optimum condition) was enhancing the mass transfer problem from the bulk to the catalyst active sites possibly exacerbated by particle agglomeration (Okoye et al., 2017).

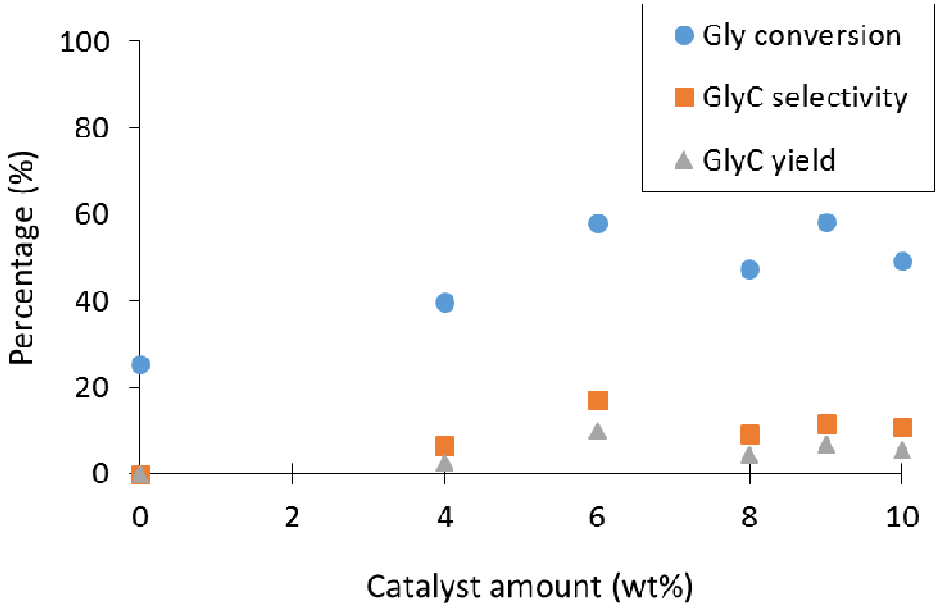

Figure 4.6. Influence of catalyst amount to reactant ratio. Reaction conditions: reaction pressure = 45 bar, catalyst = La_2O_3-C, 22.5 mmol glycerol, 45 mmol adiponitrile, 18 h and reaction temperature = 160 °C.

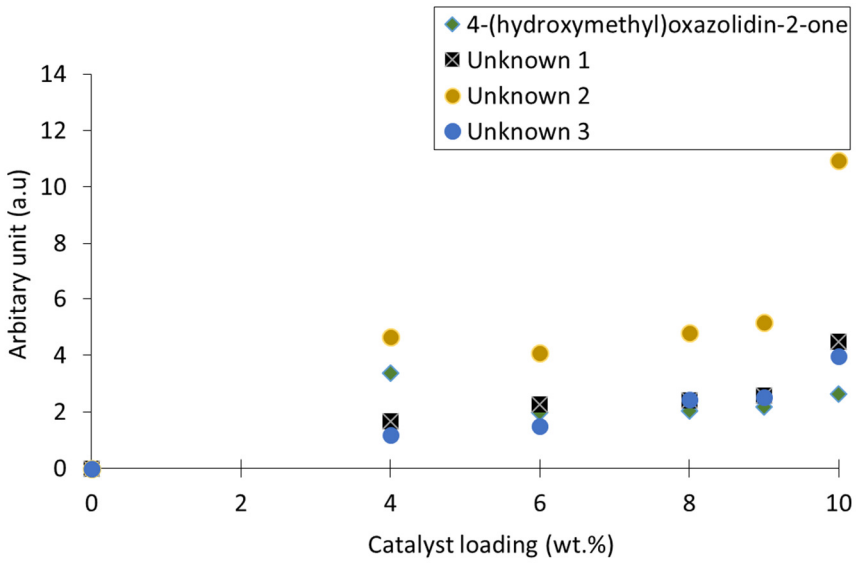

Figure 4.7. The by-products formation during the carboxylation of glycerol in presence of 0 to 10 wt.% La_2O_3-C to glycerol ratio. Reaction conditions: reaction pressure = 45 bar, catalyst = La_2O_3-C, 22.5 mmol glycerol, 45 mmol adiponitrile, 18 h and reaction temperature = 160 °C. The by-products detected from the reaction were measured qualitatively, value shown in the graph correspond to chromatogram peak area.

The initial tests have focused on the reaction temperature and catalyst to reactant ratio. Following this, a study into the influence of dehydrating agent to reactant ratio was undertaken of 6 wt.% of La_2O_3-C at 160 °C (Figure 4.8). Glycerol conversion and selectivity to GlyC were observed to increase from 38 to 58% and 14 to 17% with increasing adiponitrile (22.5 to 50 mmol). Further addition of adiponitrile decreased the GlyC selectivity to 12% (67.5 mmol) and 3% (90 mmol) respectively. A possible explanation was with regards to the mass transfer between the solid catalyst, CO_2, glycerol and adiponitrile. Activation of these species took place at the basic sites of catalysts; therefore a high quantity of adiponitrile lowers the chance for the diffusion and the adsorption of CO_2 to the catalytic sites. In this case, diffusion and activation of adiponitrile was favourable resulting in the decrease in glycerol conversion and selectivity to GlyC.

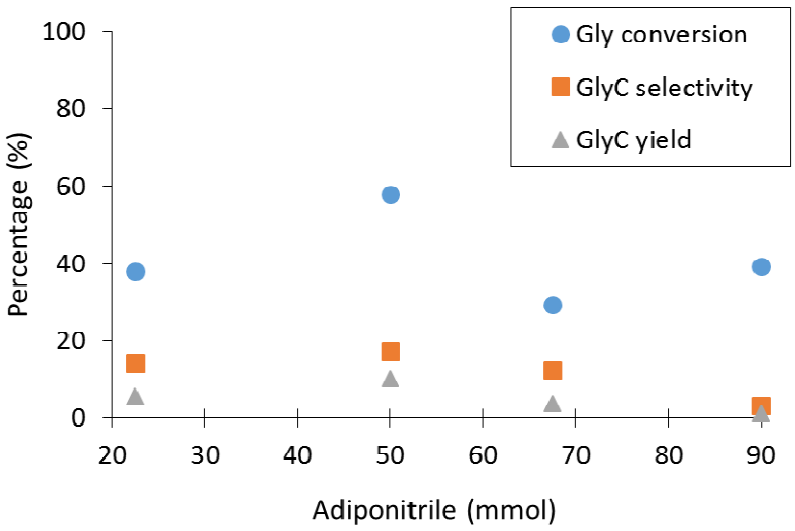

Figure 4.8. Influence of dehydrating agent volume to reactant ratio. Reaction conditions: reaction pressure = 45 bar, 6 wt.% La_2O_3-C to glycerol ratio, 22.5 mmol glycerol, 22.5 to 90 mmol adiponitrile, 18 h and reaction temperature = 160 ℃.

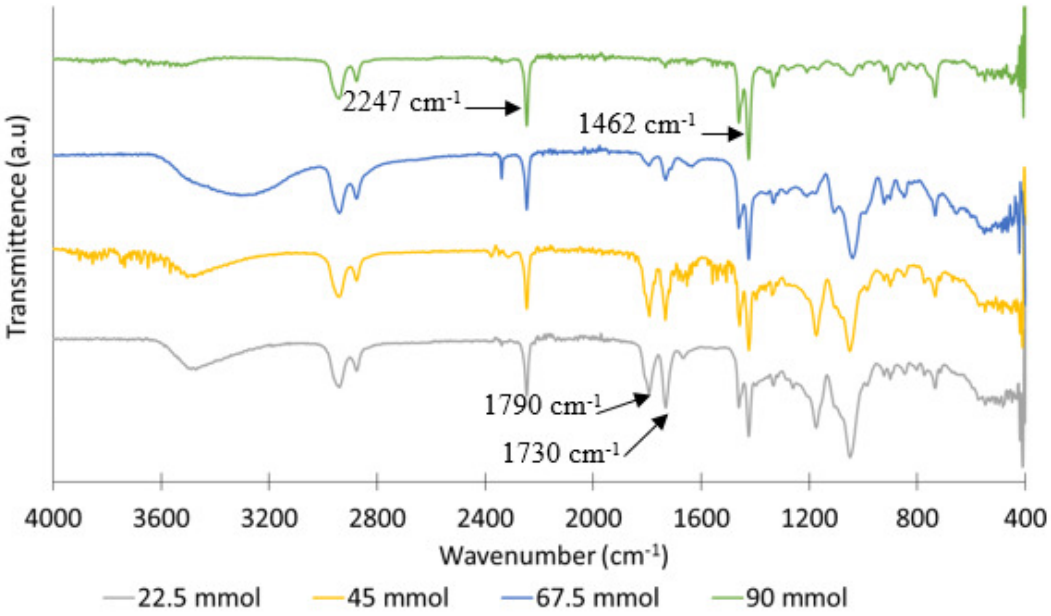

Figure 4.9. The FTIR spectra of glycerol, adiponitrile and reaction products of carboxylation of glycerol with varying amounts of dehydrating agent and all of these samples were collected at 18 h. Reaction conditions: reaction pressure = 45 bar, 6 wt.% La_2O_3-C to glycerol ratio, 22.5 mmol glycerol, 22.5 to 90 mmol, adiponitrile, 18 h and reaction temperature = 160 °C.

Alongside GC-MS, the liquid products produced were characterised by FTIR as shown in Figure 4.9. Liquid samples from the carboxylation of glycerol in the presence of 22.5, 45, 67.5 and 90 mmol of adiponitrile were analysed. The peak appearing at 2247 cm^{-1} indicated the presence of C≡N while that at 1462 cm^{-1} confirmed the presence of-CH_2- bend of adiponitrile. The peaks at 1462 and 2247 cm^{-1} appear strongly in the spectra of 67.5 and 90 mmol, and may indicate a high quantity of unreacted adiponitrile. Notably, low intensity of peaks at 1730 and 1790 cm^{-1} were observed from those spectra which suggested that a high quantity of adiponitrile lowered the chances for CO_2 activation and thus inhibited the formation of GlyC and 4HMO. The study presented in this section provides an understanding that the optimisation of the amount of dehydrating agent to reactant ratio is crucial to maximise the GlyC synthesis, limit the formation of by-products and reduce waste formed from the unreacted adiponitrile.

4.6 **Chapter conclusion**

Experimental work reported within this chapter has shown the efficacy of heterogeneous catalysts to synthesise GlyC *via* the direct carboxylation of glycerol. The carboxylation reaction shows a significantly increased selectivity to GlyC (17.1%) upon the introduction of La_2O_3-C as compared to the blank reaction (0%). In order to understand the influence of catalyst preparation methods and the impact on the products formation, lanthanum-based catalysts prepared *via* sol-gel, hydrothermal and co-precipitation methods have been employed. Small surface areas of La_2O_3-C, 14 m^2/g and large surface areas of $La_2O_2CO_3$-HT, $La_2O_2CO_3$-CP and $La_2O_2CO_3$-SG, > 28 m^2/g, were observed. High selectivity to GlyC was observed upon the introduction of $La_2O_2CO_3$-CP (18%) while only 3% selectivity to GlyC was observed in $La_2O_2CO_3$-SG (194 m^2/g). These findings suggest that the selectivity to GlyC does not simply correlate with the surface area of the catalyst. However, average pore diameter plays an important role in by-product formation. A large amount of 4HMO was formed by the $La_2O_2CO_3$-HT and $La_2O_2CO_3$-CP catalytic systems; where those catalysts have large pore diameters in comparison to $La_2O_2CO_3$-SG and La_2O_3-C. One of the significant findings to emerge from this study is the influence of the number of basic sites on products formation. TPD-CO_2 measurements of La_2O_3-C and $La_2O_2CO_3$

based catalysts yield a basicity of 0.8 to 1 mmol/$g_{catalyst}$, The case revealed that the basic catalysts favour the formation of GlyC and supported the findings of previous work (Zhang and He, 2014b). The experimental work demonstrated the highest GlyC yield was 18%, obtained at glycerol: dehydrating agent ratio of 22.5:45 in the presence of adiponitrile, 6 wt.% of $La_2O_2CO_3$-CP and the reaction was carried out at 160 °C, 18 hours and 45 bar of CO_2 (reaction pressure).

5 EFFECT OF DEHYDRATING AGENTS

This chapter results the catalytic performance of La_2O_3-C in the carboxylation of glycerol over a range of dehydrating agents. This reaction was thermodynamically limited and the presence of a dehydrating agent was crucial in order to improve the glycerol conversion by shifting the reaction equilibrium into the product site. The performance of both acidic and nitrile based dehydrating agents was tested. The selectivity to glycerol carbonate increased upon the introduction of adiponitrile (dicyanated dehydrating agent).

5.1 Catalyst and catalyst characterisation technique

In this section, only commercial La_2O_3 (La_2O_3-C) was investigated. The characterisation of this catalyst has been discussed in section 4.2.

5.2 Influence of acidity and basicity of media (dehydrating agent) on product formation

Chapter 4 (section 4.3 and 4.4) reported on the synthesis of GlyC over La_2O_3-C and $La_2O_2CO_3$ catalysts. What is not clear from these studies is the impact of dehydrating agents on the carboxylation of glycerol and on product formation. Herein, it is shown for the first time that the dehydrating agents employed can significantly affected the production of GlyC, 4HMO and acetin. Only 2% of glycerol conversion was observed in the absence both catalyst and dehydrating agent as shown in (Table 5.1). The glycerol conversion was increased to 26% (to solketal) upon the introduction of adiponitrile. This finding shows the importance of dehydrating agents for the carboxylation of GlyC. As previously stated in the literature review (Chapter 2), this reaction suffers from a thermodynamic limitation, therefore, the dehydrating agents employed play an important role as a water trap, thus shifting the reaction equilibrium to the product side (Li *et al.*, 2013; Zhang and He, 2014a). A series of experiments with nitrile based and acidic based dehydrating agents in the presence of La_2O_3-C were conducted; the results is summarised Table 5.1.

Table 5.1. Summary of product formation from the carboxylation of glycerol over a range of dehydrating agents. Reaction conditions: reaction pressure = 45 bar, 6 wt.% La_2O_3-C to glycerol ratio, 22.5 mmol glycerol, 45 mmol dehydrating agent, 18 h and reaction temperature = 160 ℃.

Dehydrating agent	Properties	Glycerol conversion (%)	Selectivity to products (%)			
			GlyC	Monoacetin	Diacetin	Triacetin
[a]Blank	-	2	0	0	0	0
Blank	-	26	0	0	0	0
Acetic anhydride	Acidic	91	0	17	60	24
[b]Acetic anhydride	Acidic	99	0	8	49	45
Acetonitrile	Base (Monocyanated)	48	4	12	3	0
Benzonitrile	Base (Monocyanated)	71	5	0	0	0
Adiponitrile	Base (Dicyanated)	58	17	0	0	0

[a]Reaction was carried out in the absence of catalyst.

[b]Reaction was carried out in absence of CO_2.

The use of monocyanated and dicyanated dehydrating agents show a significant impact on selectivity to GlyC. Using acetonitrile as the dehydrating agent, a selectivity of 4% is achieved, increasing to 5% in the presence of benzonitrile and 17% with adiponitrile. These were achieved at conversion of 48%, 71% and 58% respectively. No GlyC was formed when acetic anhydride was employed as the dehydrating agent and the glycerol conversion was 97%. It was proposed that more GlyC was produced

in the presence of adiponitrile because dicyanated dehydrating agents have better performance as the water trap as compared to monocyanated dehydrating agents (Silva *et al.*, 2012).

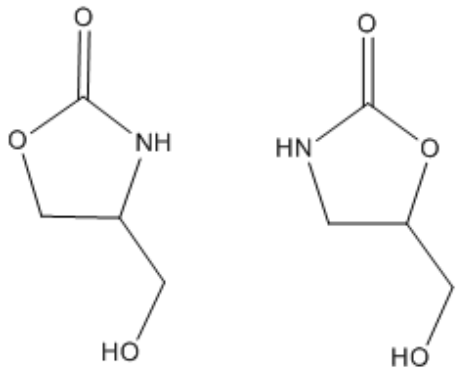

Figure 5.1. The isomers of 4-(hydroxymethyl)oxazolidin-2-one (4HMO).

The introduction of dehydrating agents will affect the formation of GlyC and by-products. The use of nitrile based dehydrating agents enhanced the formation of GlyC along with the formation of 4HMO (Figure 5.1). Alongside GC-MS, the liquid products produced have been characterised by FTIR. Peaks at 1730 and 1790 cm^{-1} were indicative of the presence of C=O for a five cyclic membered ring, with the peak at 1790 cm^{-1} confirming the formation of GlyC and that at 1730 cm^{-1} indicating the formation of 4HMO (Figure 5.2) (Indran *et al.*, 2014).

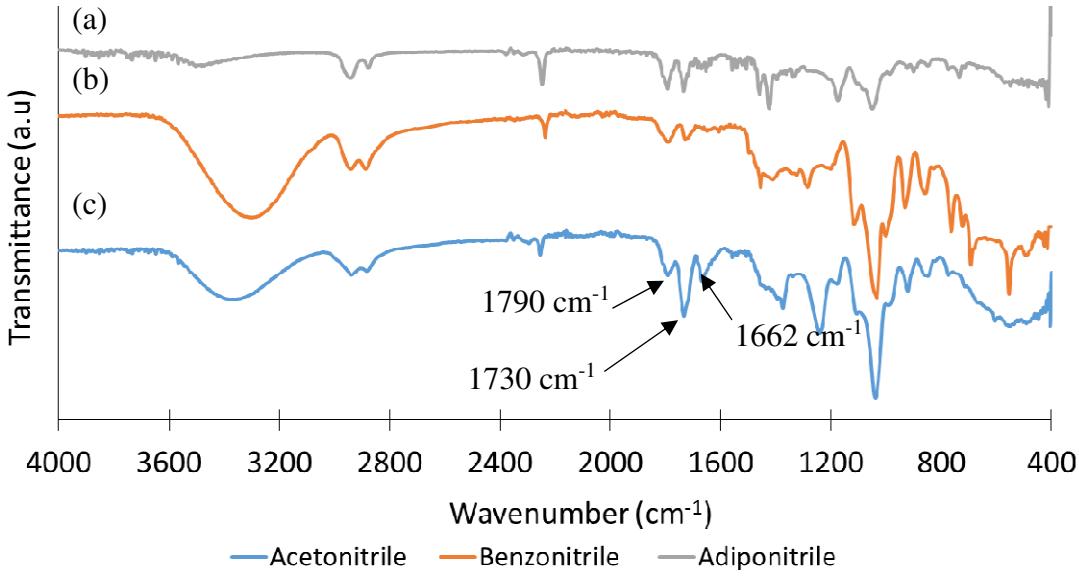

Figure 5.2. FTIR spectra of liquid reaction mixture sample using (a) acetonitrile, (b) benzonitrile and (c) adiponitrile as dehydrating agents. Reaction conditions: reaction pressure = 45 bar, 6 wt.% La_2O_3-C to glycerol ratio, 22.5 mmol glycerol, 45 mmol dehydrating agent 18 h and reaction temperature = 160 °C.

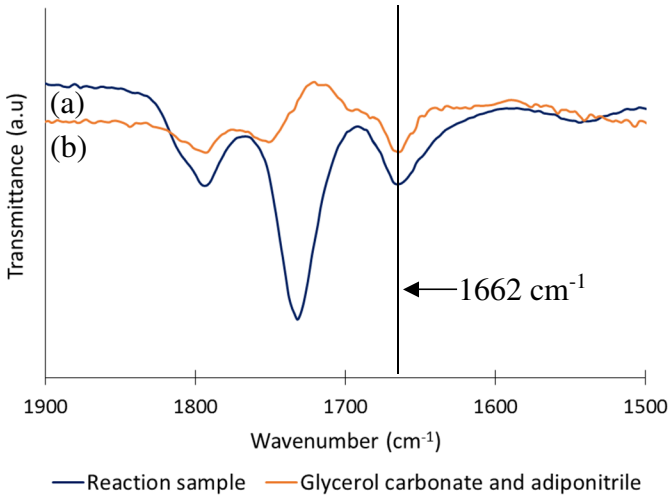

Figure 5.3. FTIR spectra of the liquid products arising from (a) the direct carboxylation of pure glycerol with CO_2 in the presence of adiponitrile and (b) the reaction of glycerol carbonate and adiponitrile in present of CO_2. Reaction conditions: reaction pressure = 45 bar, 6 wt.% La_2O_3-C to glycerol ratio, 22.5 mmol glycerol, 45 mmol adiponitrile, 18 h and reaction temperature = 160 °C.

The high intensity of the peak at 1730 cm^{-1} detected when using acetonitrile as the dehydrating agent suggests that this favours the formation of 4HMO. This spectrum also shows a strong band at 1662 cm^{-1}. This is representative of C=O in an amide bond and hence was postulated to indicate the product of a secondary reaction of GlyC and adiponitrile. In order to investigate this, GlyC and adiponitrile were reacted directly in both the presence and absence of CO_2. FTIR analysis of the reaction products, Figure 5.3, clearly shows the presence of a peak at 1662 cm^{-1}, supporting this hypothesis.

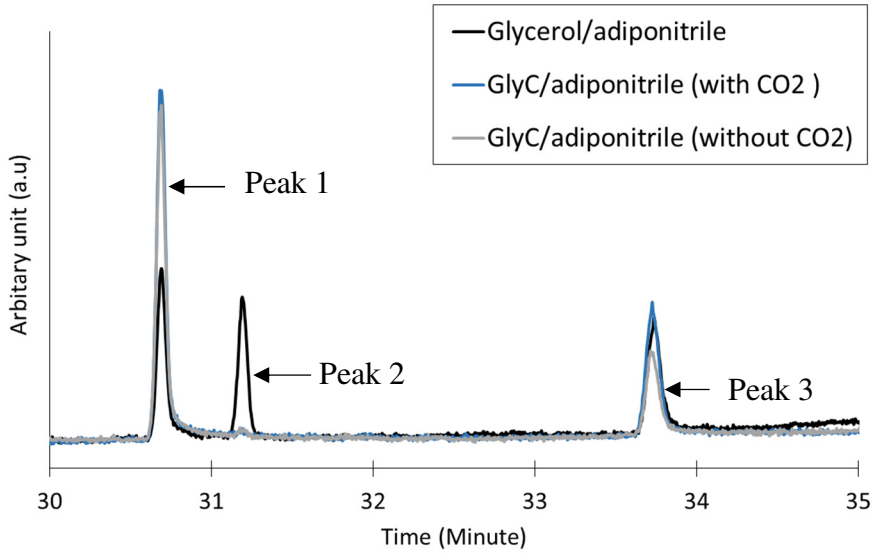

Figure 5.4. The unidentified peak detected from the reaction of (a) glycerol, CO_2 and adiponitrile, (b) glycerol carbonate, CO_2 and adiponitrile and (c) glycerol carbonate and adiponitrile. Reaction conditions: reaction pressure = 45 bar, 6 wt.% La_2O_3-C to glycerol/glycerol carbonate ratio, 22.5 mmol glycerol, 45 mmol adiponitrile, 18 h and reaction temperature = 160 °C.

The liquid products were also analysed using GC-MS; in which the GC-MS chromatogram of glycerol, CO_2 and adiponitrile were compared with the reaction GlyC and adiponitrile and GlyC, adiponitrile and CO_2. The by-products (Unknown 1 and 3) were detected which confirmed the hypothesis that the secondary reaction (reaction of GlyC and adiponitrile) had occurred (Figure 5.4). It is expected that the aminolysis of GlyC had occurred (Nohra *et al.*, 2012; Camara, Caillol and Boutevin,

2014). GlyC itself has a potential to be utilised as a chemical intermediate, for example in polymer production (Sonnati *et al.*, 2013; Camara, Caillol and Boutevin, 2014). The mass spectrometry (ion fragment) of peaks detected at 30.3 and 33.4 minutes were analysed. The ion fragments were detected at m/z 45, 59, 89, 133 and 151 (peak at 30.3 minutes). The ion fragments were also detected at m/z 45, 59, 89, 151, 177, 221 and 235 (for the peak at 33.4 minutes).

The reaction of glycerol and CO_2 in the presence of acetonitrile shows the production of GlyC along with the formation of mono- and diacetin. Strong intensity peaks at 1000 to 1300 cm^{-1} in the IR spectrum indicated the present of C-O of ester species (Figure 5.6) (Pavia et al., 2009) and supported the evidence that acetins were produced during the reaction. Acetonitrile reacted with water and formed acetamide, while the acetic acid was formed from the hydrolysis of acetamide. Acetic acid underwent acetylation of glycerol to synthesise acetins (Zhang and He, 2014a). The acetylation of glycerol and acetic acid is shown in Figure 5.5 and is thermodynamically favourable for monoacetin and diacetin, but is unfavourable for triacetin production due the endothermic nature of this process (L. N. Silva et al., 2010). Large amounts of energy (28.03 kJ/mol) are required for the replacement of –OH by –CH_3– group (Liao *et al.*, 2010).

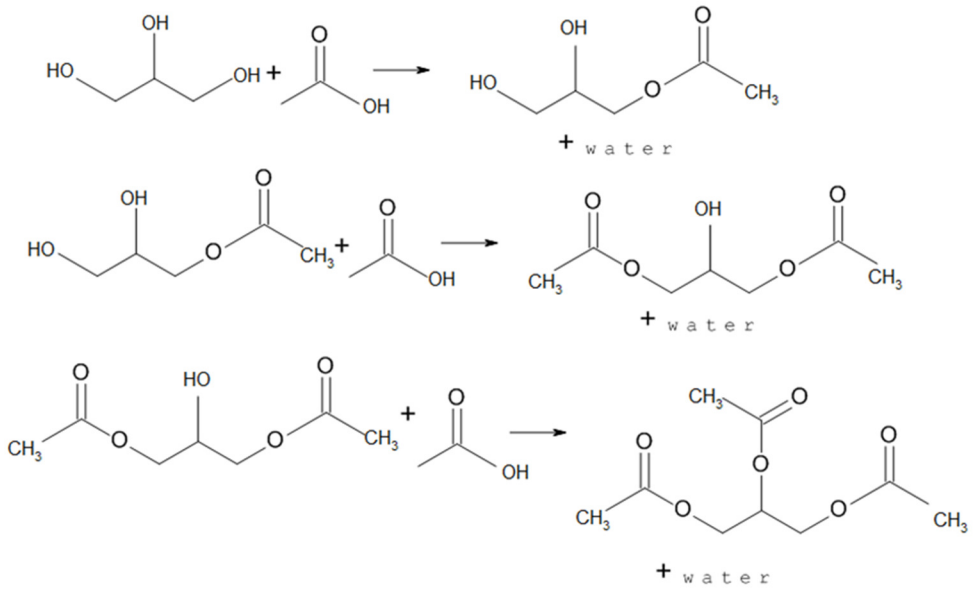

Figure 5.5. Glycerol acetylation mechanism to synthesise mono-, di- and triacetin.

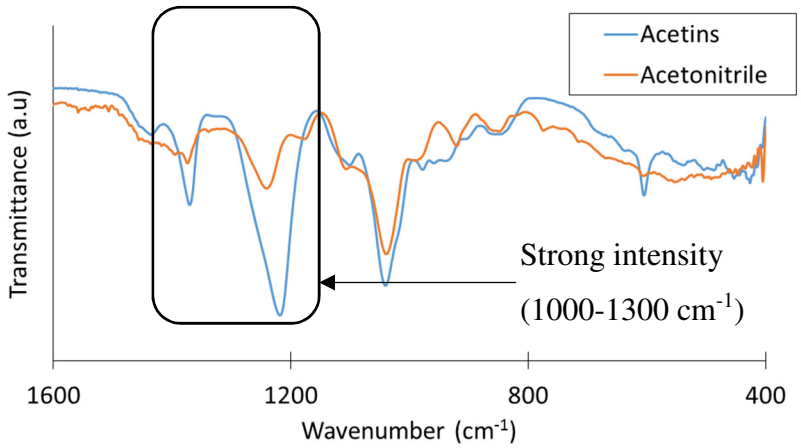

Figure 5.6. The FTIR spectra of mono-, di- and triacetin and the sample for the carboxylation of glycerol in presence of La_2O_3-C over acetonitrile. Reaction conditions: reaction pressure = 45 bar, 6 wt.% La_2O_3-C to glycerol ratio, 22.5 mmol glycerol, 45 mmol acetonitrile, 18 h, and reaction temperature = 160 °C.

The carboxylation of glycerol upon the introduction of benzonitrile produces GlyC and water as the by-product. It was proposed that the benzamide will form from the hydrolysis of benzonitrile and benzoic acid will be the product from the hydrolysis of benzamide (Figure 5.7). However, neither benzamide nor benzoic acid were detected by GC-MS; as a result it is concluded that the esterified product was not obtained from this reaction (Figure 5.8) (Silva *et al.*, 2012).

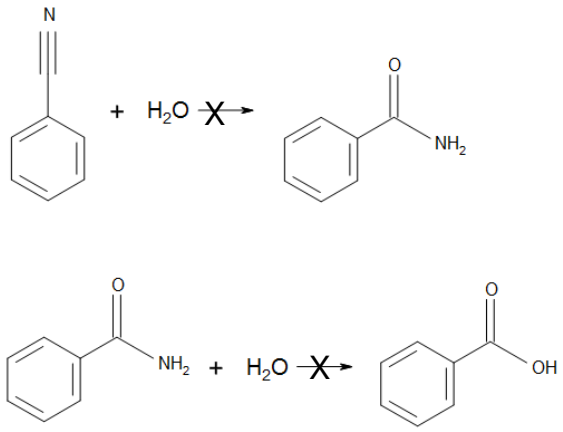

Figure 5.7. The process of hydrolysis of benzonitrile, however, neither products was observed from this reaction.

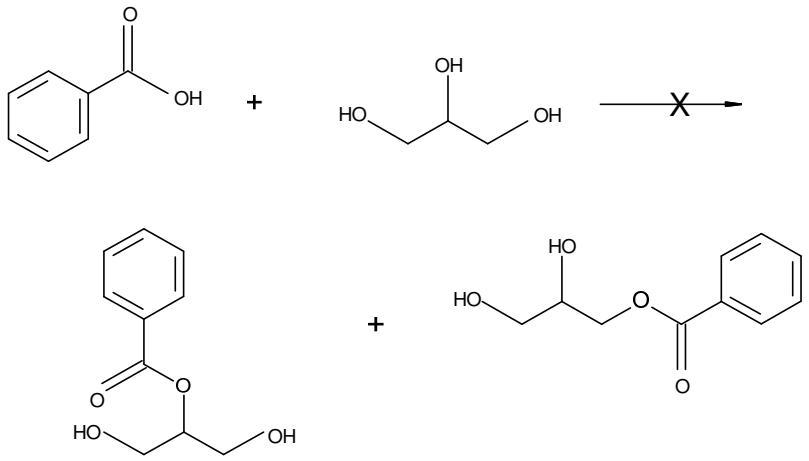

Figure 5.8. Esterified products that could be formed from the esterification of benzoic acid and glycerol.

Acetic anhydride was the only acidic dehydrating agent tested for this reaction. This dehydrating agent results in the formation of mono-, di- and triacetin with no GlyC observed. The acidic medium is therefore not suitable for GlyC synthesis in agreement with previous study by Teng *et al.*, 2014. High selectivity to triacetin, 24%, diacetin, 60%, and monoacetin, 17%, have been observed upon the introduction of acetic anhydride. The acetylation glycerol with acetic anhydride is an exothermic (negative free gibbs energy of reaction) process, therefore less energy is required for triacetin formation (Silva, Goncalves and Mota, 2010). This reaction was also conducted in the absence of CO_2. The selectivity to diacetin decreases to 49%, while the triacetin production has increased from 24 to 45%. This finding shows that the reaction of acetic anhydride and glycerol was faster at low pressure. The formation of triacetin can be improved by introduced the reaction with an acid catalyst, *e.g.*, H-Y (Konwar *et al.*, 2015), H-β (Silva, Goncalves and Mota, 2010) or CsPWA (Sandesh et al., 2015).

Anisole regarded as a green solvent was also employed for the direct carboxylation of glycerol over La_2O_3-C. Anisole was tested in order to study the ability of green solvents to replace the function of nitrile based dehydrating agent to synthesise GlyC. However, no GlyC was detected from this reaction. Natalie and Phillip studied the hydrolysis of anisole to phenol (Rebacz and Savage, 2013). Due to the large activation energy of this system, 31 kcal mol^{-1} (in the presence of 5 mol% of $In(OTf)_3$), the

reaction must be carried out at high temperature > 300 ℃ (Rebacz and Savage, 2013). The anisole hydrolysis rate constant was also investigated; only 0.0002 L mol^{-1} s^{-1} was observed at 200 ℃ while 0.04 L mol^{-1} s^{-1} at 300 ℃ (Rebacz and Savage, 2013). The present study was designed to determine the influence of acidic and nitrile based dehydrating agents on GlyC, acetins and by-products synthesis over La_2O_3-C. Although the current study is based on a small number of dehydrating agents, this finding suggest that acidic media favour the formation of acetins, while nitrile based dehydrating agents create the basic medium for the desired reaction to take place and promote the formation of GlyC. In addition, 4HMO was produced as a result of the reaction of glycerol, CO_2 and NH_3.

5.3 Reaction mechanism for the carboxylation of glycerol in the presence of nitrile based dehydrating agents

The reaction between CO_2 and glycerol produces GlyC and water and its reaction mechanism is shown in Figure 5.9. The small equilibrium constant, 0.0015 at 180 ℃ and 5 MPa, (Li and Wang, 2011) for the carboxylation of glycerol leads to a low yield of GlyC. Removal of the water using both physical and chemical water trap (dehydrating agents) are the available methods to increase the conversion of glycerol and selectivity to GlyC (Styring, Quadrelli and Amstrong, 2015).

Previous studies show a positive impact on the yield and selectivity to GlyC upon the addition of dehydrating agents such as acetonitrile and 2-cynopyridine. There have been a number of studies that describe the hydrolysis of acetonitrile employed in the reaction of CO_2 and glycerol. Acetonitrile reacted with water and formed acetamide, while the acetic acid was formed from the hydrolysis of acetamide (Li *et al.*, 2013). Acetic acid underwent acetylation of glycerol to synthesise acetins. However, the presence of other products, *e.g.*, 4HMO has never been discussed. Further investigation is required to confirm the impact of the nitrile based dehydrating agents and understand the origin of these products.

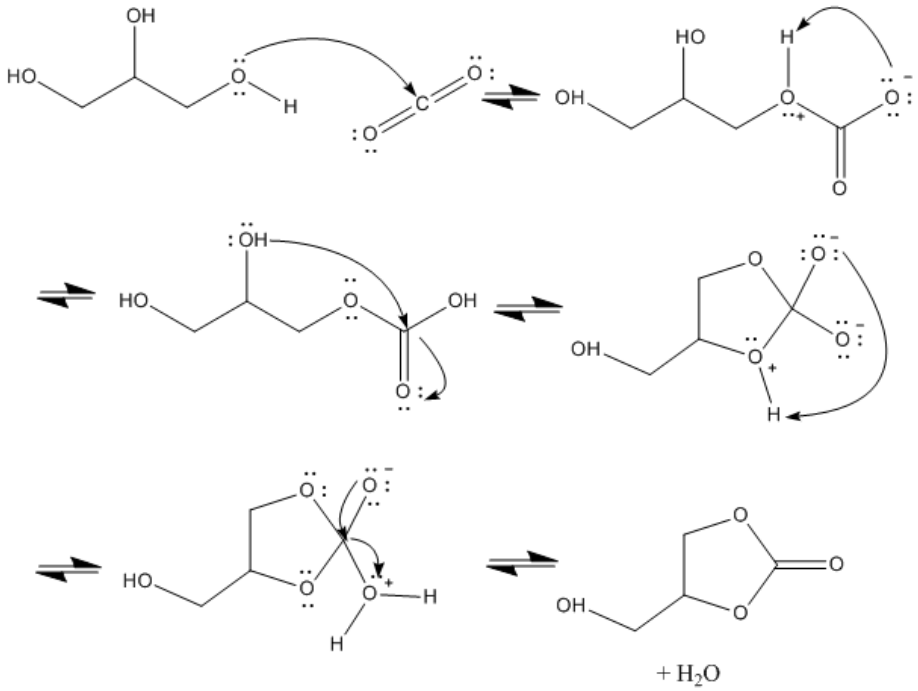

Figure 5.9. The reaction mechanism of glycerol and carbon dioxide to glycerol carbonate and water.

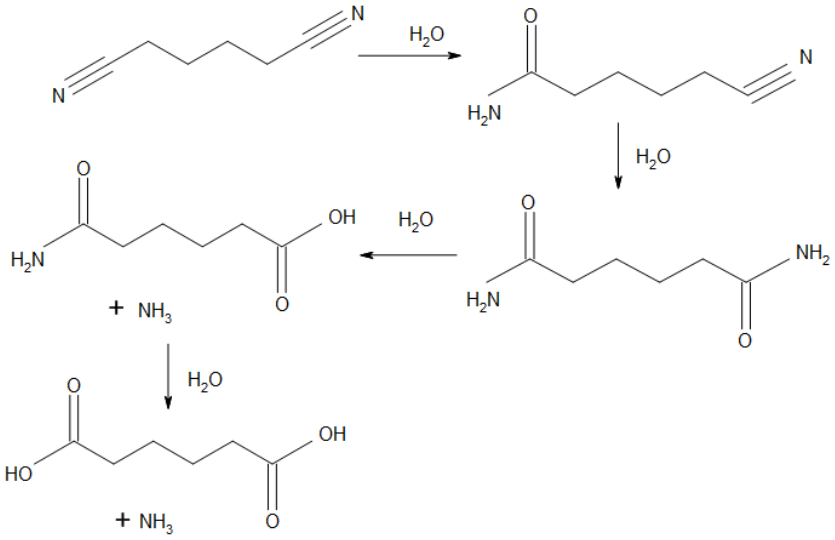

Figure 5.10. The hydrolysis of adiponitrile.

Despite the simplicity of the carboxylation reaction, it can proceed *via* a number of different pathways. Other pathways are showed in Figure 5.12. This further adds to the complexity of the reaction mechanism. This reaction also synthesised a range of

by-products due to the addition of adiponitrile as the dehydrating agent. It is suggested that the hydrolysis of adiponitrile produces 5-cyanovaleramide, adipamide, 5-cyanovaleric acid and adipic acid as summarised in Figure 5.10 (Duan *et al.*, 2008). Adiponitrile reacted with water and formed 5-cyanovaleramide and adipamide. The adipic acid was formed from the hydrolysis of adipamide (Li *et al.*, 2013); where NH_3 is eliminated. Figure 5.11 shows the general reaction mechanism to synthesise carboxylic acid from amide. All these products mention are not detected on the GC chromatogram. Both adipamide (98% Sigma Aldrich) and adipic acid (99% Sigma Aldrich) cannot be detected using the HP Innowax capillary column because of its high boiling point. Boiling point of adipic acid is 337.5 °C at 760 mmHg.

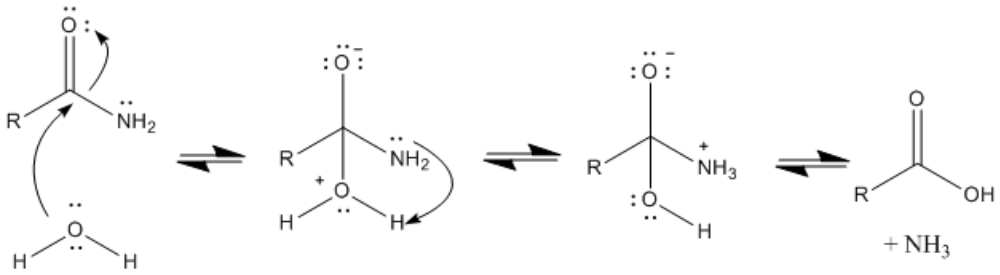

Figure 5.11. Reaction mechanism for the reaction of amide and water, where R= $NH_2C{=}OCH_2CH_2CH_2CH_2$.

Figure 5.12 shows the possible reaction pathway to synthesise GlyC, 4HMO and 6-cyclic ring. It is suggested that the 4HMO can be synthesised by reacting glycerol, CO_2 and NH_3. NH_3 is the by-product formed from the decomposition of adipamide. Reaction of glycerol and CO_2 may promote the formation of the reaction intermediates (Figure 5.12); where the CO_2 attacks the carbon on the primary and secondary alcohol to form A and D. The reaction of A and D with NH_3 promotes the formation of compound B and E. The lone pair of nitrogen (amine group) attacks the electropositive carbonyl group and the electron resonates onto the oxygen which allows for the proton transfer between the positively charged nitrogen and negatively charged oxygen after which dehydration process takes place to reform the carbonyl group (Figure 5.13). Cyclisation of compound B and E leads to the formation of 4HMO (B_1 and E_1). The

presence of 4HMO was later confirmed by GC-MS analysis using (S)-4-(Hydroxymethyl)oxazolidin-2-one purchased from Sigma Aldrich. NMR analysis must be carried out in the future in order to confirm the presence of both 4HMO isomers and also reaction intermediates proposed in Figure 5.12. It is also noteworthy that the 6-ring carbonates (A_1 and C_1) were not detected in any of the experiments performed.

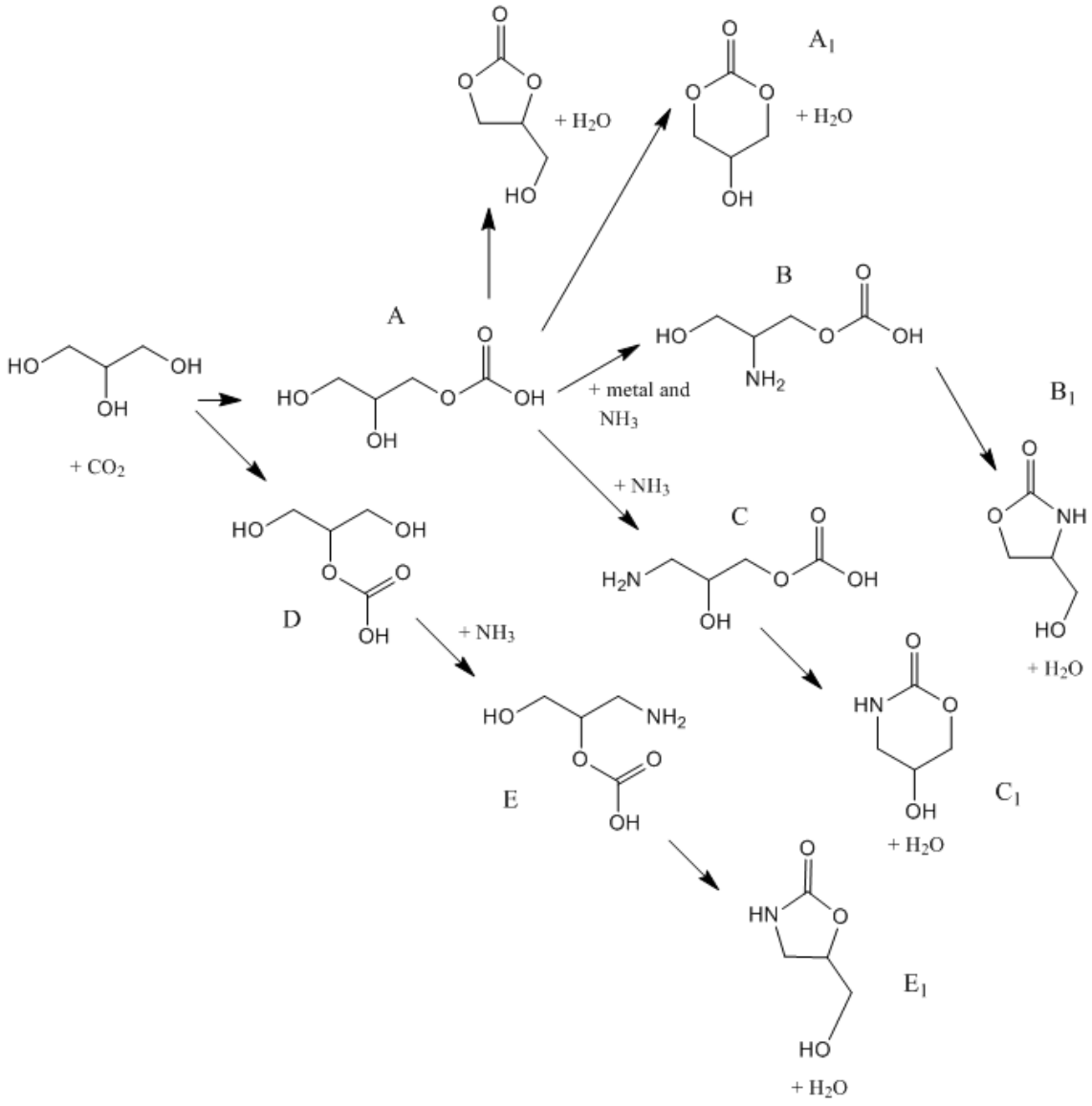

Figure 5.12. The proposed reaction pathway to synthesised glycerol carbonate, 4HMO isomers (B_1 and E_1). 6-ring carbonates (A_1 and C_1) were not detected from the GC chromatogram and the presence of intermediate A-E need further analysis.

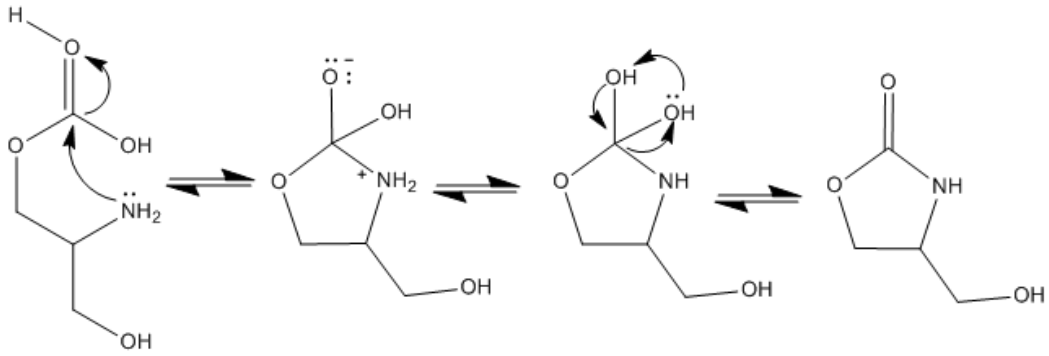

Figure 5.13. The reaction mechanism of the ring closing of compound B.

4HMO cannot be synthesised from the reaction of GlyC and NH_3 (Figure 5.14). The lone pair on NH_3 attacks the electropositive carbonyl group of GlyC and leads to the formation of imine (C=N). The C=N is stable in the presence of base. However, the process of amination is highly reversible in the presence of acid.

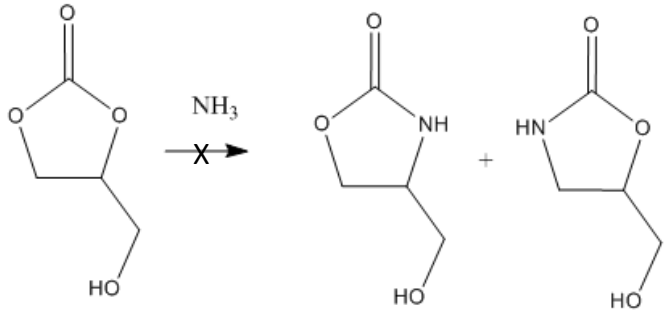

Figure 5.14. 4-hydroxymethyl oxazolidin-2-one cannot be synthesised from the reaction of glycerol carbonate and ammonia.

5.4 **Comparison with previous studies**

Several catalysts, dehydrating agents and reaction conditions have been introduced and tested for the carboxylation reaction. The results of these studies will now be compared to the findings of previous work as summarised in Table 5.2.

Table 5.2. Comparative study of catalysts with different reaction conditions.

Catalyst	Dehydrating agent (Glycerol to D.A mol ratio)	Reaction condition			Gly. Conv. (%)	Selectivity (%)	Yield (%)	Ref.
		Temp (°C)	Time (hr)	[a]P (MPa)				
CeO_2	[b]2-cyanopyridine (10:30)	150	5	3 (4)	N/A	N/A	20	(J. Liu *et al.*, 2016)
Zn/Al/La F	Acetonitrile (50:95)	170	12	4 (N/A)	30.6	46	14	(Li et al. 2015)
Zn/Al/La -Li	Acetonitrile (50:95)	170	12	4 (N/A)	35.7	42.2	15.1	(H. Li, Jiao, *et al.*, 2015)
Cu/La_2O_3	Acetonitrile (50:190)	150	3	4 (7)	8.9	29.3	N/A	(Zhang and He, 2014b)
2.3 wt.% Cu/La_2O_3	Acetonitrile (50:190)	150	12	4 (7)	33.4	45.4	15.2	(Zhang and He, 2014a)
$La_2O_2CO_3$ -ZnO	Acetonitrile (50:95)	170	12	4 (N/A)	30.3	47.3	14.3	(Li *et al.*, 2013)
CaO	Acetonitrile (50:95)	170	12	4 (N/A)	5.3	0	0	(Li *et al.*, 2013)
CaO	Acetonitrile (50:190)	150	3	4 (7)	0.6	15	N/A	(Zhang and He, 2014b)
MgO/ Al_2O_3 (2:1)	Acetonitrile (50:95)	170	12	4 (N/A)	2.4	0	0	(Li *et al.*, 2013)
MgO	Acetonitrile (50:190)	150	3	4 (7)	0.9	24.4	N/A	(Zhang and He, 2014b)
ZrO_2	Acetonitrile (50:95)	170	12	4 (N/A)	1.2	0	0	(H. Li, Jiao, *et al.*, 2015)

Catalyst	Dehydrating agent (Glycerol to D.A mol ratio)	Reaction condition			Gly. Conv. (%)	Selectivity (%)	Yield (%)	Ref.
		Temp (℃)	Time (hr)	[a]P (MPa)				
La_2O_3	Acetonitrile (50:190)	150	12	4 (7)	0.8	6.3	0.1	(Zhang and He, 2014a)
La_2O_3-C	Adiponitrile (22.5:45)	160	18	3.4 (4.5)	58.1	17.2	9.9	This work
$La_2O_2CO_3$ -CP	Adiponitrile (22.5:45)	160	18	3.4 (4.5)	57.0	18.2	10.4	This work

[a]Initial pressure of CO_2 at room temperature and reaction pressure at reaction temperature.

[b]Reaction was carried out in the presence of 10 ml of dimethyl formamide.

Previous studies propose the efficacy of acetonitrile and 2-cynopyridine, as chemical water traps, to shift the reaction equilibrium towards the products side, thus improving the selectivity to GlyC (Li *et al.*, 2013; Zhang and He, 2014a). High GlyC yield (20%) was observed from the carboxylation of glycerol in the present of 2-cyanopyridine and CeO_2, however a high amount of catalyst was used in this reaction: 20 mmol% based on the quantity of the reactant ratio. High selectivity to GlyC was observed in the presence of acetonitrile, but it was corresponded to the high reaction pressure (~.70 bar); which is beyond of the scope of this study. This work was focusing on the ability of dehydrating agents and efficacy of La_2O_3-C to synthesise GlyC at low pressure, 45 bar. Li and co-worker reported only 5.3 and 2.4% glycerol conversion with no GlyC formation in the presence of CaO and 2:1 MgO/Al_2O_3 catalysts. Alkaline earth metals are not active for this catalytic reaction. All these works contributed to the knowledge in improving the GlyC synthesis *via* direct carboxylation of glycerol, from the influence of range of heterogeneous catalysts, the influence of dehydrating agents and the influence of catalyst preparation methods

5.5 **Chapter conclusions**

A range of dehydrating agents were employed and affected product formation (GlyC, 4HMO and acetins) in different ways. Nitrile based dehydrating agents favour the formation of GlyC and 4HMO. The reaction mechanism of the carboxylation of glycerol to GlyC and by-products in the presence of adiponitrile is summarised in Figure 5.12. In contrast to nitrile based dehydrating agents, acidic dehydrating agents promote the production of acetins. However, neither GlyC nor acetins were observed in carboxylation reaction in the absence of dehydrating agent. The selectivity to GlyC increases to 4, 5 and 17% upon the addition of acetonitrile, benzonitrile and adiponitrile. It is proposed that dicyanated dehydrating agents have better performance as the water trap (Silva et al., 2012). In contrast, 100% selectivity to mono-, di and triacetin and no GlyC were observed from reaction over acid anhydride. This study has demonstrated for the first time that the yield and selectivity to GlyC and acetins are shown to be dependent upon the presence of dehydrating agents.

6 CARBOXYLATION OF CRUDE GLYCEROL

Transesterification of vegetable oils or animal fats and methanol generates biodiesel and crude glycerol. Crude glycerol contain impurities such as methanol, fatty acid methyl esters and salts. This chapter investigates the direct carboxylation of crude glycerol into glycerol carbonate in the presence of ZrO_2-based catalysts, La_2O_3-C and $La_2O_2CO_3$-CP. The study shows that the presence of impurities in crude glycerol can significantly lower the selectivity to glycerol carbonate. These catalysts must be resistant to a range of impurities including water, sodium methoxide and methanol. The characterisation of crude glycerol was also conducted. Experimental works were designed by reacting a range of model crude glycerol with CO_2. Model crude glycerol was the combination of pure glycerol with varying impurities including fatty acid methyl esters, methanol, sodium methoxide and water. Finally, direct carboxylation of crude glycerol over modified lanthanum-based catalysts and in the presence of adiponitrile has been carried out.

6.1 Catalyst synthesis

All catalysts employed within this section have been prepared using a standard co-precipitation method discussed in section 3.2. Based on the promising results of the catalyst that has been prepared *via* co-precipitation (Chapter 4), modified $La_2O_2CO_3$ catalysts including $ZrO_2/La_2O_2CO_3$ and $ZrO_2/La_2O_2CO_3/Ga_2O_3$ catalysts were prepared using the same method.

6.2 Solid catalyst characterisation

6.2.1 SEM

Figure 6.1 (a-e) show the SEM micrograph of La_2O_3-C, $La_2O_2CO_3$-CP, ZrO_2, $ZrO_2/La_2O_2CO_3$ and $ZrO_2/La_2O_2CO_3/Ga_2O_3$. The SEM analysis was carried out using JEOL JSM-6010LA and particle size of those catalysts were analysed using ImageJ software as summarised in Table 6.1. All images were magnified for 250 times and the acceleration voltage was 15 to 20 kV.

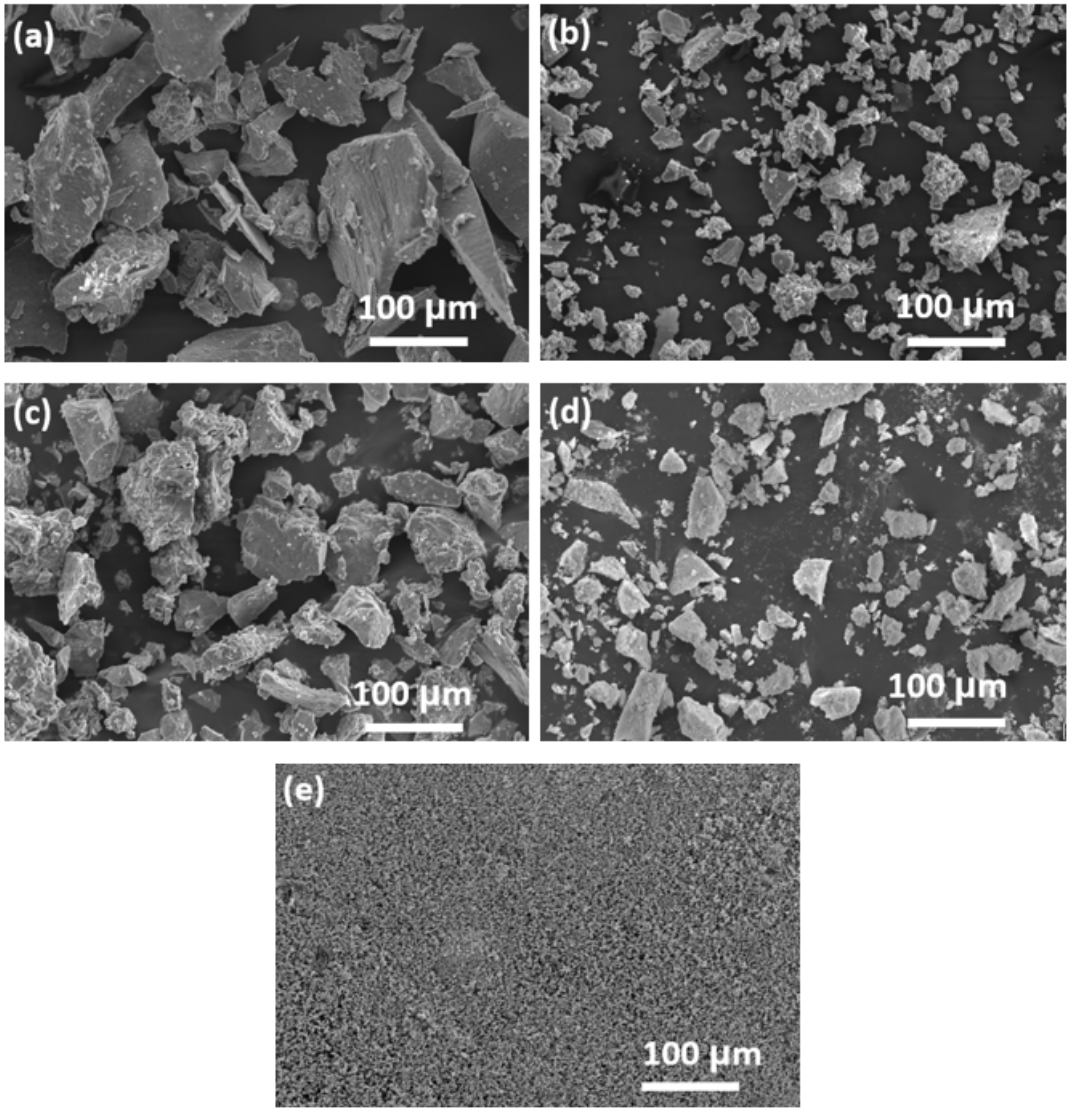

Figure 6.1. Scanning electron micrographs for (a) ZrO_2 (b) $ZrO_2/La_2O_2CO_3$ (c) $ZrO_2/La_2O_2CO_3/Ga_2O_3$ (d) $La_2O_2CO_3$-CP and (e) La_2O_3-C. All catalysts prepared from co-precipitation method except for (e) La_2O_3-C and magnified 250 times and acceleration voltage was set up at 15 to 20 kV.

The morphology of ZrO_2 shows a significant difference to the $ZrO_2/La_2O_2CO_3$ (70:30) catalyst. It was observed that the particle size of $ZrO_2/La_2O_2CO_3$ (Figure 6.1 (b)) was smaller, ~ 7 µm, than the ZrO_2 (~ 20 µm). 5 wt.% of Ga_2O_3 was introduced to the $ZrO_2/La_2O_2CO_3$ catalyst giving a $ZrO_2/La_2O_2CO_3/Ga_2O_3$ of 65:30:5. This catalyst (Figure 6.1 (c)) shows a particle size of ~ 15 µm. Figure 6.1 (d and e) show the image of La_2O_3-C and $La_2O_2CO_3$-CP catalysts. These micrographs clearly show that all

catalysts have an irregular shape. In general, small particle size of catalysts have a high surface area. It is expected that catalysts with small particle size have a better catalytic performance; presumably due its high number of catalytic active sites.

Table 6.1. The particle size of solid catalysts.

Catalysts	Particle size (μm)
La_2O_3-C	1
$La_2O_2CO_3$-CP	5
ZrO_2	20
$ZrO_2/La_2O_2CO_3$	7
$ZrO_2/La_2O_2CO_3/Ga_2O_3$	15

6.2.2 **BET**

A Micrommetrics 3-Flex was employed to determine the BET surface area of catalyst and pore volume and average pore diameter were measured from the desorption branch of isotherm *via* the BJH method. BET measurement of ZrO_2 yield a surface area of 59 m^2/g; while surface area of only 26 m^2/g and 35 m^2/g were obtained from $ZrO_2/La_2O_2CO_3$ and $ZrO_2/La_2O_2CO_3/Ga_2O_3$ catalysts.

ZrO_2 has a larger surface area, pore volume and average pore diameter than La_2O_3 (Adeleye *et al.*, 2014). $ZrO_2/La_2O_2CO_3$ and $ZrO_2/La_2O_2CO_3/Ga_2O_3$ catalysts are also show large average pore diameter 33 and 34 nm as compared with La_2O_3-C (3 nm) and $La_2O_2CO_3$-CP (14 nm). These catalysts are considered as mesoporous in nature. For comparison, the molecular length of glycerol and GlyC are 0.52 nm and 0.65 nm (Saiyong *et al.*, 2012), hence mass transfer of the reactant within the catalyst pores is expected to be relatively facile; it therefore more likely that mass transfer between the

gas-phase (CO_2) and the catalyst surface in the liquid (glycerol) phase is likely to be the dominant transport effect.

Table 6.2. BET surface area, pore volume and average pore diameter for solid catalysts.

Catalysts	BET surface area (m^2g^{-1})	[a]Pore volume (cm^3g^{-1})	[a]Average pore diameter (nm)
La_2O_3-C	14	0.02	3
$La_2O_2CO_3$-CP	60	0.34	14
ZrO_2	59	0.06	26
$ZrO_2/La_2O_2CO_3$	26	0.04	33
$ZrO_2/La_2O_2CO_3/Ga_2O_3$	35	0.05	34

[a]Measured from the desorption branch according to the BJH method.

6.2.3 **TPD-NH_3**

TPD-NH_3 analysis has been employed in order to study the total number of acid sites of the catalysts. La_2O_3-C presents the lowest acidic sites (0.07 mmol of $NH_3/g_{catalyst}$) as compared to the Zr-based catalysts (> 0.1 mmol of $NH_3/g_{catalyst}$). The number of acidic sites calculated is summarised in Table 6.3. The total acidity of Zr-based catalysts was affected by the composition of La and Ga catalysts and decrease in the order of $ZrO_2 < ZrO_2/La_2O_2CO_3 < ZrO_2/La_2O_2CO_3/Ga_2O_3$. Ga_2O_3 is an acidic catalyst; addition of Ga_2O_3 is therefore to increase the acidity of $ZrO_2/La_2O_2CO_3/Ga_2O_3$ (Lee *et al.*, 2011, 2012).

Table 6.3. The acid site densities for the series of La_2O_3-C, ZrO_2, $ZrO_2/La_2O_2CO_3$ and $ZrO_2/La_2O_2CO_3/Ga_2O_3$ catalysts.

Catalysts	[a]Total acidity (mmol of $NH_3/g_{catalyst}$)
La_2O_3-C	0.07
$La_2O_2CO_3$-CP	0.13
ZrO_2	0.11
$ZrO_2/La_2O_2CO_3$	0.12
$ZrO_2/La_2O_2CO_3/Ga_2O_3$	0.12

[a]NH_3 desorption peak for all catalysts at $T_{max} > 400$ °C.

6.3 **Characterisation of crude glycerol**

Figure 6.2 (a) shows the sample of crude glycerol used for the direct carboxylation of crude glycerol and adiponitrile. The sample of crude glycerol was obtained from biodiesel synthesis from sunflower oil and methanol and catalysed by sodium hydroxide (NaOH). The reaction was carried out on a Golden Ray biodiesel processer at Department of Chemical and Biological Engineering, University of Sheffield. Crude glycerol (Figure 5.2 (b)) was separated using a 50 ml separating funnel in order to remove the methanol and ash content. The purity of the crude glycerol was tested by GC-MS and the water content was tested using Karl Fisher titration technique. The pH of the crude glycerol was analysed using pH paper. 74% of glycerol with 5 wt.% of water and < 1% of methanol were present in crude glycerol. The crude glycerol also contained 7 g/l of Na as analysed using ICP-MS technique. The sodium originated from the NaOMe homogenous catalyst residual in the crude glycerol sample.

Table 6.4. The summary of impurities contain in crude and 99% purity of glycerol.

Properties	Crude glycerol with purity 74%	Pure glycerol with purity 99%
Appearance	Brownish viscous liquid	Colourless viscous liquid
Moisture/water (wt/wt.%)	5%	1%
Glycerol purity (wt/wt.%)	74%	99%
FAMEs	20%	-
Methanol (wt/wt.%)	<1%	-
pH	8	7
Salt, Na (g/l)	7	-

'-' indicates that the presence of a component was not detected.

In addition to the impurities listed in Table 6.4, the crude glycerol also contained 20% of FAMEs, which were analysed *via* GC-MS with compound identification through comparison with the NIST database. The chain-length of the detected FAMEs ranged from C_{17} (methyl palmitate) to C_{20} (ethyl linoleate). Such compounds are well established constituents of biodiesel synthesised from oil feedstocks (Knothe, 2008; Joshi *et al.*, 2010).

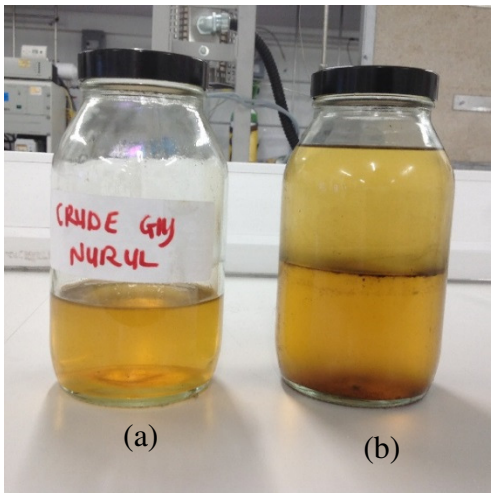

Figure 6.2. Crude glycerol was separated using a 50 ml separating funnel in order to remove the methanol and ash content; samples show the crude glycerol (a) after and (b) before separation process.

6.4 Influence of catalysts and supports on the direct carboxylation of glycerol

The catalyst screening test was carried out over a range lanthanum-based catalysts supported on ZrO_2 and with Ga_2O_3 as the catalyst promoter. ZrO_2 was selected because of its previously reported high activity in synthesising dimethyl carbonate (linear carbonate) from methanol and CO_2 (Jung and Bell, 2001; Chen *et al.*, 2014). The catalytic activity ZrO_2, with Lewis acid site was tested. Result summarised in Table 6.5 show that high selectivity to GlyC was observed from the carboxylation of pure glycerol over $ZrO_2/La_2O_2CO_3/Ga_2O_3$. A similar trend was also observed from the reaction over $La_2O_2CO_3$-CP and La_2O_3-C at the same reaction conditions. Although the catalytic activity of $ZrO_2/La_2O_2CO_3/Ga_2O_3$ was highest, the high cost of Ga_2O_3 means it was less suitable for scale up for industrial use. Therefore, $La_2O_2CO_3$-CP and La_2O_3-C were suggested to be employed for the direct carboxylation of crude glycerol along with $ZrO_2/La_2O_2CO_3/Ga_2O_3$ catalyst. Li and co-worker investigated the impact of ZrO_2 and only 1.2% glycerol conversion was observed. However, introduction of ZrO_2 into the 4:1:1 Zn/Al/La hydrotalcite increased the number of catalyst basic sites; thus improved the selectivity to GlyC from 13 to 14%. This work is still in developing stage and currently there is no sufficient data available for rigorous comparison.

Table 6.5. A range of heterogeneous catalyst employed in reaction of CO_2 and glycerol in presence of adiponitrile. Reaction conditions: reaction pressure = 45 bar, 6 wt.% catalyst to glycerol ratio, 22.5 mmol glycerol, 45 mmol adiponitrile, 18 h and reaction temperature = 160 ℃.

Catalyst	Conversion	Selectivity	Yield
La_2O_3 –C	58	17	10
$La_2O_2CO_3$-CP	57	18	10
ZrO_2	66	9	6
$ZrO_2/La_2O_2CO_3$ (70:30)	61	16	10
$ZrO_2/La_2O_2CO_3/Ga_2O_3$ (65:30:5)	60	19	12

Research to-date has tended to focus on the efficacy of the basic catalysts to synthesise GlyC rather than the acidic catalysts. Therefore, this study will focus and investigate the impact of acid catalysts to the products synthesis. Honda and co-workers highlighted the important of acid-base properties of catalysts; where -OH group of glycerol was adsorbed onto the Lewis acid sites of CeO_2 (Honda *et al.*, 2014). The TPD-NH_3 measurements of ZrO_2 show a high number of acid sites, 0.11 mmol/$g_{catalyst}$, as compared to La_2O_3-C (0.07 mmol/$g_{catalyst}$). A high number of acid sites was also observed from the $ZrO_2/La_2O_2CO_3$ (0.12 mmol/$g_{catalyst}$) and $ZrO_2/La_2O_2CO_3/Ga_2O_3$ (0.12 mmol/$g_{catalyst}$). The selectivity to GlyC decreases from 17% to 9% upon the employing of ZrO_2 in comparison to La_2O_3-C. The by-products produced from this reaction have been analysed and production of 4HMO was increased by thirty-fold. As summarised in Figure 6.3, a high quantity of by-products were produced from the decomposition of GlyC to amide products (Unknown 1 and 3). A similar trend was also observed from the reaction over $ZrO_2/La_2O_2CO_3$ and $ZrO_2/La_2O_2CO_3/Ga_2O_3$. These findings support the hypothesis that acidic catalysts favour the formation of the 4HMO and promote the decomposition of GlyC.

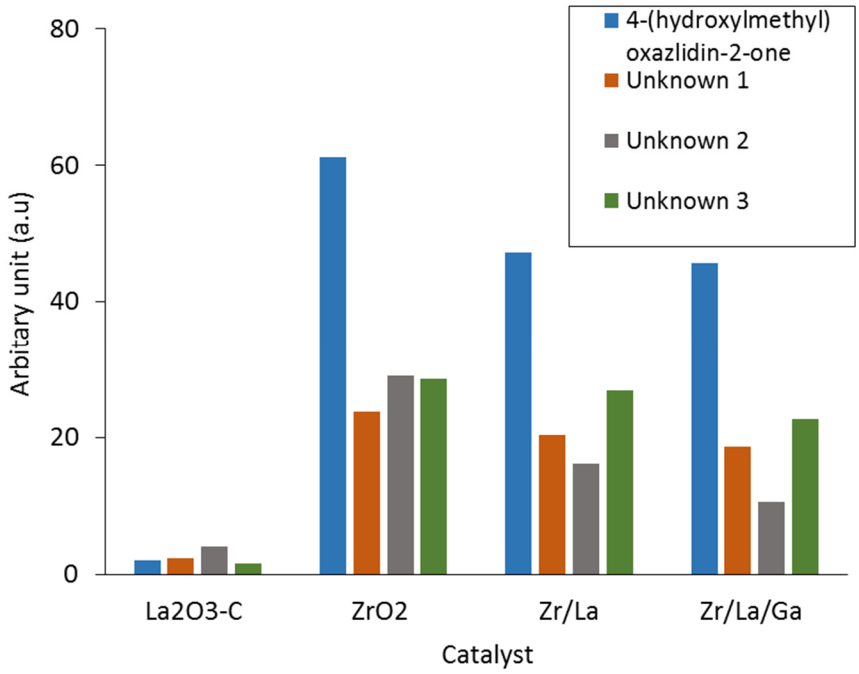

Figure 6.3. Influence of the catalyst loading on by-products formation. Reaction conditions: reaction pressure = 45 bar, 6 wt.% catalyst to glycerol ratio, 22.5 mmol glycerol, 45 mmol adiponitrile, 18 h and reaction temperature = 160 ℃. The by-products detected from the reaction was measured qualitatively, value shown in the table correspond to chromatogram peak area.

FTIR is used in the characterisation of liquid products. Figure 6.4 shows the FTIR spectra for liquid samples from the carboxylation of glycerol over a range of heterogeneous catalysts taken at 18 hours of reaction. Peaks at 1730 and 1790 cm^{-1} confirmed the formation of 4HMO and GlyC (Nguyen-Phu, Park and Eun, 2016). The peak at 1662 cm^{-1} was detected in all reaction samples with differing intensities and indicates the presence of C=O of amide; this peak confirmed that the GlyC has decomposed to by-products (Indran *et al.*, 2014). The used catalysts were also analysed; no peak was detected at 1950 cm^{-1} on any of those catalyst (Figure 6.5). These data indicate that the metal glycerolate was not formed during the carboxylation of glycerol reaction (Li *et al.*, 2013; H. Li, Jiao, *et al.*, 2015).

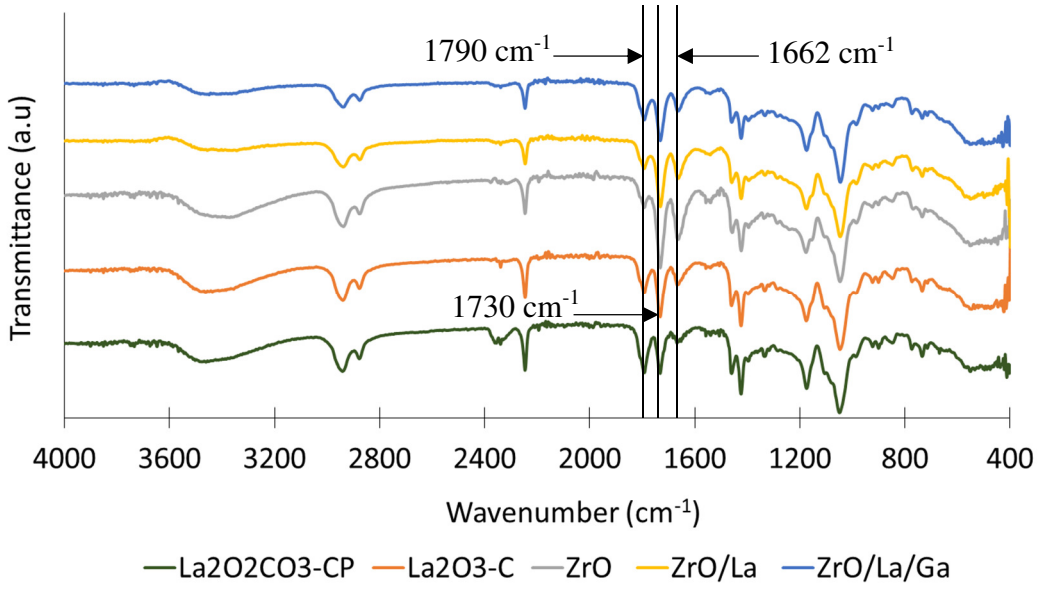

Figure 6.4. FTIR spectra of reaction samples taken at 18 hours over a range of catalyst. Reaction conditions: Pressure = 45 bar, 6 wt.% catalyst to glycerol ratio, 22.5 mmol glycerol, 45 mmol adiponitrile, 18 h and reaction temperature = 160 ℃.

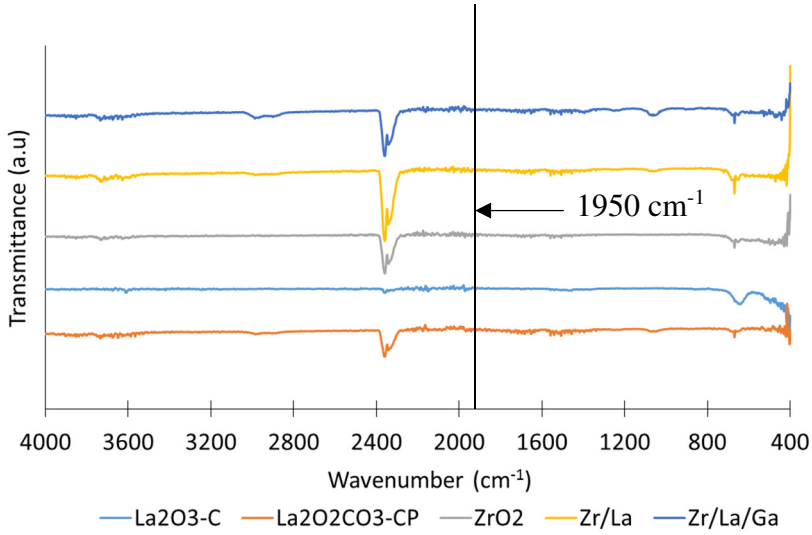

Figure 6.5. FTIR spectra of used catalysts show no peak detected on 1950 cm^{-1}, indicate that none of metal glycerolate formed during the carboxylation of glycerol reaction. Reaction conditions: reaction pressure = 45 bar, 6 wt.% catalyst to glycerol ratio, 22.5 mmol glycerol, 45 mmol adiponitrile, 18 h and reaction temperature = 160 °C.

6.5 Influence of impurities on the carboxylation of glycerol (Model crude glycerol and single impurities)

Crude glycerol is a combination of glycerol and impurities including FAMEs, methanol, water and NaOMe (He *et al.*, 2017). The individual impact of each impurity was studied by preparing model crude glycerol samples comprising of methanol, FAME (methyl palmitate, 97%), water or NaOMe (Table 5.6). Transesterification of pure glycerol and 20 wt.% of methanol shows a slight increase in the selectivity to GlyC from 7 to 8%; while introduction of 1 wt.% of NaOMe shows a negative impact on GlyC formation (Teng *et al.*, 2016). Indran and co-worker investigated the impact of water on the glycerolysis of urea; the selectivity to GlyC was decreased by half upon the addition of 10wt.% of water (Indran *et al.*, 2016).

Addition of methanol to glycerol over La_2O_3-C increased the glycerol conversion from 58 to 61% and selectivity to GlyC from 17 to 22%. Introduction of $La_2O_2CO_3$-CP to the carboxylation of glycerol and methanol (80:20 mol%) improve the selectivity to GlyC to 30%. This is a noteworthy observation and may be related to improve mass transfer by improving the immiscibility of glycerol and CO_2. CO_2 is slightly miscible in glycerol (Nunes *et al.*, 2013), however the equilibrium of CO_2, methanol and glycerol is improve upon the increasing of methanol concentration (Pinto *et al.*, 2011). Additionally, methanol may hinder the secondary reaction of GlyC thereby increasing the reaction selectivity. A more detailed study on the effect of methanol is required in order to determine its precise role.

Table 6.6. The effect of individual impurities on the carboxylation of glycerol. Reaction conditions: reaction pressure = 45 bar, 6 wt.% La_2O_3-C, 22.5 mmol glycerol and 45 mmol adiponitrile, 18 h and reaction temperature = 160 °C.

Model crude glycerol (%)	Conversion	Selectivity	Yield
Glycerol	58	17	10
Glycerol:MeOH (80:20 mol%)	61	22	13
[a]Glycerol:MeOH (80:20 mol%)	56	30	17
Glycerol and 1 wt.% NaOMe	51	11	6
[b]Glycerol and 1 wt.% NaOMe	43	7	3
Glycerol and 10 wt.% FAME	76	1	1
Glycerol and 10 wt.% water	19	3	1

[a]$La_2O_2CO_3$-CP.

[b]Reaction was carried out in absence of catalyst.

Addition of 1 wt.% of NaOMe to the carboxylation reaction results in a reduced in the glycerol conversion (51%) and selectivity to GlyC (10.6%) (Table 6.6). The reduced selectivity to GlyC was reflected in the increased formation of 4HMO by eight fold as summarised in Table 6.7. As the NaOMe acts as homogeneous catalyst in biodiesel synthesis, the impact of NaOME is tested upon the absence of La_2O_3-C. The results obtained showed only 43% glycerol conversion along with a further drop in GlyC selectivity to 7%, consistent with the hypothesis that NaOMe acts as an active homogeneous catalyst favouring the synthesis of 4HMO.

Table 6.7. The qualitative analysis of by-products detected from the reaction upon the addition of NaOMe. Reaction conditions: reaction pressure = 45 bar, 6 wt.% La_2O_3-C, 22.5 mmol glycerol and 45 mmol adiponitrile, 18 h and reaction temperature = 160 °C. The by-products detected from these reactions were measured qualitatively, value shown in the table correspond to chromatogram peak area.

Products	Glycerol	Glycerol and NaOMe	[a]Glycerol and NaOMe
4HMO	2	16	7
Unknown 1 (minute 30.8)	2	6	3
Unknown 2 (minute 31.3)	4	N/A	12
Unknown 3 (minute 33.9)	2	N/A	7

[a]absence of catalyst.

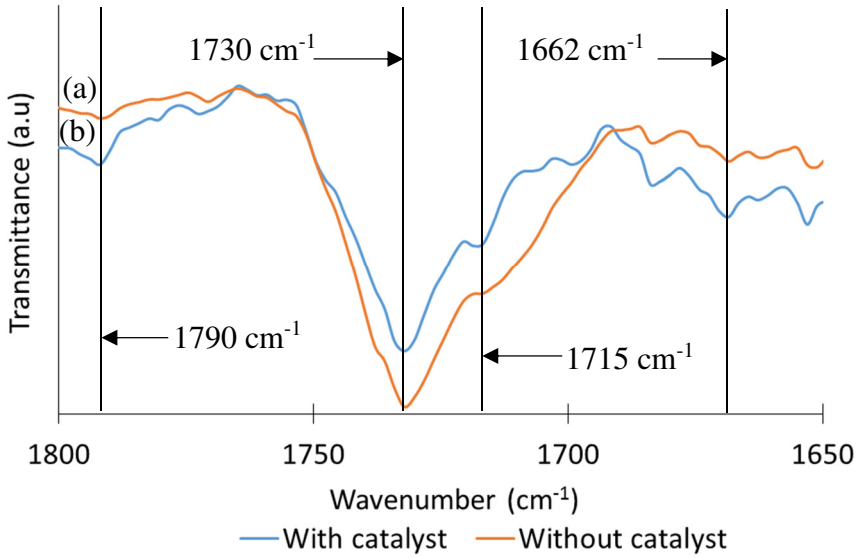

Figure 6.6. FTIR spectra from the reaction of glycerol with NaOMe and CO_2 in (a) absence and (b) present of La_2O_3-C catalsyst. Reaction conditions: reaction pressure = 45 bar, 0 and 6 wt.% La_2O_3-C to glycerol ratio, 22.5 mmol glycerol and 45 mmol adiponitrile and was carried out at 160 °C for 18 hour.

FTIR analysis was conducted to explain impact of addition of NaOMe on the carboxylation reaction. Strong intensity peaks at 1662 and 1730 cm^{-1} confirmed that the decomposition of GlyC to amide products and the formation of 4HMO were favourable even in the absence of the catalyst (Figure 6.6). The strong band at 1730 cm^{-1} was assigned to the formation of GlyC; therefore it is concluded that the NaOMe is able to catalyse the carboxylation reaction, synthesise GlyC and acts as a homogeneous catalyst.

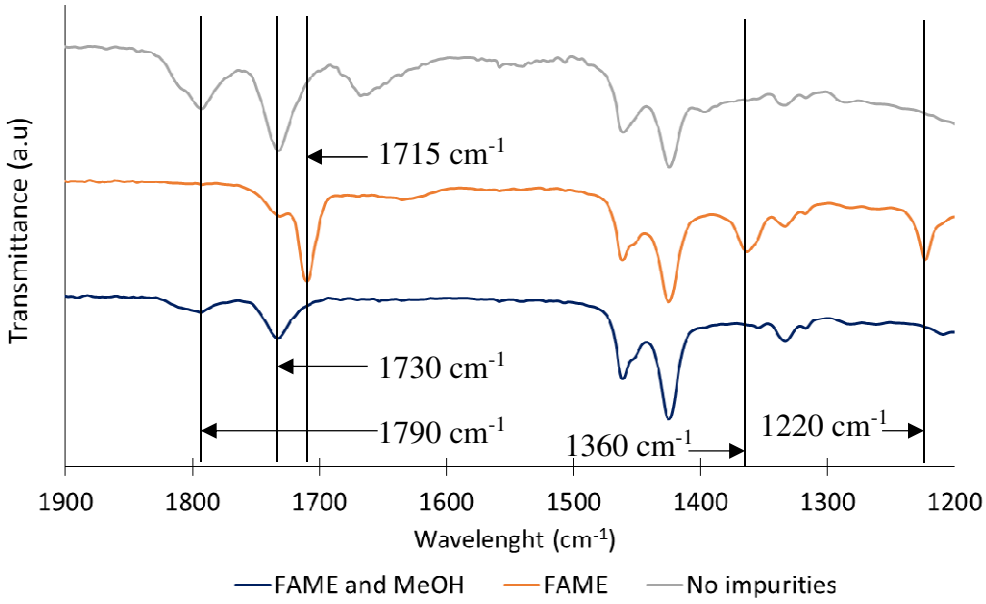

Figure 6.7. FTIR spectra for the reaction of glycerol and/or impurities and CO_2 over La_2O_3-C catalyst. Model crude glycerol was prepared by blending 80:20 mol% glycerol and methanol and also 80:20 mol% glycerol and methanol with 10 wt.% FAME.

Addition of 10 wt.% FAME (methyl palmitate, 97%) to the glycerol resulted in high glycerol conversion, (76%), however, selectivity to GlyC reduced to only 1%. Due the high conversion and low selectivity to GlyC, it was expected that the glycerolysis of FAME to synthesise monoglyceride occurs during the reaction (Bancquart *et al.*, 2001; Ferretti, Apesteguía and Cosimo, 2011). FTIR analysis was conducted in order to investigate the origin of the reduced conversion (Figure 6.7). In comparison to the reaction with pure glycerol the peak at 1790 cm^{-1} is no longer present, co-incident with

a reduced intensity of the 1730 cm^{-1} peak, and with the appearance of new peaks at 1715, 1360 and 1220 cm^{-1}. A high intensity of the peak at 1715 cm^{-1} indicative of C=O of ketone (stretch) was detected alongwith the formation of phenolic species (1220 cm^{-1}) and R-NO_2 species (1360 cm^{-1}). High intensity of peak at 1715 cm^{-1} indicates that a high amount of by-products formed in this reaction. This supported the fact that high glycerol conversion has been achieved with low yield and selectivity to GlyC.

The influence of water was also studied. 10 wt.% of water resulted a significantly decreased in glycerol conversion of 19% and a selectivity to GlyC (3%); this is likely attributed to the selective strong adsorption of water molecules on the active sites of La_2O_3-C (Okoye, Abdullah and Hameed, 2017), thus leading to catalyst deactivation.

6.6 Influence of impurities on the carboxylation of glycerol (Effect of multiple impurities)

As the impurities in crude glycerol are likely to interact with one another and any subsequent products produced from the impurities, the behaviour of model feedstocks containing two or more impurities has also been investigated. The presence of methanol was kept constant across all model systems with glycerol and methanol in an 80:20 mol%. Addition of 1 wt.% of NaOMe appears to have positive impact on the catalytic system; in which highest selectivities to GlyC were achieved in the presence of La_2O_3-C and $La_2O_2CO_3$-CP, 25 and 42% respectively (Table 6.8). However, this was achieved a reduced conversion to 46 and 31% which compared with 58% for pure glycerol and 61% for the glycerol/methanol mixture.

Table 6.8. Effect of multiple impurities on carboxylation of glycerol over La_2O_3-C. Reaction conditions: reaction pressure = 45 bar, 6 wt.% La_2O_3-C to glycerol ratio, 80:20 mol% of glycerol to methanol (22.5 mmol in total) and 45 mmol adiponitrile, 18 h and reaction temperature = 160 °C.

Model crude glycerol (%)	Conversion	Selectivity	Yield
Glycerol:MeOH (80:20 mol%)	61	22	13
Glycerol:MeOH (80:20 mol%) 1 wt.% NaOMe	46	25	12
[a]Glycerol:MeOH (80:20 mol%) 1 wt.% NaOMe	31	42	13
Glycerol:MeOH (80:20 mol%) 10 wt.% FAME	85	3	3
Glycerol:MeOH (80:20 mol%) 10 wt.% FAME +1 wt.% NaOMe	73	4	3
[b]Glycerol:MeOH (80:20 mol%) 10 wt.% FAME +1 wt.% NaOMe	48	21	10

[a]$La_2O_2CO_3$-CP.

[b]$ZrO_2/La_2O_2CO_3/Ga_2O_3$ was employed.

The by-products formed from this reaction have been analysed. The formation of 4HMO increased upon the addition of single impurity such as methanol or NaOMe as summarised in Table 6.9. In contrast to what is observed with the single impurity, a glycerol mixture containing both methanol and NaOMe favours the formation of by-products (Unknown 1, 2 and 3) produced from the decomposition of GlyC.

Table 6.9. By-products detected from the reaction of glycerol in presence of impurities and CO_2 over La_2O_3-C was measured qualitatively, value shown in the table correspond to chromatogram peak area.

Products	Glycerol	Glycerol: MeOH	Glycerol: NaOMe	Glycerol:MeOH :NaOMe
4HMO	2	4	7	5
Unknown 1 (minute 30.8)	2	11	3	11
Unknown 2 (minute 31.3)	4	10	12	12
Unknown 3 (minute 33.9)	2	8	7	17

Addition of FAME to the glycerol and methanol mixture results in a significantly reduced selectivity alongside high conversion, as it did in the absence of methanol. 85% glycerol conversion and 3% selectivity to GlyC were observed. This trend was also observed if methanol, NaOMe and FAME were all present; suggesting that the effect of FAME is to inhibit GlyC formation. FTIR data (Figure 6.7) do not show significant intensity at 1715 cm^{-1} suggesting that the formation of by-product (C=O stretch for ketone) was not formed in the presence of methanol. When the reaction mixture comprised glycerol, methanol, FAME and CO_2, phenolic and R-NO_2 species were not observed by FTIR. The intensity of peak at 1715 cm^{-1} observed in the presence of FAME and methanol is decreased while the intensity of peak detected at 1730 cm^{-1} (C=O of 4HMO) appears to be increased. In reviewing the literature, no prior data was found on the role of FAMEs and their impact on the carboxylation of pure or crude glycerol. In fact, the reaction of crude glycerol and urea and the reaction of crude glycerol and dimethyl carbonate studied by Indran *et al.* (2016) and Teng *et al.* (2016) were carried out using the crude glycerol with < 2% of FAMEs. Therefore, the separation of FAMEs and crude glycerol is crucial in order to obtain high purity of crude glycerol.

The impact of multiple impurities in the mixture comprising glycerol and methanol (80:20 mol%), 10 wt.% of FAME and 1 wt.% of NaOMe was tested over La_2O_3-C. Glycerol conversion and selectivity to GlyC decreased to 73% and 4% respectively. However, only 48% conversion and 21% selectivity to GlyC was observed over $ZrO_2/La_2O_2CO_3/Ga_2O_3$ tested under the same reaction conditions. This catalyst system ($ZrO_2/La_2O_2CO_3/Ga_2O_3$) favours the formation of 4HMO and Unknown 1, 2 and 3 production (Table 6.10). It was likely that the high number of acid sites of $ZrO_2/La_2O_2CO_3/Ga_2O_3$ (0.11 mmol/$g_{catalyst}$) enhance the 4HMO synthesis and promotes the GlyC decomposition to amide products; consistent with the hypothesis that acidic catalysts favour the synthesis of by-products. Little is known about Ga_2O_3 as the catalyst promoter, for this reaction and it is not clear how this promoter suppresses the glycerol conversion. However, gallium-based catalysts been successfully employed in various catalytic reaction including cycloaddition reactions for organic transformations (Gupta and O'Sullivan, 2013). Indeed, Ga_2O_3 was successful in the field of the direct synthesis of dimethyl carbonate (linear carbonate), but the focus on employing gallium as catalyst promoter in synthesising the cyclic carbonate seems very limited.

Table 6.10. The qualitative analysis of by-products detected from the reaction of glycerol and impurities over La_2O_3-C and $ZrO_2/La_2O_2CO_3/Ga_2O_3$. Reaction conditions: pressure = 45 bar, 6 wt.% catalyst to glycerol ratio, 80:20 mol% glycerol to methanol (22.5 mmol in total) and 45 mmol adiponitrile, 18 h and reaction temperature = 160 °C. The by-products detected from these reactions were measured qualitatively, value shown in the table correspond to chromatogram peak area.

Products	La_2O_3-C	$ZrO_2/La_2O_2CO_3/Ga_2O_3$
4HMO	7	24
Unknown 1 (minute 30.8)	3	3
Unknown 2 (minute 31.3)	N/A	14
Unknown 3 (minute 33.9)	N/A	10

So far there has been little literature discussion about the single and multiple impact of impurities on the carboxylation of glycerol, of which detailed investigation and experimentation regarding to the role of impurities would be interesting. Overall, water and FAME have a negative impact on the carboxylation of glycerol and significantly lowered the GlyC selectivity to < 3%. A similar trend is observed from the reaction of: (1) glycerol, methanol and FAME and (2) glycerol, methanol, NaOMe and FAME in comparison with the reaction of glycerol and FAME; suggesting that the presence of FAME lowers the selectivity to GlyC (> 4%).

This study shows that the selectivity to GlyC was decreased to 11% and 7% upon the addition of NaOMe and favours synthesis of 4HMO. In contrast, addition methanol to glycerol improves the glycerol conversion and selectivity to GlyC to 61% and 22%. Addition of NaOMe to the glycerol and methanol mixture shows a positive impact on GlyC synthesis, where the highest selectivity (42%) was observed from all systems employed and achieved in the presence of $La_2O_2CO_3$-CP.

6.7 Optimisation of reaction parameters

6.7.1 Influence of reactant to methanol ratio

Given the observation that the addition of methanol to glycerol improves the catalytic performance with respect to the GlyC production, the optimisation of the methanol to glycerol ratio will be investigated over $La_2O_2CO_3$-CP. Optimisation of reaction conditions is very important in order to obtain a high selectivity to GlyC, by eliminating or/and limiting the formation of by-products. As shown in Figure 6.8, in mixture of glycerol and methanol (80:20 mol%) resulted in an increase in selectivity to GlyC, from 18% (pure glycerol) to 30%, while further increasing methanol concentration (60:40 glycerol:methanol mol%) showed a major reduction in selectivity to GlyC (13%).

This observation suggested that the addition of methanol improves mass transfer by improving the immiscibility of glycerol and CO_2. However, the high methanol

concentration (40:60 methanol:glycerol mol%) added shows a negative impact on the carboxylation reaction. A possible explanation is with regard to the mass transfer between the solid catalyst, CO_2, glycerol and adiponitrile. However, the dimethyl carbonate may be synthesised from this reaction. An excess amount of methanol introduced to this reaction increased the chances for the reaction of CO_2 and methanol to dimethyl carbonate to take place.

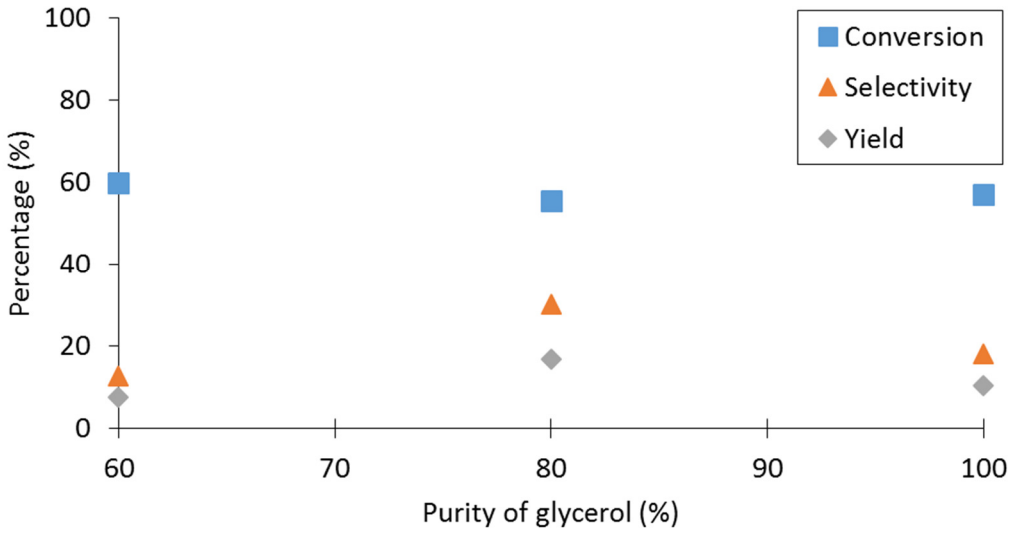

Figure 6.8. The influence of glycerol to methanol molar ratio to the formation of GlyC. Reaction conditions: reaction pressure = 45 bar, 6 wt.% $La_2O_2CO_3$ -CP to glycerol ratio, glycerol:methanol (22.5 mmol in total) and 45 mmol adiponitrile, 18 h and reaction temperature = 160 ℃.

Relatively low intensity of peaks at 1730 and 1790 cm^{-1} were observed from the FTIR spectrum with 60:40 of glycerol to methanol (Figure 6.9). The peaks at 1730 and 1790 cm^{-1} were previously assigned to the GlyC and 4HMO, this may therefore confirmed that the low selectivity to GlyC was observed from the carboxylation reaction employing the 60:40 glycerol to methanol mixture.

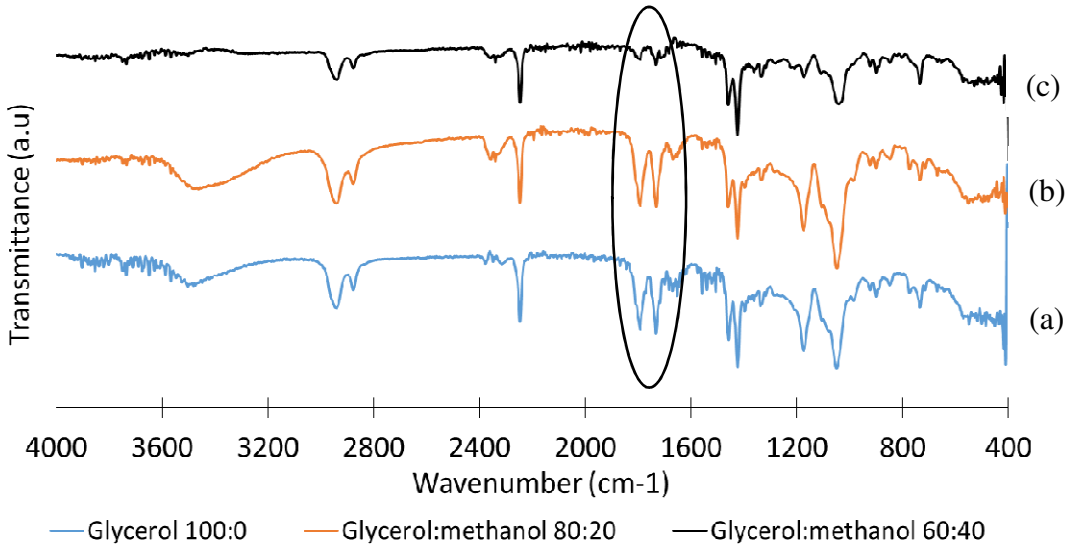

Figure 6.9. FTIR spectra from the reaction of glycerol with (a) 0, (b) 20 and (c) 40 mol% of methanol and CO_2 over $La_2O_2CO_3$-CP catalyst. Reaction conditions: reaction pressure = 45 bar, 6 wt.% $La_2O_2CO_3$ -CP to glycerol ratio, glycerol:methanol (22.5 mmol in total) and 45 mmol adiponitrile, 18 h and reaction temperature = 160 ℃.

6.7.2 **Influence of reaction time**

As shown in Figure 6.10, a detailed investigation of the impact of different reaction time was consideration for the carboxylation of glycerol and methanol in the ratio of 80:20 mol% over $La_2O_2CO_3$-CP. It illustrated that glycerol conversion increased from 56 from 75% for the reaction sample collected at 13 to 25 hours. The selectivity to GlyC increased from 7 to 30% (18 hours) and then decreased to only 10% after 25 hours of reaction. This observation suggests that the decrease of selectivity to GlyC may be related to the increase of 4HMO and by-products formation. The GC chromatogram has been analysed and the by-products were measured qualitatively as summarised in Figure 6.11. By-product (Unknown 1 and 3) formation increased by eleven and six fold within 12 hours. In conclusion, reaction time has a significant impact on the GlyC and by-products formation. Prolonged reaction times (> 18 hours) resulted in lowering the selectivity to GlyC and increasing the formation of by-products; where these were the products formed from the transformation of GlyC to amide product.

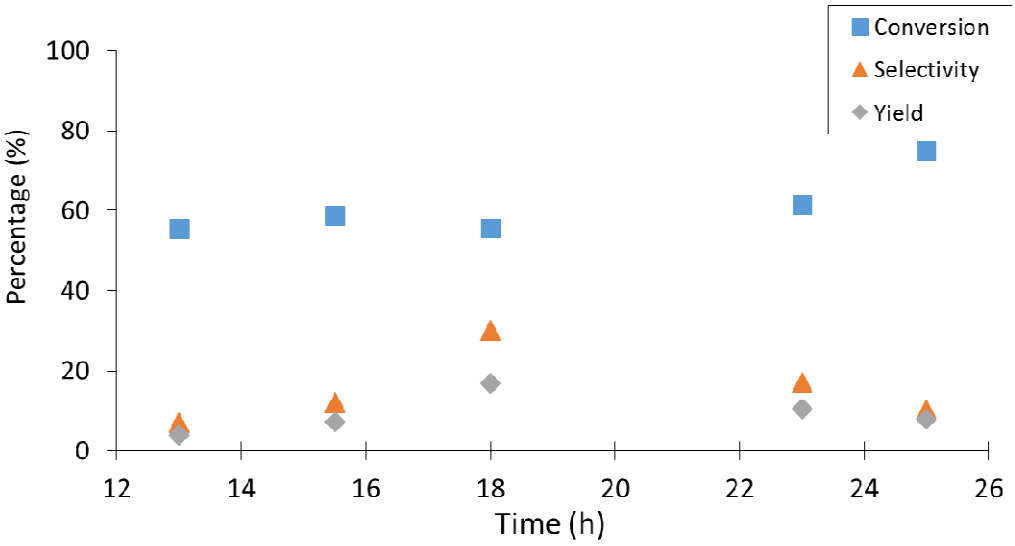

Figure 6.10. The time-on-stream analysis of glycerol conversion and selectivity and yield of GlyC from 13 to 25 h. Reaction conditions: reaction pressure = 45 bar, 6 wt.% $La_2O_2CO_3$-CP to glycerol ratio, glycerol:methanol (80:20 mol%), 45 mmol adiponitrile, 13 to 25 h and reaction temperature = 160 ℃.

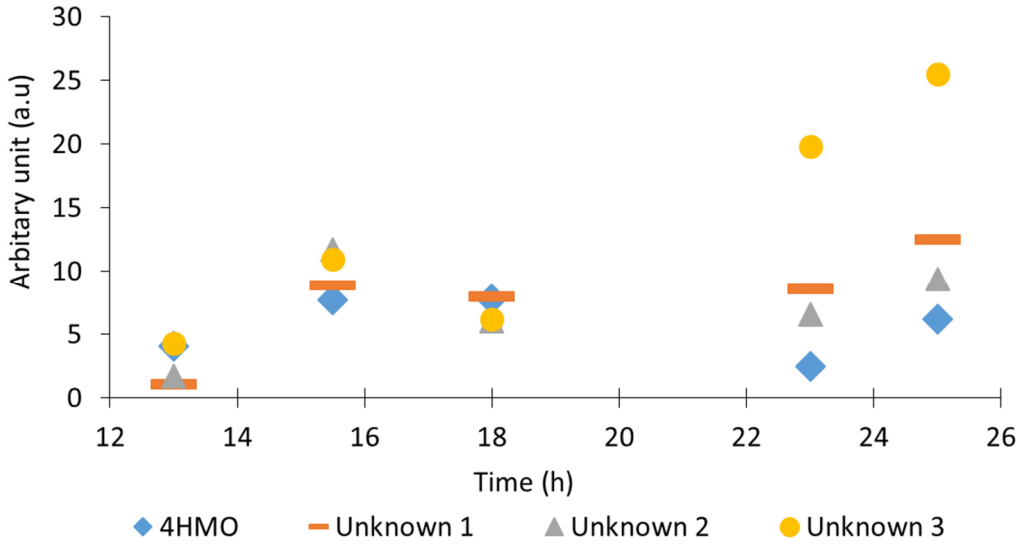

Figure 6.11. The by-products formation over time. Reaction conditions: reaction pressure = 45 bar, 6 wt.% $La_2O_2CO_3$ -CP to glycerol ratio, glycerol:methanol (80:20 mol%), 45 mmol adiponitrile, 13 to 25 h, and reaction temperature = 160 °C. By-products was measured qualitatively, value shown in the graph correspond to chromatogram peak area.

In order to corroborate the GC-MS analysis for the impact of reaction time on products formation, reaction samples taken at 13, 15.5, 18, 23 and 25 hours were also analysed using FTIR. As observed from the spectra shown in Figure 6.12, glycerol was not completely reacted during the reaction. The band at 3100 to 3500 cm^{-1} was assigned to the presence of –OH species of glycerol. It was observed that the C=O stretch (1730 cm^{-1}) was increased from 13 to 15 hours as shown in Figure 6.13. From 18 hours onward, the C=O stretch (1730 cm^{-1}) intensity decreased coincident with an increase in intensity of the band at 1790 cm^{-1}. Strong intensity of peak at 1662 cm^{-1} were observed over prolonged time. The peak at 1662 cm^{-1} was previously assigned to an amide product formed from GlyC (Indran *et al.*, 2014). This may therefore support the suggestion that the lower selectivity observed is indicative of the secondary conversion of synthesised GlyC to by-products.

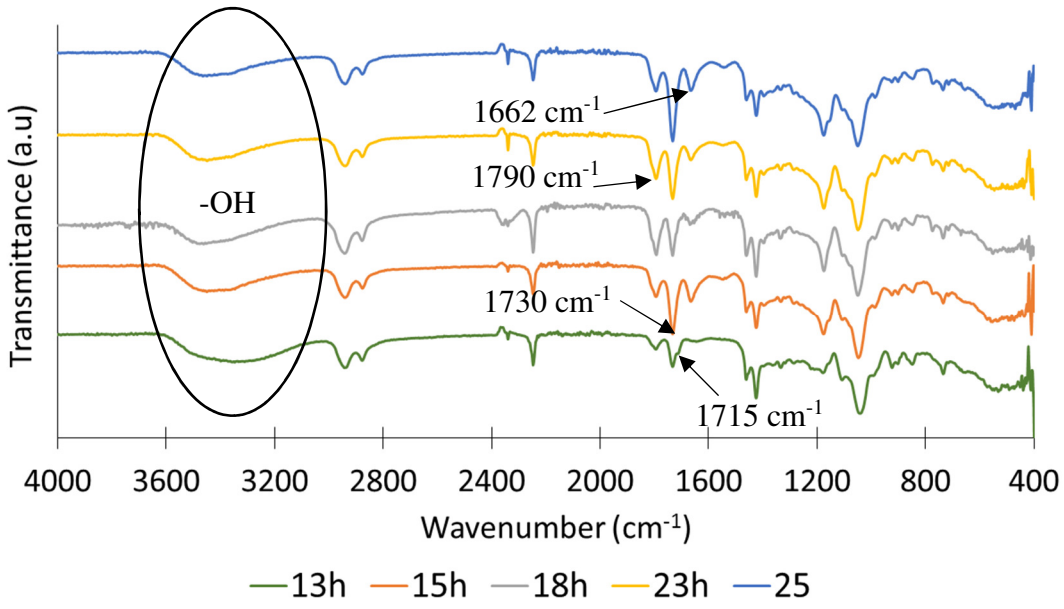

Figure 6.12. FTIR spectra for time-on-stream analysis of glycerol:methanol (80:20 mol%) over $La_2O_2CO_3$-CP from 13 to 25 h. Reaction conditions: reaction pressure = 45 bar, 6 wt.% $La_2O_2CO_3$ -CP to glycerol ratio, glycerol:methanol (80:20 mol%), 45 mmol adiponitrile, 13 to 25 h and reaction temperature = 160 °C.

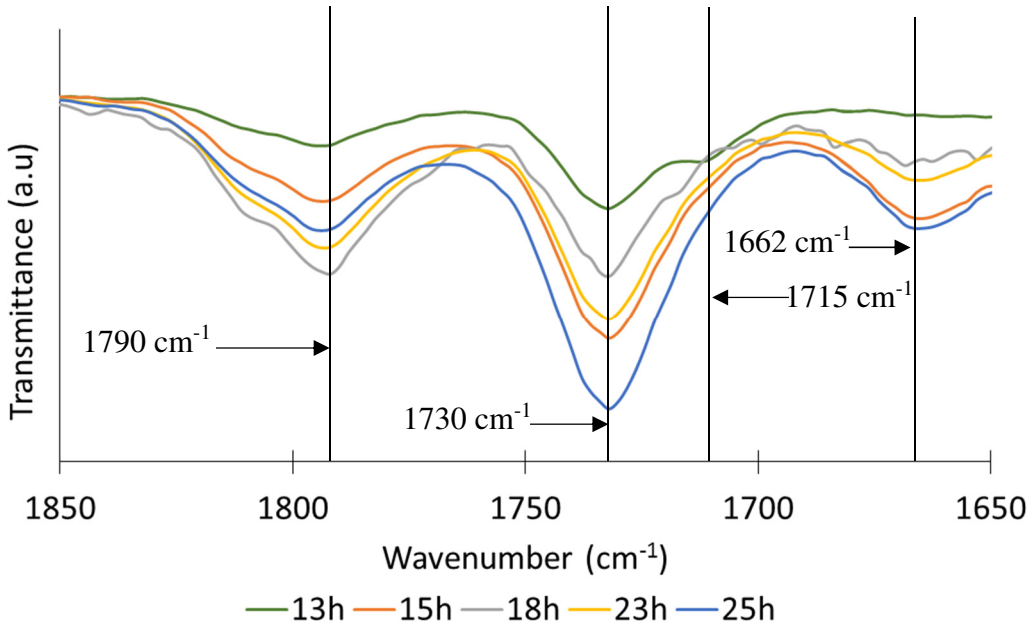

Figure 6.13. FTIR spectra for time-on-stream analysis of glycerol:methanol (80:20 mol%) over $La_2O_2CO_3$-CP from 13 to 25 h. Reaction conditions: reaction pressure = 45 bar, 6 wt.% $La_2O_2CO_3$-CP to glycerol ratio, glycerol:methanol (80:20 mol%), 45 mmol of adiponitrile and reaction temperature = for 160 °C.

6.8 **Direct carboxylation of crude glycerol to synthesise glycerol carbonate**

This work demonstrated for the first time the efficacy of La_2O_3 and $La_2O_2CO_3$ catalysts to synthesise GlyC *via* the carboxylation of crude glycerol. Direct carboxylation of crude glycerol discarded the process of glycerol separation and purification (Figure 6.14). CyclicCO_2R highlighted the four great opportunities of using crude glycerol (CyclicCO_2R, 2013):

1) Large scale of crude glycerol produce from biodiesel production (Europe approx. 800 to 1000 kt 2013).
2) Low price of crude glycerol (~ 300 €/tonne) if compared with the purified glycerol (~ 600 €/tonne).
3) The presence of impurities such as H_2O (15 to 20%), salts (7 to 15 wt.%) and organics limits the direct use of crude glycerol.

4) Some fraction of glycerol from biodiesel is purified to serve the demands of chemical industry (~ 20%).

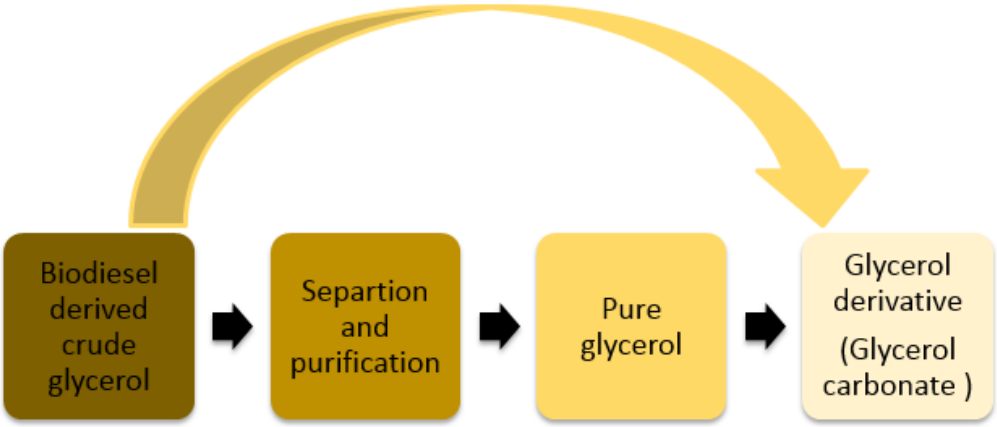

Figure 6.14. The direct transformation of glycerol carbonate from crude glycerol.

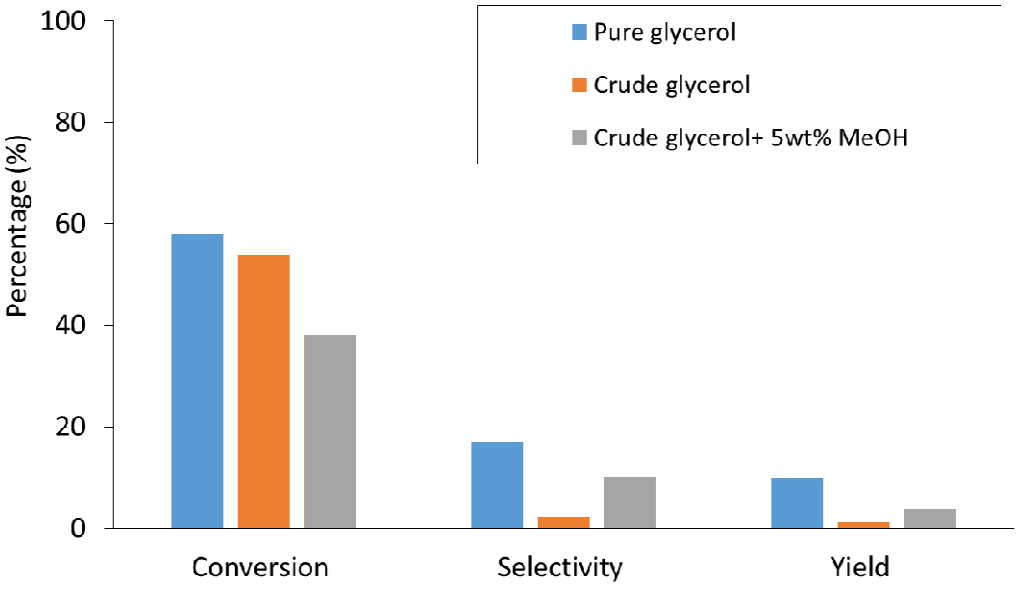

Figure 6.15. Carboxylation of pure/crude glycerol and compared with the crude glycerol mixture with added impurities. Reaction conditions: reaction pressure = 45 bar, 6 wt.% La_2O_3-C to glycerol ratio, 2.1 g crude glycerol (17 mmol glycerol), 5 wt.% methanol, 45 mmol adiponitrile, 18 h and reaction temperature = 160 °C.

Carboxylation of crude glycerol (74% purity) was carried out in the presence of La_2O_3-C and adiponitrile. The impurities present in crude glycerol have a relatively insignificant impact on glycerol conversion, which drops from 58 to 54%, however they have a stark impact upon GlyC selectivity, which drops from 17% to only 2%. This indicated that alternative reaction pathways were operating in the presence of the impurities in crude glycerol. The influence of methanol on the production of GlyC from pure glycerol was tested individually in previous section (Table 6.6). Due to the beneficial impact of methanol promoting the synthesis of GlyC, methanol was added into crude glycerol. As shown in Figure 6.15, the addition of 5 wt.% methanol to crude glycerol resulted in a decreased in glycerol conversion to 38%; this was coupled with an increased in selectivity to GlyC to 10%.

Table 6.11. Carboxylation of crude glycerol over a range of catalysts. Reaction conditions: reaction pressure = 45 bar, 6 wt.% catalyst to glycerol ratio, 2.1 g crude glycerol (17 mmol glycerol) and 45 mmol adiponitrile, 18 h and reaction temperature = 160 °C.

Crude glycerol composition	Catalyst	Conversion	Selectivity	Yield
Crude glycerol+ 5 wt.% MeOH	La_2O_3-C	38	10	4
Crude glycerol+ 5 wt.% MeOH	$La_2O_2CO_3$-CP	34	6	3
Crude glycerol+ 5 wt.% MeOH	$ZrO_2/La_2O_2CO_3/Ga_2O_3$	39	5	2

Given the observation that high selectivity to GlyC was observed from the carboxylation of pure glycerol over $La_2O_2CO_3$-CP (18%) and $ZrO_2/La_2O_2CO_3/Ga_2O_3$ (19%), the performances of these two catalysts were tested in the direct carboxylation of crude glycerol and methanol. Contrary to earlier findings, carboxylation of crude

glycerol over $ZrO_2/La_2O_2CO_3/Ga_2O_3$ and $La_2O_3CO_3$-CP produced low selectivity to GlyC, 5.1 and 5.6 respectively (Table 6.11). The reason for this low selectivity to GlyC was not clear but may be related to the composition of FAMEs in the crude glycerol. Model crude glycerol was prepared by adding only 10% methyl palmitate; while crude glycerol may consist of several type of FAMEs with higher composition.

Table 6.12. The by-products formed from the carboxylation of crude glycerol over heterogeneous catalyst in presence of methanol as the impurities. Reaction conditions: reaction pressure = 45 bar, 6 wt.% catalyst to glycerol ratio, 2.1 g crude glycerol (17 mmol glycerol), 5 wt.% methanol and 45 mmol adiponitrile, 18 h and reaction temperature = 160 °C. The by-products detected from the reaction was measured qualitatively, value shown in the graph correspond to chromatogram peak area.

By product	La_2O_3-C	$La_2O_2CO_3$-CP	$ZrO_2/La_2O_2CO_3/Ga_2O_3$
[a]Adiponitrile	450	410	364
Pentanoic acid, 5-cyano-, methyl ester	9	28	37
4HMO	1	15	4
Unknown 2	3	7	10
Unknown 3	12	10	-

[a]Adiponitrile left unreacted after the reaction.

Another possible explanation for the reduction in selectivity to GlyC may involve the high number of acid sites present on $ZrO_2/La_2O_2CO_3/Ga_2O_3$ and $La_2O_2CO_3$-CP; consistent with the hypothesis that acid catalysts favour the synthesis of 4HMO and the decomposition of GlyC (Table 6.12). Pentanoic acid 5-cyano methyl ester was observed from the GC chromatogram and analysed *via* GC-MS with compound

identification through comparison with the NIST database. It is proposed that the pentanoic acid 5-cyano- methyl ester was formed from the reaction of FAMEs with adiponitrile. The greatest quantity of adiponitrile was reacted over $ZrO_2/La_2O_2CO_3/Ga_2O_3$, 20% higher than the amount of adiponitrile reacted over La_2O_3-C. This is reflected in a four-fold increase in production of pentanoic acid 5-cyano methyl ester. Further investigation of the interplay between acid and base catalytic sites and how this affects by-product formation must be investigated. In general, the composition of crude glycerol highly affected the catalytic performance and contributed to a high quantity of by-products being synthesised. In reviewing the literature, no prior data was found on the role of FAMEs and their impact on the carboxylation of pure or crude glycerol; the separation of FAMEs and crude glycerol is therefore crucial in order to obtain high purity of crude glycerol.

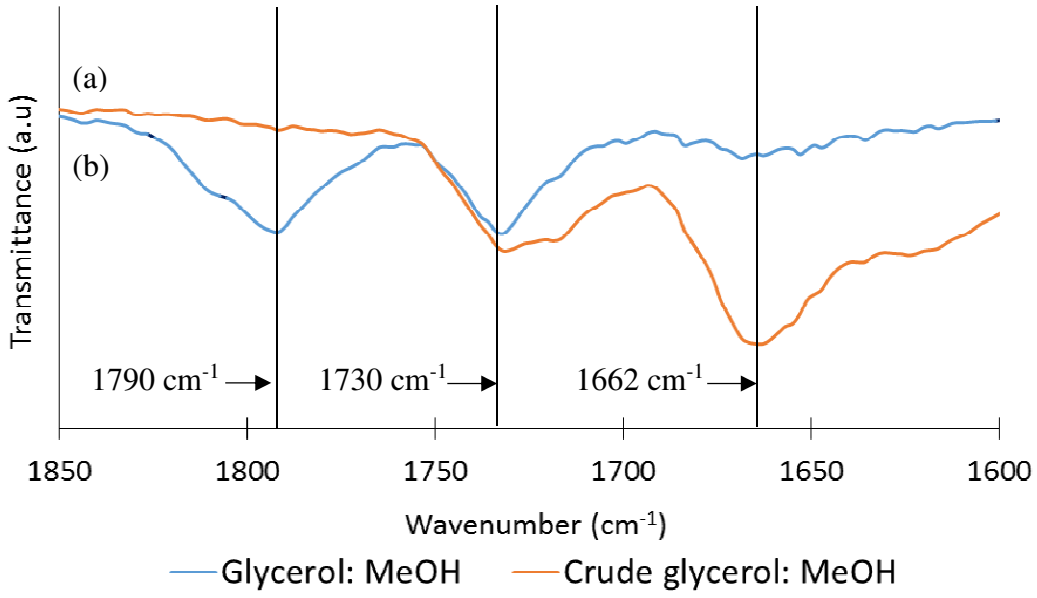

Figure 6.16. The carboxylation of (a) crude glycerol and methanol and (b) pure glycerol and methanol were studied in presence of adiponitrile. Reaction conditions: reaction pressure = 45 bar, 6 wt.% La_2O_3-C to glycerol ratio, 2.1 g crude glycerol (17 mmol glycerol) and 3.3 mmol methanol or 80:20 mol% glycerol to methanol, 45 mmol adiponitrile, 18 h and reaction temperature = 160 °C.

Figure 6.16 shows the comparison of FTIR spectra for the reaction sample of: (a) crude glycerol and methanol and (b) glycerol and methanol (80:20 mol%). The peak at 1790 cm^{-1} (GlyC) was not observed in the sample arising from crude glycerol; however strong peak intensities were observed for the peaks at 1730 cm^{-1} (4HMO) and 1662 cm^{-1}. The peak at 1662 cm^{-1} was previously assigned to an amide product formed from GlyC. This may therefore support the suggestion that the lower selectivity observed was indicative of the secondary conversion of synthesised GlyC rather than an absence of formation of this product.

6.9 **Chapter conclusions**

Impurities contained in the crude glycerol such as water, methanol, NaOMe and FAMEs are believed to limit the catalytic activity of a reaction. The impact of individual impurities on the carboxylation reaction was tested in order to gain a better understanding on how they influence this reaction. The introduction of methanol to glycerol (20:80) was investigated over La_2O_3-C; the selectivity to GlyC was found to be higher (25%) as compared to the carboxylation of pure glycerol (17%). 10 wt.% water loading significantly affected the glycerol conversion (19%) and selectivity to GlyC (3%); water caused catalyst deactivation. The highest glycerol conversion (76%), alongside low selectivity to GlyC, 1%, was observed upon the addition of FAME; co-incident with the presence of a high quantity of C=O stretch of ketone species alongside the formation of phenolic species and R-NO_2 species. It was proposed that addition of FAME limits/inhibits the formation of GlyC. The reaction was then carried out in the presence of NaOMe. Interestingly, NaOMe may also act as homogeneous catalyst, and was able to synthesise GlyC either in the presence or absence of La_2O_3-C. This however greatly reduced the selectivity to GlyC (11 and 7%) as NaOMe itself favoured the formation of 4HMO. As the impurities in crude glycerol were likely to interact with one another, the behaviour of model feedstocks containing two or more impurities were also investigated. The presence of methanol is kept constant across all model systems with glycerol and methanol in an 80:20 mol% ratio. FAME and NaOMe were added into the system. A similar trend is observed as per reaction of glycerol, methanol and FAME in comparison with the reaction of glycerol and FAME, suggesting that the presence of FAME lowered the selectivity to GlyC.

Overall, FAME and NaOMe have a negative impact on the carboxylation of crude glycerol; therefore, the separation of FAMEs and crude glycerol is crucial in order to obtain high purity of crude glycerol.

Introduction of 5 wt.% of methanol to the crude glycerol improved the selectivity to GlyC from 2% to 10, 6 and 5% in the presence of La_2O_3-C, $La_2O_2CO_3$-CP and $ZrO_2/La_2O_2CO_3/Ga_2O_3$ catalysts. These findings suggest that the acidity of catalysts plays an important role to influence product formation; where acid catalysts show a negative impact on GlyC synthesis and promote the formation of by-products. Indeed, the composition of crude glycerol itself affected the catalytic activity. This research has thrown up many questions in need of further investigation, and provide many opportunities for developing new active catalysts.

7 CONCLUSIONS AND FUTURE WORK

This chapter summarises the major conclusions of the experimental works conducted for the direct carboxylation of pure and crude glycerol over a range of heterogeneous catalysts in the presence of dehydrating agents. This field of research is new and an ongoing work and this chapter also suggests some recommendations and improvements for further studies.

7.1 Influence of heterogeneous catalysts on the carboxylation of pure glycerol

The catalysts employed herein were able to synthesise GlyC *via* the carboxylation of glycerol. This therefore provides a potential routes to utilise both abundant CO_2 and waste glycerol produced from biodiesel production. A preliminary study was carried out over ZnO, La_2O_3-C and ZnO/$La_2O_2CO_3$. ZnO/$La_2O_2CO_3$ was prepared *via* impregnation and co-precipitation methods. Of the ZnO/$La_2O_2CO_3$ catalysts, only the prepared *via* co-precipitation successfully synthesised GlyC; GlyC was not produced over ZnO/$La_2O_2CO_3$-I. Indeed, a similar extent of glycerol conversion was observed in the absence of catalyst and in the presence of ZnO/$La_2O_2CO_3$-I. The catalyst preparation methods significantly affected the BET surface area and pore volume of the catalysts.

High selectivity to GlyC (14.7%) was observed upon the introduction of La_2O_3-C, while only 7% and 11% selectivity to GlyC was observed in the presence of ZnO and ZnO/$La_2O_2CO_3$-CP respectively. BET measurements on ZnO/$La_2O_2CO_3$-CP showed a large surface area of 47 m^2/g; as compared with La_2O_3-C and ZnO, which had a surface area of 14 and 11 m^2/g respectively. It is concluded that the glycerol conversion and GlyC formation do not therefore simply correlate with the surface areas of the catalysts; however, large average pore diameter of catalysts promote the formation of by-products with large molecular diameter.

A set of $La_2O_2CO_3$-based catalysts prepared *via* co-precipitation, sol-gel and hydrothermal methods were tested for the direct carboxylation of glycerol as reported in Chapter 4. The greatest GlyC selectivity (18%) was observed over $La_2O_2CO_3$-CP, followed by La_2O_3-C, (17%), $La_2O_2CO_3$-HT, (11%), and $La_2O_2CO_3$-SG, (3%). CO_2-TPD measurements confirmed the basic properties of these catalysts, consistent with the hypothesis that basic catalysts favour the formation of GlyC.

Prior research has to-date has tended to focus on the efficacy of basic catalysts to synthesise GlyC; however, the impact of acidic catalyst and how they affect the production of products has commonly been neglected. The introduction of transition metal oxide, ZrO_2 (acidic/base) resulted in an increased of glycerol conversion from 58 to 66%. Nevertheless, it is found to be less selective to GlyC (17 to 10%) and favours the formation of 4HMO by thirty-fold in comparison to the 4HMO formed in the presence of La_2O_3-C. A high quantity of 4HMO was also observed upon the introduction of $ZrO_2/La_2O_2CO_3$ and $ZrO_2/La_2O_2CO_3/Ga_2O_3$. Work conducted thus far supports the hypothesis that the acidic sites promotes the formation of 4HMO and decomposition of GlyC.

7.2 **Influence of dehydrating agents**

The influence of acidic and basic dehydrating agents was discussed in Chapter 4. A range of dehydrating agents were employed and affected product formation (GlyC, 4HMO and acetins) in different ways. Acidic dehydrating agents favour the formation of acetins, with GlyC not observed from this reaction. Hydrolysis of acetonitrile produced acetamide and further hydrolysis occurred synthesising acetic acid. Acetic acid reacted with glycerol to synthesise mono- and diacetin. Both mono- and dicyanated dehydrating agents were employed including acetonitrile, benzonitrile and adiponitrile favouring the formation of GlyC. GlyC selectivity increased to 17% in the presence of adiponitrile while only 4 and 5% of selectivity to GlyC was observed in the presence of acetonitrile and benzonitrile. This case clearly demonstrates the importance of dehydrating agents and how they can influence product formation. It was demonstrated for the first time that adiponitrile was successfully able to assist the

synthesis of GlyC *via* carboxylation of pure and crude glycerol by shifting the reaction equilibrium to the product side; introduction of adiponitrile greatly improved both the yield and selectivity to GlyC.

7.3 Influence of impurities on catalytic activity of carboxylation of glycerol

In reviewing the literature it is noted that very few previous studies have been carried out to synthesise GlyC from crude glycerol and no data were found on the direct carboxylation of crude glycerol with CO_2 to synthesise GlyC. The study reported herein was designed to synthesis GlyC from crude glycerol in the presence of adiponitrile over heterogeneous catalysts. Crude glycerol contains a number of impurities; the impact of impurities such as water, methanol, FAME and NaOMe were first tested individually. Later, the behaviour of model feedstocks containing two or more impurities was also investigated as these impurities are likely to interact with one another. Carboxylation of pure glycerol resulted in 58% glycerol conversion and 17% selectivity to GlyC. Addition of methanol to glycerol greatly improved the GlyC selectivity; and may be related to improve mass transfer through enhancing the miscibility of glycerol and CO_2. In contrast, the addition of 1 wt.% NaOMe, 10 wt.% water and 10 wt.% FAME all have a negative impact on selectivity to GlyC reducing this to 11%, 3% and 1% respectively. A high conversion of glycerol, > 73%, and low selectivity to GlyC, > 4%, were observed upon the addition of FAME (methyl palmitate, 97%). It is assumed that the addition of FAME was promoted the glycerolysis of methyl ester. The separation of FAMEs and crude glycerol is crucial in order to obtain high purity of crude glycerol, thus improved the chances of the production of GlyC from the direct carboxylation of crude glycerol.

7.4 Direct carboxylation of crude glycerol

This is the first study reporting the successful of the direct carboxylation of crude glycerol from glycerol and CO_2 in presence of adiponitrile. La_2O_3-C was adversely affected by the impurities contained in crude glycerol where GlyC selectivity reduced from 17% to 2%. However, the selectivity to GlyC increased from 2% to 10% upon

the addition of 5 wt.% of methanol to crude glycerol. Catalytic activity of $ZrO_2/La_2O_2CO_3/Ga_2O_3$ shows a positive impact when tested in model crude glycerol with multiple impurities; therefore, the efficacy of $ZrO_2/La_2O_2CO_3/Ga_2O_3$ was tested on the direct carboxylation of crude glycerol and methanol. This test resulted in only 6% selectivity to GlyC, 4% lower than the reaction with La_2O_3-C. This finding was correlated with the amount of acid sites on $ZrO_2/La_2O_2CO_3/Ga_2O_3$ and the high quantity of pentanoic acid 5-cyano-methyl ester formed from this reaction; supported the hypothesis that acid catalysts favour the formation of by-products.

7.5 Recommendations for future work

The results obtained from this work are highly valuable and demonstrated the ability of CO_2 and glycerol to be converted into valuable chemicals: GlyC and acetins respectively. Other possible areas of future research would to be investigated are listed below:

- Running the experimental work using semi-batch or flow reactors. The comparison between batch, semi-batch and flow reactors would be interesting and beneficial in developing ways to prolong the stability of catalysts and improving the yield and selectivity to GlyC. Ongoing research is essential in order to utilise glycerol and CO_2; and thus improve the chances of GlyC synthesis being commercialised at an industrial scale.
- The influence of supercritical carbon dioxide ($scCO_2$) on the carboxylation of glycerol was not investigated in this work and it is beyond of the aim of this study. However, the use of scCO2 might help in improving the GlyC yield, catalyst lifetime, and also the reaction rate and activation of CO_2.
- Study the influence of green solvents on the carboxylation of glycerol. An alternative solvent or/and dehydrating agent is necessary to replace the function of nitrile based dehydrating agents, thus minimise the use and generation of hazardous substance.

- Studies on recyclability of catalysts as well as the recyclability of unreacted dehydrating agents are also important from the point of view of industrial (large scale) and economic application.
- The effect of mass transfer of solid catalyst in liquid and gas reactants is subject to the efficacy of the mixing and thus affects the rate of reaction and product formation. The correlation between the dehydrating agent chosen, stirring speed, concentration of reactant and time-on-stream should be studying in order to improve the success of solid catalysts to catalyse this reaction. The intersection of mass transfer and kinetics have been explored by (Machado, 2007) and could be applied to this carboxylation reaction system: (a) study the pressure profile during batch CO_2 adsorption with induction agitator and (b) study the influence of agitation on liquid and gas mass transfer coefficient.
- La_2O_3 has been used as the catalyst and is shown to improve the catalytic activity of this reaction; however it has recently been recognised as a material of limited availability with a future risk to supply. It is worthwhile to employ a more abundant element as the catalyst or as the catalyst support, such as char and ash. Char is the waste product from pyrolysis process. Identifying the by-products formed from the carboxylation of glycerol. There remain some unidentified by-products were formed from the decomposition of GlyC detected by GC-MS.
- Identifying the 4HMO isomers and reaction intermediate that formed from the carboxylation reaction. The formation of 4HMO isomers and reaction intermediate cannot be detected using a GC-MS analysis, therefore, the reaction sample must be further analysed using NMR.

REFERENCES

Ab Rahim, M. H., He, Q., Lopez-Sanchez, J. A., Hammond, C., Dimitratos, N., Sankar, M., Carley, A. F., Kiely, C. J., Knight, D. W. and Hutchings, G. J. (2012) 'Gold, palladium and gold-palladium supported nanoparticles for the synthesis of glycerol carbonate from glycerol and urea', *Catalysis Science & Technology*, 2, pp. 1914–1924.

Abboudi, M., Messali, M., Kadiri, N., Ali, A. Ben and Moran, E. (2011) 'Synthesis of CuO, La_2O_3 and La_2CuO_4 by the thermal-decomposition of oxalates precursors using a new method', *Synthesis and Reactivity in Organic, Metal-Organic and nano-Metal Chemistry*, 41, pp. 683–688.

Abu-Dahrieh, J., Rooney, D., Goguet, A. and Saih, Y. (2012) 'Activity and deactivation studies for direct dimethyl ether synthesis using CuO–ZnO–Al_2O_3 with NH_4ZSM-5, HZSM-5 or γ-Al_2O_3', *Chemical Engineering Journal*, 203, pp. 201–211.

Adeleye, A. I., Patel, D., Niyogi, D. and Saha, B. (2014) 'Efficient and greener synthesis of propylene carbonate from carbon dioxide and propylene oxide', *Industrial & Engineering Chemistry Research*, 53, p. 18647−18657.

Adhikari, S., Fernando, S. D. and Haryanto, A. (2008) 'Hydrogen production from glycerin by steam reforming over nickel catalysts', *Renewable Energy*, 33, pp. 1097–1100.

Aguayo, A. T., Ereña, J., Sierra, I., Olazar, M. and Bilbao, J. (2005) 'Deactivation and regeneration of hybrid catalysts in the single-step synthesis of dimethyl ether from syngas and CO_2', *Catalysis Today*, 106, pp. 265–270.

Algoufi, Y. T. and Hameed, B. H. (2014) 'Synthesis of glycerol carbonate by transesterification of glycerol with dimethyl carbonate over K-zeolite derived from coal fly ash', *Fuel Processing Technology*, 126, pp. 5–11.

Alper, E. and Orhan, O. Y. (2017) 'CO_2 utilization: Developments in conversion processes', *Petroleum*, 3, pp. 109–126.

Ampelli, C., Perathoner, S. and Centi, G. (2015) 'CO_2 utilization: An enabling element to move to a resource-and energy-efficient chemical and fuel production', *Philosophical Transactions of the Royal Society A: Mathematical, Physical and*

Engineering Sciences, 373, pp. 1–35.

An, X., Zuo, Y., Zhang, Q., Wang, D. and Wang, J. (2008) 'Dimethyl ether synthesis from CO_2 hydrogenation on a CuO-ZnO-Al2O_3-ZrO_2 / HZSM-5 bifunctional catalyst', *Industrial & Engineering Chemistry Research*, 47, pp. 6547–6554.

Annino, R. and Villalobos, R. (1992) *Process gas chromatography: fundamentals and applications : on-line analysis for process monitoring and control*. Research Triangle Park, NC: Instrument Society of America.

AOCS Lipid Library (2017) *X-ray powder diffractometer*, *AOCS Lipid Library*. Available at: http://lipidlibrary.aocs.org/Biochemistry/content.cfm?ItemNumber=40299 (Accessed: 1 November 2017)

Aresta, M. (2010) 'Carbon dioxide: Utilization options to reduce its ccumulation in the atmosphere', in *Carbon Dioxide as Chemical Feedstock*, pp. 1–13.

Aresta, M. and Dibenedetto, A. (2007) 'Utilisation of CO_2 as a chemical feedstock: opportunities and challenges.', *Dalton transactions*, 0, pp. 2975–92.

Aresta, M., Dibenedetto, A., Nocito, F. and Pastore, C. (2006) 'A study on the carboxylation of glycerol to glycerol carbonate with carbon dioxide: The role of the catalyst, solvent and reaction conditions', *Journal of Molecular Catalysis A: Chemical*, 257, pp. 149–153.

Ateka, A., Sierra, I., Ereña, J., Bilbao, J. and Aguayo, A. T. (2016) 'Performance of CuO–ZnO–ZrO_2 and CuO–ZnO–MnO as metallic functions and SAPO-18 as acid function of the catalyst for the synthesis of DME co-feeding CO_2', *Fuel Processing Technology*, 152, pp. 34–45.

AZO Material (2017) *Different Types of SEM Imaging – BSE and Secondary Electron Imaging*, *AZO Material*. Available at: https://www.azom.com/article.aspx?ArticleID=14309 (Accessed: 13 November 2017).

Bahruji, H., Bowker, M., Hutchings, G., Dimitratos, N., Wells, P., Gibson, E., Jones, W., Brookes, C., Morgan, D. and Lalev, G. (2016) 'Pd/ZnO catalysts for direct CO_2 hydrogenation to methanol', *Journal of Catalysis*, 343, pp. 133–146.

Baiker, A. (1999) ‘Supercritical fluids in heterogeneous catalysis.’, *Chemical Reviews*, 99, pp. 453–474.

Bancquart, S., Vanhove, C., Pouilloux, Y. and Barrault, J. (2001) ‘Glycerol transesterification with methyl stearate over solid basic catalysts: I. Relationship between activity and basicity’, *Applied Catalysis A : General*, 218, pp. 1–11.

Behrens, M. (2016) ‘Promoting the synthesis of methanol: Understanding the requirements for an industrila catalyst for thr conversion of CO_2’, *Angewandte Chemie International Edition*, 55, pp. 14906–14908.

Bienholz, A., Blume, R., Knop-gericke, A., Girgsdies, F., Behrens, M. and Claus, P. (2011) ‘Prevention of catalyst deactivation in the hydrogenolysis of glycerol by Ga_2O_3 - Modified copper/zinc oxide catalysts’, *Journal of Physical Chemistry C*, 115, pp. 999–1005.

Bond, G. C. (1974) ‘The descriptive chemistry of heterogeneous catalysis’, in *Heterogeneous Catalysis Principles and Application*. Oxford: Oxford University Press, pp. 13–39.

Boot-Handford, M. E., Abanades, J. C., Anthony, E. J., Blunt, M. J., Brandani, S., Mac Dowell, N., Fernandez, J. R., Ferrari, M.-C. M.-C., Gross, R., Hallett, J. P., Haszeldine, R. S., Heptonstall, P., Lyngfelt, A., Makuch, Z., Mangano, E., Porter, R. T. J., Pourkashanian, M., Rochelle, G. T., Shah, N., Yao, J. G., Fennell, P. S., Fernández, J. R., Ferrari, M.-C. M.-C., Gross, R., Hallett, J. P., Haszeldine, R. S., Heptonstall, P., Lyngfelt, A., Makuch, Z., Mangano, E., Porter, R. T. J., Pourkashanian, M., Rochelle, G. T., Shah, N., Yao, J. G. and Fennell, P. S. (2014) ‘Carbon capture and storage update’, *Energy & Environmental Science*, 7, pp. 130–189.

Bowker, M. (1998) *The basis and application of heterogeneous catalysis*. New York: Oxford University Press.

Cai, M., Wen, J., Chu, W., Cheng, X. and Li, Z. (2011) ‘Methanation of carbon dioxide on Ni/ZrO_2-Al_2O_3 catalysts: Effects of ZrO_2 promoter and preparation method of novel ZrO_2-Al_2O_3 carrier’, *Journal of Natural Gas Chemistry*, 20, pp. 318–324.

Camara, F., Caillol, S. and Boutevin, B. (2014) ‘Free radical polymerization study of glycerin carbonate methacrylate for the synthesis of cyclic carbonate functionalized

polymers', *European Polymer Journal*, 61, pp. 133–144.

Campanati, M., Fornasari, G. and Vaccari, A. (2003) 'Fundamental in the preparation of heterogeneous catalysts', *Catalysis Today*, 77, pp. 299–314.

Centi, G. and Perathoner, S. (2004) 'Heterogeneous catalytic reactions with CO_2: Status and perspectives', *Studies in Surface Science and Catalysis*, 153, pp. 1–8.

Chen, C.-S., Cheng, W.-H. and Lin, S.-S. (2001) 'Enhanced activity and stability of a Cu/SiO_2 catalyst for the reverse water gas shift reaction by an iron promoter', *Chemical Communications*, pp. 1770–1771.

Chen, C.-S., Cheng, W.-H. and Lin, S.-S. (2003) 'Study of reverse water gas shift reaction by TPD, TPR and CO_2 hydrogenation over potassium-promoted Cu/SiO_2 catalyst', *Applied Catalysis A: General*, 238, pp. 55–67.

Chen, C.-S., Cheng, W.-H. and Lin, S.-S. (2014) 'Study of iron-promoted Cu/SiO_2 catalyst on high temperature reverse water gas shift reaction', *Applied Catalysis A: General*, 257, pp. 97–106.

Chen, L., Wang, S., Zhou, J., Shen, Y., Zhao, Y. and Ma, X. (2014) 'Dimethyl carbonate synthesis from carbon dioxide and methanol over CeO_2 versus over ZrO_2: comparison of mechanisms', *Royal Society of Chemistry Advance*, 4, pp. 30968–30975.

Chromacademy (2013) *Theory and instrumentation of GC: Introduction to gas chromatograpy*. Available at: http://www.chromacademy.com/lms/sco10/01-Gas-chromatography-Aims-and-Objectives.html (Accessed: 1 March 2016).

Climent, M. J., Corma, A., De Frutos, P., Iborra, S., Noy, M., Velty, A. and Concepción, P. (2010) 'Chemicals from biomass: Synthesis of glycerol carbonate by transesterification and carbonylation with urea with hydrotalcite catalysts. The role of acid-base pairs', *Journal of Catalysis*, 269, pp. 140–149.

CO_2 thermodynamics (2017) *Global CCS institute*. Available at: https://hub.globalccsinstitute.com/publications/co2-liquid-logistics-shipping-concept-llsc-–-business-model-report/appendix-1-co2 (Accessed: 6 December 2016).

CO_2earth (2016) *Global carbon emmision*, *CO_2 Earth*. Available at: https://www.co2.earth/global-co2-emissions (Accessed: 30 August 2016).

CO_2now (2017) *The most current CO_2 data on earth*. Available at: http://co2now.org/Current-CO2/CO2-Now/global-co2-board.html (Accessed: 30 September 2017).

Collins, S. E., Chiavassa, D. L., Bonivardi, A. L. and Baltanás, M. A. (2005) 'Hydrogen spillover in Ga_2O_3-Pd/SiO_2 catalysts for methanol synthesis from CO_2/H_2', *Catalysis Letters*, 103, pp. 83–88.

Cullity, B. D. and Stock, S. R. (2001) *Elements of x-ray diffraction*. Prentice Hall. Available at: http://books.google.co.uk/books/about/Elements_of_X_ray_Diffraction.html?id=IiXwAAAAMAAJ&pgis=1 (Accessed: 20 August 2014).

CyclicCO_2R (2013) *Production of cyclic carbonates from CO_2 using renewable feedstocks*. Available at: http://www.cyclicco2r.eu/wp-content/uploads/2013/03/Kimball_ECCE9_CyclicCO2R.pdf (Accessed: 6 February 2016).

Dadgar, F., Myrstad, R., Pfeifer, P., Holmen, A. and Venvik, H. J. (2016) 'Direct dimethyl ether synthesis from synthesis gas: The influence of methanol dehydration on methanol synthesis reaction', *Catalysis Today*, 270, pp. 76–84.

Dalil, M., Carnevali, D., Edake, M., Auroux, A., Dubois, J.-L. and Patience, G. S. (2016) 'Gas phase dehydration of glycerol to acrolein: Coke on WO_3/TiO_2 reduces by-products', *Journal of Molecular Catalysis A: Chemical*, 421, pp. 146–155.

Daza, Y. and Kuhn, J. N. (2016) 'CO_2 conversion by reverse water gas shift catalysis: Comparison of catalysts and mechanisms and their consequences for CO_2 conversion to liquid fuels', *Royal Society of Chemistry Advance*, 6, pp. 49675–49691.

Dewajani, H., Rochmadi, Purwono, S. and Budiman, A. (2016) 'Effect of modification ZSM-5 catalyst in upgrading quality of organic liquid product derived from catalytic cracking of Indonesian Nyamplung Oil (Calophyllum inophyllum)', *AIP Conference Proceedings*, 1755, pp. 1–6.

Dibenedetto, A., Angelini, A. and Stufano, P. (2014) 'Use of carbon dioxide as feedstock for chemicals and fuels: homogeneous and heterogeneous catalysis', *Journal of Chemical Technology & Biotechnology*, 89, pp. 334–353.

Donga, X., Li, F., Zhao, N., Xiao, F., Wang, J. and Tan, Y. (2016) 'CO_2 hydrogenation

to methanol over Cu/ZnO/ZrO_2 catalysts prepared by precipitation-reduction method', *Applied Catalysis B: Environmental*, 191, pp. 8–17.

Du, G., Lim, S., Yang, Y., Wang, C., Pfefferle, L. and Haller, G. L. (2007) 'Methanation of carbon dioxide on Ni-incorporated MCM-41 catalysts: The influence of catalyst pretreatment and study of steady-state reaction', *Journal of Catalysis*, 249, pp. 370–379.

Duan, P.-G., Niu, Y.-L., Wang, Y.-Y. and Dai, L.-Y. (2008) 'Hydrolysis of adiponitrile in near critical water', *Chinese Journal of Chemistry*, 26, pp. 1741–1744.

Duckett, S. and Gilbert, B. (2000) 'Infra-red spectroscopy', in *Foundation of Spectroscopy*. New York: Oxford University Press, pp. 23–42.

Dutrow, B. L. and Clark, C. M. (2017) *X-ray powder diffraction*, *Geochemical instrumentation and analysis*. Available at: https://serc.carleton.edu/research_education/geochemsheets/techniques/XRD.html (Accessed: 13 November 2017).

Falconer, J. (1980) 'Adsorption and methanation of carbon dioxide on a nickel/silica catalyst', *Journal of Catalysis*, 62, pp. 280–285.

Ferreira, P., Fonseca, I. M., Ramos, A. M., Vital, J. and Castanheiro, J. E. (2009) 'Esterification of glycerol with acetic acid over dodecamolybdophosphoric acid encaged in USY zeolite', *Catalysis Communications*, 10, pp. 481–484.

Ferretti, C. A., Apesteguía, C. R. and Cosimo, J. I. Di (2011) 'MgO-based catalysts for monoglyceride synthesis from methyl oleate and glycerol: Effect of Li promotion', *Applied Catalysis A: General*, 399, pp. 146–153.

Figueiredo, J. lLis (2008) 'Heterogeneous catalysis: An overview', in *Catalysis from Theory to Application- An Intergrated Course*. Maio: Coimbra University Press, pp. 1–29.

Fleish, T., McCarthy, C., Basu, A. and Udovich, A. (1995) 'A new clean diesel technology: demonstration of ULEV emissions on a Navistar diesel engine fueled with dimethyl ether', *Society of Automotive Engineers Technical Paper Series*, 1129, pp. 39–50.

Fogler, H. S. (2006) *Elements of chemical reaction engineering*. Upper Saddle River,

NJ: Pearson International Edition.

Fonseca, I. M. de F. L. da (2008) 'Bulk catalysts', in *Catalysis from Theory to Application- An Intergrated Course*. Maio: Imprensa Da Universidade De Coimbra, pp. 33–52.

Frusteri, F., Bonura, G., Cannila, C., Ferrante, G. D., Aloise, A. and Catizzone, E. (2015) 'Stepwise tuning of metal-oxide and acid sites of CuZnZr-MFI hybrid catalysts for the direct DME synthesis by CO_2 hydrogenation', *Applied Catalysis B: Environmental*, 176, pp. 522–531.

Fujita, S., Arai, M. and Bhanage, B. M. (2014) 'Direct transformation of carbon dioxide to value-added products over heterogeneous catalysts', in *Transformation and Utilization of Carbon Dioxide, Green Chemistry and Sustainable Technology*. Springer-Verlag Berlin Heidelberg, pp. 39–53.

Fujita, S., Nakamura, M., Doi, T. and Takezawa, N. (1993) 'Mechanisms of methanation of carbon dioxide and carbon monoxide over nickel/alumina catalysts', *Applied Catalysis A: General*, 104, pp. 87–100.

Fujitani, T., Saito, M., Kanai, Y., Watanabe, T., Nakamura, J. and Uchijima, T. (1995) 'Development of an active Ga_2O_3 supported palladium catalyst for the synthesis of methanol from carbon dioxide and hydrogen', *Applied Catalysis A: General*, 125, pp. 199–202.

Gangwar, B. P., Palakollu, V., Singh, A., Kanvah, S. and Sharma, S. (2014) 'Combustion synthesized La_2O_3 and $La(OH)_3$: Recyclable catalytic activity towards Knoevenagel and Hantzsch reactions', *Royal Society of Chemistry Advances*, 4, pp. 55407–55416.

Gao, P., Yang, H., Zhang, L., Zhang, C., Zhong, L., Wang, H., Wei, W. and Sun, Y. (2016) 'Fluorinated Cu/Zn/Al/Zr hydrotalcites derived nanocatalysts for CO_2 hydrogenation to methanol', *Journal of CO_2 Utilization*, 16, pp. 32–41.

Garbarino, G., Riani, P., Magistri, L. and Busca, G. (2014) 'A study of the methanation of carbon dioxide on Ni/Al_2O_3 catalysts at atmospheric pressure', *International Journal of Hydrogen Energy*, 39, pp. 11557–11565.

Gas Encyclopedia (2016) *Air Liquide*. Available at: http://encyclopedia.airliquide.com/encyclopedia.asp?GasID=26 (Accessed: 10

December 2016).

Ghoreishi, K. B. and Yarmo, M. A. (2013) 'Sol-gel sulfated silica as a catalyst for glycerol acetylation with acetic acid', *Journal of Science and Technology*, pp. 65–78.

Global energy trends – BP statistical review 2014 (2014) *Energy Matters*. Available at: http://euanmearns.com/global-energy-trends-bp-statistical-review-2014/ (Accessed: 12 October 2016).

Goeppert, A., Czaun, M., Jones, J.-P., Surya Prakash, G. K. and Olah, G. A. (2014) 'Recycling of carbon dioxide to methanol and derived products – closing the loop', *Chemical Society Reviews*, 43, pp. 7995–8048.

GPS Instrument Ltd. (2017) *Measuring principle Karl Fischer titration*, *GPS Instrument Ltd.* Available at: https://www.gpsil.co.uk/our-products/karl-fischer-titrators/measuring-principle/#affixMenu8 (Accessed: 13 November 2017).

Guo, M. and Lu, G. (2014) 'The difference of roles of alkaline-earth metal oxides on silica-supported nickel catalysts for CO_2 methanation', *Royal Society of Chemistry Advance*, 4, pp. 58171–58177.

Gupta, M. K. and O'Sullivan, T. P. (2013) 'Recent applications of gallium and gallium halides as reagents in organic synthesis', *Royal Society of Chemistry Advance*, 3, pp. 25498–25522.

Hammond, C., Lopez-Sanchez A., J., Ab Rahim, M. H., Dimitratos, N., Jenkins L., R., Carley F., A., He, Q., Kiely J., C., Knight W., D. and Hutchings, G. J. (2011) 'Synthesis of glycerol carbonate from glycerol and urea with gold-based catalysts', *Dalton Transactions*, 40, pp. 3927–3937.

Homs, N., Toyir, J. and Piscana, P. R. de la (2013) 'Catalytic processes for activation of CO_2', in *New and Future Developments in Catalysis Activation of Carbon Dioxide*. Elsevier B.V., pp. 1–26.

Honda, M., Tamura, M., Nakao, K., Suzuki, K., Nakagawa, Y. and Tomishige, K. (2014) 'Direct cyclic carbonate synthesis from CO_2 and diol over carboxylation/hydration cascade catalyst of CeO_2 with 2-cyanopyridine', *American Chemical Society Catalysis*, 4, pp. 1893–1896.

Hou, Y.-H., Han, W.-C., Xia, W.-S. and Wan, H.-L. (2015) 'Structure sensitivity of

$La_2O_2CO_3$ catalysts in the oxidative coupling of methane', *American Chemical Society Catalysis*, 5, pp. 1663–1674.

Hu, S., Luo, X., Wan, Ca. and Li, Y. (2012) 'Characterisation of crude glycerol from biodiesel plant', *Journal of Agricultural and Food Chemistry*, 60, pp. 5915–5921.

Hu, W., Zhang, Y., Huang, Y., Wang, J., Gao, J. and Xu, J. (2015) 'Selective esterification of glycerol with acetic acid to diacetin using antimony pentoxide as reusable catalyst', *Journal of Energy Chemistry*. Elsevier B.V., 24, pp. 632–636.

Huang, C.-H. (2014) 'A review: CO_2 utilization', *Aerosol and Air Quality Research*, 14, pp. 480–499.

Huntsman (2016) *Glycerine carbonate in beauty & personal care*, *www.huntsman.com*. Available at: http://www.huntsman.com/performance_products/Media Library/a_MC348531CFA3EA9A2E040EBCD2B6B7B06/Home_MC348531CFA8BA9A2E040EBCD2B6B7B06/Functional Chemicals_M4667C4C202148ACBE053D96BEBCD2D43/Beauty personal ca_M46647F551109F5F8E053D96BEBCD1EDB/files/JEFFS (Accessed: 26 July 2017).

Hutchings, G. J. and Vedrine, J. C. (2004) 'Heterogeneous catalyst preparation', in *Basic Principles in Applied Catalysis*. Heidelberg, Berlin: Springer-Verlag Berlin Heidelberg, pp. 217–255.

Ibrahim, M. Y., Ghazali, Z. and Rahman, H. U. (2016) 'The feasibility of carbon capturing, storage and utilization projects in developing countries: A case of Malaysia', *International Journal of Economics and Financial Issues*, 6, pp. 6–11.

Indran, V. P., Saud, A. S. H., Maniam, G. P., Taufiq-Yap, Y. H. and Rahim, M. H. A. (2016) 'Viable glycerol carbonate synthesis through direct crude glycerol utilization from biodiesel industry', *Waste and Biomass Valorization*, pp. 1–11.

Indran, V. P., Syuhada Zuhaimi, N. A., Deraman, M. A., Maniam, G. P., Yusoff, M. M., Yun Hin, T.-Y. and Ab. Rahim, M. H. (2014) 'An accelerated route of glycerol carbonate formation from glycerol using waste boiler ash as catalyst', *Royal Society of Chemistry Advance*, 4, pp. 25257–25267.

Ishak, Z. I., Sairi, N. A., Alias, Y., Aroua, M. K. T. and Yusoff, R. (2016) 'Production

of glycerol carbonate from glycerol with aid of ionic liquid as catalyst', *Chemical Engineering Journal*, 297, pp. 128–138.

Jacquemin, M., Beuls, A. and Ruiz, P. (2010) 'Catalytic production of methane from CO_2 and H_2 at low temperature: Insight on the reaction mechanism', *Catalysis Today*, 157, pp. 462–466.

Jagadeeswaraiah, K., Kumar, C. R., Prasad, P. S. S., Loridant, S. and Lingaiah, N. (2014) 'Synthesis of glycerol carbonate from glycerol and urea over tin-tungsten mixed oxide catalysts', *Applied Catalysis A: General*, 469, pp. 165–172.

Jiang, Z., Xiao, T., Kuznetsov, V. L. and Edwards, P. P. (2010) 'Turning carbon dioxide into fuel.', *Philosophical Transactions of the Royal Society A: Mathematical Physical and Engineering Sciences*, 368, pp. 3343–64.

Joo, O.-S., Jung, K.-D., Moon, I., Rozovskii, A. Y., Lin, G. I., Han, S.-H. and Uhm, S.-J. (1999) 'Carbon dioxide hydrogenation to form methanol via a reverse water gas shift reaction (The CAMERE Process)', *Industrial & Engineering Chemistry Research*, 38, pp. 1808–1812.

Joshi, H., Moser, B. R., Toler, J. and Walker, T. (2010) 'Preparation and fuel properties of mixtures of soybean oil methyl and ethyl esters', *Biomass and Bioenergy*, 34, pp. 14–20.

Jung, K. T. and Bell, A. T. (2001) 'An in situ infrared study of dimethyl carbonate synthesis from carbon dioxide and methanol over zirconia', *Journal of Catalysis*, 204, pp. 339–347.

Kale, S., Armbruster, U., Umbarkar, S., Dongare, M. and Martin, A. (2013) 'Esterification of glycerol with acetic acid for improved production of triacetin using toluene as an entrainer', in *10th Green Chemistry Conference*, pp. 70–71.

Kharaji, A. G., Shariati, A. and Takassi, M. A. (2013) 'A novel γ-Alumina supported Fe-Mo bimetallic catalyst for reverse water gas shift reaction', *Chinese Journal of Chemical Engineering*, 21, pp. 1007–1014.

Kim, I., Kim, J. and Lee, D. (2014) 'A comparative study on catalytic properties of solid acid catalysts for glycerol acetylation at low temperatures', *Applied Catalysis B: Environmental*, 148–149, pp. 295–303.

Knothe, G. (2008) '"Designer" biodiesel: Optimizing fatty ester composition to improve fuel properties', *Energy & Fuels*, 22, pp. 1358–1364.

Kong, P. S., Aroua, M. K., Daud, Wan, W. M. A., Lee, H. V., Cognetc, P. and Peres, Y. (2016) 'Catalytic role of solid acid catalysts in glycerol acetylation for the production of bio-additives: a review', *Royal Society of Chemistry Advance*, 6, pp. 68885–68905.

Konwar, L. J., Mäki-Arvela, P., Begum, P., Kumar, N., Thakur, A. J., Mikkola, J. P., Deka, R. C. and Deka, D. (2015) 'Shape selectivity and acidity effects in glycerol acetylation with acetic anhydride: Selective synthesis of triacetin over Y-zeolite and sulfonated mesoporous carbons', *Journal of Catalysis*, 329, pp. 237–247.

Kulawska, M. and Madej-Lachowska, M. (2013) 'Copper/zinc catalysts in hydrogenation of carbon oxides', *Chemical and Process Engineering*, 34, pp. 479–496.

Lee, H. J., Joe, W., Jung, J. C. and Song, I. K. (2012) 'Direct synthesis of dimethyl carbonate from methanol and carbon dioxide over Ga_2O_3-CeO_2-ZrO_2 catalysts prepared by a single-step sol-gel method: Effect of acidity and basicity of the catalysts', *Korean Journal of Chemical Engineering*, 29(8), pp. 1019–1024. doi: 10.1007/s11814-012-0017-0.

Lee, H. J., Park, S., Song, I. K. and Jung, J. C. (2011) 'Direct synthesis of dimethyl carbonate from methanol and carbon dioxide over $Ga_2O_3/Ce_{0.6}Zr_{0.4}O_2$ catalysts: Effect of acidity and basicity of the catalysts', *Catalysis Letters*, 141(4), pp. 531–537.

Lee, H. V., Juan, J. C. and Tau, Y. H. (2015) 'Preparation and application of binary acid-base CaO-La_2O_3 catalyst for biodiesel production', *Renewable Energy*, 74, pp. 124–132.

Leofanti, G., Tozzola, G., Padovan, M., Petrini, G., Bordiga, S. and Zecchina, A. (1997) 'Catalyst characterization: characterization techniques', *Catalysis Today*, 34, pp. 307–327.

Levy, J. M. (2007) *GC Fundamental*, *Chrome Academy*. Available at: http://www.chromacademy.com/lms/webcasts/presentation/06/load.html (Accessed: 14 November 2017).

Li, C., Yuan, X. and Fujimoto, K. (2014) 'Development of highly stable catalyst for

methanol synthesis from carbon dioxide', *Applied Catalysis A: General*, 469, pp. 306–311.

Li, F., Li, H., Wang, L., He, P. and Cao, Y. (2015) 'Magnesium oxide nanosheets as effective catalysts for the synthesis of diethyl carbonate from ethyl carbamate and ethanol', *Catalysis Science & Technology*, 5, pp. 1021–1034.

Li, H., Gao, D., Gao, P., Wang, F., Zhao, N., Xiao, F., Wei, W. and Sun, Y. (2013) 'The synthesis of glycerol carbonate from glycerol and CO_2 over $La_2O_2CO_3$–ZnO catalysts', *Catalysis Science & Technology*, 3, pp. 2801–2809.

Li, H., Jiao, X., Li, L., Zhao, N., Xiao, F., Wei, W., Sun, Y. and Zhang, B. (2015) 'Synthesis of glycerol carbonate by direct carbonylation of glycerol with CO_2 over solid catalysts derived from Zn/Al/La and Zn/Al/La/M (M = Li, Mg and Zr) hydrotalcites', *Catalysis Science & Technology*, 5, pp. 989–1005.

Li, H., Xin, C., Jiao, X., Zhao, N., Xiao, F., Li, L., Wei, W. and Sun, Y. (2015) 'Direct carbonylation of glycerol with CO_2 to glycerol carbonate over Zn/Al/La/X (X = F, Cl, Br) catalysts: The influence of the interlayer anion', *Journal of Molecular Catalysis A: Chemical*, 402, pp. 71–78.

Liao, X., Zhu, Y., Wang, S.-G., Chen, H. and Li, Y. (2010) 'Theoretical elucidation of acetylating glycerol with acetic acid and acetic anhydride', *Applied Catalysis B: Environmental*, 94, pp. 64–70.

Lim, J. Y., McGregor, J., Sederman, A. J. and Dennis, J. S. (2016) 'Kinetic studies of CO_2 methanation over a Ni/γ-Al_2O_3 catalyst using a batch reactor', *Chemical Engineering Science*, 141, pp. 28–45.

Limaa, S. H., Forrester, A. M. S., Palacio, L. A. and Faro, A. C. (2014) 'Niobia-alumina as methanol dehydration component in mixed catalyst systems for dimethyl ether production from syngas', *Applied Catalysis A: General*, 488, pp. 19–27.

Lin, P.-C., Lin, S., Wang, P. C. and Sridhar, R. (2014) 'Techniques for physicochemical characterization of nanomaterials', *National Institute of Health*, 32, pp. 711–726.

Liu, C., Guo, X., Guo, Q., Mao, D., Yu, J. and Lu, G. (2016) 'Methanol synthesis from CO_2 hydrogenation over copper catalysts supported on MgO-modified TiO_2', *Journal of Molecular Catalysis A: Chemical*, 425, pp. 86–93.

Liu, J., Li, Y., Zhang, J. and He, D. (2016) 'Glycerol carbonylation with CO_2 to glycerol carbonate over CeO_2 catalyst and the influence of CeO_2 preparation methods and reaction parameters', *Applied Catalysis A: General*, 513, pp. 9–18.

Liu, Z., Wang, J., Kang, M., Yin, N., Wang, X., Tan, Y. and Zhu, Y. (2015) 'Structure-activity correlations of $LiNO_3/Mg_4AlO_{5.5}$ catalysts for glycerol carbonate synthesis from glycerol and dimethyl carbonate', *Journal of Industrial and Engineering Chemistry*, 21, pp. 394–399.

Llewellyn, P. L., Bloch, E. and Bourrelly, S. (2012) 'Surface area/porosity, adsorption and diffusion', in *Characterization of solid materials and heterogeneous catalysts-From structure to surface reactivity*. Wiley-VCH, pp. 853–880.

Lok, M. (2009) 'Coprecipitation', in *Synthesis of solid catalytsts*. Weinheim: Wiley-VCH, pp. 135–149.

LPD Lab Services (2017) *FTIR / Fourier transform infra-red spectrophotometer*. Available at: https://www.lpdlabservices.co.uk/analytical_techniques/chemical_analysis/ftir.php (Accessed: 13 November 2017).

Lu, B. and Kawamoto, K. (2014) 'Transition metal-rich mesoporous silicas and their enhanced catalytic properties', *Catalysis Science & Technology*, 4, pp. 4313–4321.

Machado, R. M. (2007) *Fundamentals of mass transfer and kinetics for the hydrogentaion of nitrobenzene and aniline*, *Air Products and Chemical Inc.*

Malyaadri, M., Jagadeeswaraiah, K., Sai Prasad, P. S. and Lingaiah, N. (2011) 'Synthesis of glycerol carbonate by transesterification of glycerol with dimethyl carbonate over Mg/Al/Zr catalysts', *Applied Catalysis A : General*, 401, pp. 153–157.

Manjunathan, P., Ravishankar, R. and Shanbhag, G. V. (2016) 'Novel bifunctional Zn–Sn composite oxide catalyst for the selective synthesis of glycerol carbonate by carbonylation of glycerol with urea', *ChemCatChem*, 8, pp. 631–639.

Mao, D., Yang, W., Xia, J., Zhang, B., Song, Q. and Chen, Q. (2005) 'Highly effective hybrid catalyst for the direct synthesis of dimethyl ether from syngas with magnesium oxide-modified HZSM-5 as a dehydration component', *Journal of Catalysis*, 230, pp. 140–149.

Marakatti, V. S. and Halgeri, A. B. (2015) 'Metal ion-exchanged zeolites as highly active solid acid catalysts for the green synthesis of glycerol carbonate from glycerol', *Royal Society of Chemistry Advance*, 5, pp. 14286–14293.

Mekki-Berrada, A. and Aurox, A. (2012) 'Thermal methods', in *Characterization of Solid Materials and Heterogeneous Catalysts- From Structure to Surface Reactivity*. Wiley-VCH. Weinheim, pp. 747–854.

Melian-Cabrera, I., Granados, M. L. and Fierro, J. L. G. (2002) 'Effect of Pd on Cu-Zn catalysts for the hydrogenation of CO_2 to methanol: Stabilization of Cu metal against CO_2 oxidation', *Catalysis Letters*, 79, pp. 165–170.

Metz, B., Davidson, O., Connick, H. De, Loos, M. and Meyer, L. (2005) *IPPC special report on carbon dioxide capture and storage*. New York: Cambridge University Press.

Mikkelsen, M., Jørgensen, M. and Krebs, F. C. (2010) 'The Teraton Challenge. A Review of Fixation and Transformation of Carbon Dioxide', *Energy & Environmental Science*, 3, pp. 43–81.

Mitran, G., Pavel, O. D., Florea, M., Mieritz, D. G. and Seo, D.-K. (2016) 'Hydrogen production from glycerol steam reforming over molybdena–alumina catalysts', *Catalysis Communications*, 77, pp. 83–88.

Mu, Q. and Wang, Y. (2011) 'Synthesis, characterization, shape-preserved transformation, and optical properties of $La(OH)_3$, $La_2O_2CO_3$, and La_2O_3 nanorods', *Journal of Alloys and Compounds*, 509, pp. 396–401.

Mufrodi, Z., Rochmadi, Sutijan and Budiman, A. (2014) 'Synthesis acetylation of glycerol using batch reactor and continuous reactive distillation column', *Engineering Journal*, 18, pp. 29–39.

Mumford, K. A., Wu, Y., Smith, K. H. and Stevens, G. (2015) 'Review of solvent based carbon-dioxide capture technologies', *Frontiers of Chemical Science and Engineering*, 9, pp. 125–141.

Munnik, P., Jongh, P. E. de and Jong, K. P. de (2015) 'Recent developments in the synthesis of supported catalysts', *Chemical Reviews*, 115, pp. 6687–6718.

Nanda, M., Yuan, Z. and Qin, W. (2014) 'Purification of crude glycerol using

acidification: effects of acid types and product characterization', *Austin Chemical Engineering*, 1, pp. 1–7.

Narkhede, N. and Patel, A. (2015) 'Facile synthesis of glycerol carbonate via glycerolysis of urea catalysed by silicotungstates impregnated into MCM-41', *Royal Society of Chemistry Advance*, 5, pp. 52801–52808.

Nerozzi, F. (2012) 'Heterogeneous catalytic hydrogenation', *Platinum Metals Review*, 56, pp. 236–241.

Nguyen-Phu, H., Park, C. Y. and Eun, W. S. (2016) 'Activated red mud-supported Zn/Al oxide catalysts for catalytic conversion of glycerol to glycerol carbonate: FTIR analysis', *Catalysis Communications*, 85, pp. 52–56.

Nohra, B., Candy, L., Blanco, J.-F., Raoul, Y. and Mouloungui, Z. (2012) 'Aminolysis reaction of glycerol carbonate in organic and hydroorganic medium', *Journal of the American Chemical Society*, 89, pp. 1125–1133.

Nunes, A. V. M., Carrera, G. V. S. M., Najdanovic-Visak, V. and Nunes Da Ponte, M. (2013) 'Solubility of CO_2 in glycerol at high pressures', *Fluid Phase Equilibria*, 358, pp. 105–107.

Ocampo, F., Louis, B. and Roger, A.-C. (2009) 'Methanation of carbon dioxide over nickel-based $Ce_{0.72}Zr_{0.28}O_2$ mixed oxide catalysts prepared by sol–gel method', *Applied Catalysis A: General*, 369, pp. 90–96.

Ochoa-Gómez, J. R., Gómez-Jiménez-Aberasturi, O., Ramírez-López, C. a., Nieto-Mestre, J., Maestro-Madurga, B. and Belsué, M. (2011) 'Synthesis of glycerol carbonate from 3-chloro-1,2-propanediol and carbon dioxide using triethylamine as both solvent and CO_2 fixation–activation agent', *Chemical Engineering Journal*, 175, pp. 505–511.

Okoye, P. U., Abdullah, A. Z. and Hameed, B. H. (2017) 'Stabilised ladle furnace steel slag for glycerol carbonate synthesis via glycerol transesterification reaction with dimethyl carbonate', *Energy Conversion and Management*, 133, pp. 477–485.

Okoye, P. U. and Hameed, B. H. (2016) 'Review on recent progress in catalytic carboxylation and acetylation of glycerol as a byproduct of biodiesel production', *Renewable and Sustainable Energy Reviews*, 53, pp. 558–574.

Olah, G. a, Goeppert, A. and Prakash, G. K. S. (2009) 'Chemical recycling of carbon dioxide to methanol and dimethyl ether: from greenhouse gas to renewable, environmentally carbon neutral fuels and synthetic hydrocarbons.', *The Journal of Organic Chemistry*, 74, pp. 487–98.

Olajire, A. a. (2013) 'Valorization of greenhouse carbon dioxide emissions into value-added products by catalytic processes', *Journal of CO_2 Utilization*, 3–4, pp. 74–92.

Owen, R. E., O'Byrne, J. P., Mattia, D., Plucinski, P., Pascu, S. I. and Jones, M. D. (2013) 'Promoter effects on iron–silica Fischer–Tropsch nanocatalysts: Conversion of carbon dioxide to lower olefins and hydrocarbons at atmospheric pressure', *ChemPlusChem*, 78, pp. 1536–1544.

Owen, R. E., Plucinski, P., Mattia, D., Torrente-Murciano, L., Ting, V. P. and Jones, M. D. (2016) 'Effect of support of Co-Na-Mo catalysts on the direct conversion of CO_2 to hydrocarbons', *Journal of CO_2 Utilization*, 16, pp. 97–103.

Ozorio, L. P., Pianzolli, R., Da Cruz MacHado, L., Miranda, J. L., Turci, C. C., Guerra, A. C. O., Souza-Aguiar, E. F. and Mota, C. J. A. (2015) 'Metal-impregnated zeolite y as efficient catalyst for the direct carbonation of glycerol with CO_2', *Applied Catalysis A: General*, 504, pp. 187–191.

Park, J. N. and McFarland, E. W. (2009) 'A highly dispersed Pd-Mg/SiO_2 catalyst active for methanation of CO_2', *Journal of Catalysis*, 266, pp. 92–97.

Particle Technology Lab (2017) *BET surface area analysis*, *Particle Lab Technology*. Available at: https://www.particletechlabs.com/analytical-testing/gas-adsorption-porosimetry-analyses/bet-specific-surface-area (Accessed: 5 December 2017).

Patel, A. and Singh, S. (2014) 'A green and sustainable approach for esterification of glycerol using 12-tungstophosphoric acid anchored to different supports: Kinetics and effect of support', *Fuel*, 118, pp. 358–364.

Patil, Y. P., Tambade, P. J., Jagtap, S. R. and Bhanage, B. M. (2009) 'Carbon dioxide: a renewable feedstock for the synthesis of fine and bulk chemicals', *Frontiers of Chemical Engineering in China*, 4, pp. 213–235.

Pavia, D. L., Lampman, G. M., Kriz, G. S. and Vyvyan, J. R. (2009) *Introduction to spectroscopy*. California: Brooks/Cole.

Perego, C. and Villa, P. (1997) 'Catalyst preparation methods', 34, pp. 281–305.

Perkin Elmer (2014) *The 30 minute guide to ICP-MS: Technical note ICP mass spectrometry*, *Perkin Elmer*. Available at: https://www.perkinelmer.com/CMSResources/Images/44-74849tch_icpmsthirtyminuteguide.pdf (Accessed: 13 November 2017).

Pinto, L. F., Ndiaye, P. M., Ramos, L. P. and Corazza, M. L. (2011) 'Phase equilibrium data of the system CO_2+glycerol+methanol at high pressures', *The Journal of Supercritical Fluids*, 59, pp. 1–7.

Pons, A., Jouin, J., Bechade, E., Julien, I., Masson, O., Geffroy, P. M., Mayet, R., Thomas, P., Fukuda, K. and Kagomiya, I. (2014) 'Study of the formation of the apatite-type phases $La_{9.33+x}(SiO_4)6O_2+3_{x/2}$ synthesized from a lanthanum oxycarbonate $La_2O_2CO_3$', *Solid State Sciences*, 38, pp. 150–155.

Porosoff, M. D., Yan, B. and Chen, J. G. (2016) 'Catalytic reduction of CO_2 and H_2 for synthesis of CO, methanol and hydrocarbon: Challenges and oppurtunities', *Energy & Environmental Science*, 9, pp. 62–73.

Puxty, G., Rowland, R., Allport, A., Yang, Q., Bown, M., Burns, R., Maeder, M. and Attalla, M. (2009) 'Carbon dioxide postcombustion capture: A novel screening study of the carbon dioxide absorption performance of 76 amines', *Environment Science Technology*, 43, pp. 6427–6433.

Quispe, C. A. G., Coronado, C. J. R. and Carvalho, J. A. (2013) 'Glycerol: Production, consumption, prices, characterization and new trends in combustion', *Renewable and Sustainable Energy Reviews*, 27, pp. 475–493.

Rastegari, H. and Ghaziaskar, H. S. (2015) 'From glycerol as the by-product of biodiesel production to value-added monoacetin by continuous and selective esterification in acetic acid', *Journal of Industrial and Engineering Chemistry*, 21, pp. 856–861.

Razali, N. A. M., Lee, K. T., Bhatia, S. and Mohamed, A. R. (2012) 'Heterogeneous catalysts for production of chemicals using carbon dioxide as raw material: A review', *Renewable and Sustainable Energy Reviews*, 16, pp. 4951–4964.

Rebacz, N. A. and Savage, P. E. (2013) 'Anisole hydrolysis in high temperature water', *Physical Chemistry Chemical Physics*, 15, pp. 3562–3569.

Redasani, V. K., Kumawat, V. S., Kabra, R. P., Kansagara, P. and Surana, S. J. (2010) 'Applications of green chemistry in organic synthesis', *International Journal of ChemTech Research*, 2, pp. 1856–1859.

Reddy, P. S., Sudarsanam, P., Gangadhara Raju and Reddy, B. M. (2010) 'Synthesis of bio-additives: Acetylation of glycerol over zirconia-based solid acid catalysts', *Catalysis Communications*, 11, pp. 1224–1228.

Rioux, R. M. (2006) *The synthesis, characterization and catalytic reaction studies of monodisperse platinum nanoparticles in mesoporous oxide materials*. University California, Berkeley.

Rodrigues, A. E. (2008) 'Chemical reaction engineering', in *Catalysis from Theory to Application- An Intergrated Course*. Maio: Imprensa Da Universidade De Coimbra, pp. 167–188.

Rodriguez, J. A., Evans, J., Feria, L., Vidal, A. B., Liu, P., Nakamura, K. and Illas, F. (2013) 'CO_2 hydrogenation on Au/TiC, Cu/TiC, and Ni/TiC catalysts: Production of CO, methanol, and methane', *Journal of Catalysis*, 307, pp. 162–169.

Saiyong, P., Liping, Z., Renfeng, N., Shuixin, X., Ping, C. and Zhaoyin, H. (2012) 'Transesterification of glycerol with dimethyl carbonate to glycerol carbonate over Na–based zeolites', *Chinese Journal of Catalysis*, 33, pp. 1772–1777.

Sakakura, T., Choi, J.-C. and Yasuda, H. (2007) 'Transformation of carbon dioxide.', *Chemical Reviews*, 107, pp. 2365–87.

Sandesh, S., Manjunathan, P., Halgeri, A. B. and Shanbhag, G. V. (2015) 'Glycerol acetins: fuel additive synthesis by acetylation and esterification of glycerol using cesium phosphotungstate catalyst', *Royal Society of Chemistry Advance*, 5, pp. 104354–104362.

Sandra, S., Konstatinovic, Danilovic, B. R., Ciric, J. T., Ilic, S. B., Savic, D. S. and Veljkovic, V. B. (2016) 'Valorization of crude glycerol from biodiesel production', *Chemical Industry and Chemical Engineering Quaterly*, 22, pp. 461–489.

Sanguineti, P. B., Baltanás, M. A. and Bonivardi, A. L. (2015) 'Copper–gallia interaction in Cu–Ga_2O_3–ZrO_2 catalysts for methanol production from carbon oxide(s) hydrogenation', *Applied Catalysis A: General*, 504, pp. 476–481.

Sankaranarayanan, S. and Srinivasan, K. (2012) 'Carbon dioxide – A potential raw material for the production of fuel, fuel additives and bio-derived chemicals', *Indian Journal of Chemistry*, 51 A, pp. 1252–1262.

Satterfield, C. N. (1980) *Chemical Engineering Series: Heterogeneous catalysis in Practice*. New York: McGraw-Hill.

Scanning Electron Microscopy (SEM) (2016) *Geochemical instrumentation and analysis*. Available at: http://serc.carleton.edu/research_education/geochemsheets/techniques/SEM.html (Accessed: 5 December 2016).

Schuth, F. and Ugner, K. (1999) 'Precipitation and coprecipitation', in *Preparation of solid catalysts*. Weinheim: Wiley-VCH, pp. 60–84.

Schwengber, C. A., Alves, H. J., Schaffner, R. A., da Silva, F. A., Sequinel, R., Bach, V. R. and Ferracin, R. J. (2016) 'Overview of glycerol reforming for hydrogen production', *Renewable and Sustainable Energy Reviews*, 58, pp. 259–266.

Seaton, N. A., Walton, J. P. R. B. and Quirke, N. (1989) 'A new analysis method for the determination of the pore size distribution of porous carbons from nitrogen adsorption measurements', *Carbon*, 27, pp. 853–861.

Shirsat, A. N., Ali, M., Kaimal, K. N. G., Bharadwaj, S. R. and Das, D. (2003) 'Thermochemistry of $La_2O_2CO_3$ decomposition', *Thermochimica Acta*, 399, pp. 167–170.

Shukla, K. and Srivastava, V. C. (2016) 'Diethyl carbonate: critical review of synthesis routes, catalysts used and engineering aspects', *Royal Society of Chemistry Advance*, 6, pp. 32624–32645.

Silva, E. Da, Dayoub, W., Mignani, G., Raoul, Y. and Lemaire, M. (2012) 'Propylene carbonate synthesis from propylene glycol, carbon dioxide and benzonitrile by alkali carbonate catalysts', *Catalysis Communications*, 29, pp. 58–62.

Silva, L. N., Goncalves, V. L. C. and Mota, C. J. A. (2010) 'Catalytic acetylation of glycerol with acetic anhydride', *Catalysis Communications*, 11, pp. 1036–1039.

Song, C. (2006) 'Global challenges and strategies for control, conversion and utilization of CO_2 for sustainable development involving energy, catalysis, adsorption

and chemical processing', *Catalysis Today*, 115, pp. 2–32.

Song, Y., Liu, X., Xiao, L., Wu, W., Zhang, J. and Song, X. (2015) 'Pd-promoter/MCM-41: A highly effective bifunctional catalyst for conversion of carbon dioxide', *Catalysis Letters*, 145, pp. 1272–1280.

Sonnati, M. O., Amigoni, S., Taffin de Givenchy, E. P., Darmanin, T., Choulet, O. and Guittard, F. (2013) 'Glycerol carbonate as a versatile building block for tomorrow: synthesis, reactivity, properties and applications', *Green Chemistry*, 15, pp. 283–306.

Spath, P. L. and Dayton, D. C. (2003) *Preliminary screening — technical and economic assessment of synthesis gas to fuels and chemicals with emphasis on the potential for biomass-derived syngas*. Colorado.

Styring, P., Jansen, D., Coninck, H. de, Reith, H. and Armstrong, K. (2011) *Carbon capture and utilisation in the green economy*. York: The centre for low carbon futures 2011 and CO_2 Chem Publishing 2012.

Styring, P., Quadrelli, E. A. and Amstrong, K. (2015) *Carbon dioxide utilisation: Closing the carbon cycle*. First Edit. Amsterdam: Elsevier.

Su, X., Lin, W., Cheng, H., Zhang, C., Wang, Y., Yu, X., Wud, Z. and Zhao, F. (2017) 'Metal-free catalytic conversion of CO_2 and glycerol to glycerol carbonate', *Green Chemistry*, 19, pp. 1775–1781.

Su, X., Xu, J., Liang, B., Duan, H., Hou, B. and Huang, Y. (2016) 'Catalytic carbon dioxide hydrogenation to methane: A review of recent studies', *Journal of Energy Chemistry*, 25, pp. 553–656.

Sun, D., Yamada, Y., Sato, S. and Ueda, W. (2016) 'Glycerol hydrogenolysis into useful C_3 chemicals', *Applied Catalysis B: Environmental*, 193, pp. 75–92.

Sun, J., Yang, G., Yoneyama, Y. and Tsubaki, N. (2014) 'Catalysis chemistry of dimethyl ether synthesis', *American Chemical Society Catalysis*, 4, pp. 3346–3356.

Sun, K., Fan, Z., Ye, J., Yan, J., Ge, Q., Li, Y., He, W., Yang, W. and Liu, C. (2015) 'Hydrogenation of CO_2 to methanol over In_2O_3 catalyst', *Journal of CO_2 Utilization*, 12, pp. 1–6.

Supasitmongkol, S. and Styring, P. (2010) 'High CO_2 solubility in ionic liquids and a tetraalkylammonium-based poly(ionic liquid)', *Energy & Environmental Science*, 3,

pp. 1961–1972.

Tada, S. and Kikuchi, R. (2014) 'Preparation of Ru nanoparticles on TiO_2 using selective deposition method and their application to selective CO methanation', *Catalysis Science & Technology*, 4, pp. 26–29.

Takeguchi, T., Yanagisawa, K., Inui, T. and Inoue, M. (2000) 'Effect of the property of solid acid upon syngas-to-dimethyl ether conversion on the hybrid catalysts composed of Cu–Zn–Ga and solid acids', *Applied Catalysis A: General*, 192, pp. 201–209.

Tan, H. W., Abdul Aziz, A. R. and Aroua, M. K. (2013) 'Glycerol production and its applications as a raw material: A review', *Renewable and Sustainable Energy Reviews*, 27, pp. 118–127.

Tao, J.-L., Jun, K.-W. and Lee, K.-W. (2001) 'Co-production of dimethyl ether and methanol from CO_2 hydrogenation: development of a stable hybrid catalyst', *Applied Organometallic Chemistry*, 15, pp. 105–108.

Teng, W. K., Ngoh, G. C., Yusoff, R. and Aroua, M. K. (2014) 'A review on the performance of glycerol carbonate production via catalytic transesterification : Effects of influencing parameters', *Energy Conversion and Management*, 88, pp. 484–497.

Teng, W. K., Ngoh, G. C., Yusoff, R. and Aroua, M. K. (2016) 'Microwave-assisted transesterification of industrial grade crude glycerol for the production of glycerol carbonate', *Chemical Engineering Journal*, 284, pp. 469–477.

The end of fossil fuels (2016) *Ecotricit, Britain green energy supply*. Available at: https://www.ecotricity.co.uk/our-green-energy/energy-independence/the-end-of-fossil-fuels (Accessed: 13 February 2017).

Thermo Scientific (no date) *Introduction to Fourier Transform Infrared Spectroscopy*, *Thermo Scientific*. Available at: http://www.thermofisher.com/us/en/home/industrial/spectroscopy-elemental-isotope-analysis/spectroscopy-elemental-isotope-analysis-learning-center/molecular-spectroscopy-information/ftir-information.html?elq_mid=13016&elq_cid=3839930 (Accessed: 13 November 2017).

Thomas, J. M. and Thomas, W. J. (1967) *Introduction to the principles of heterogeneous catalysis*. London: Academic Press.

Thomas, J. M. and Thomas, W. J. (2015) *Principles and practice of heterogeneous catalysis*. Second Edi. Weinheim: Wiley-VCH.

Tiede, K., Boxall, A. B. A., Tear, S. P., Lewis, J., David, H. and Hassellöv, M. (2008) 'Detection and characterization of engineered nanoparticles in food and the environment', *Food Additives and Contiminants: Part A*, 25, pp. 795–821.

Toemen, S., Abu Bakar, W. A. W. and Ali, R. (2016) 'Effect of ceria and strontia over $Ru/Mn/Al_2O_3$ catalyst: Catalytic methanation, physicochemical and mechanistic studies', *Journal of CO_2 Utilization*, 13, pp. 38–49.

Unnikrishnan, P. and Darbha, S. (2016) 'Direct synthesis of dimethyl carbonate from CO_2 and methanol over CeO_2 catalysts of different morphologies', *Journal of Chemical Sciences*, 128, pp. 957–965.

Vieville, C., Yoo, J. W., Pelet, S. and Mouloungui, Z. (1998) 'Synthesis of glycerol carbonate by direct carbonatation of glycerol in supercritical CO_2 in the of zeolites and ion exchange resins', *Catalysis Letters*, 56, pp. 245–247.

Vujic, B. and Lyubartsev, A. P. (2016) 'Transferable force-field for modeling of CO_2, N_2, Ar and O_2 in all silica and Na^+ exchnaged zeolite', *Modelling and Simulation in Material Science and Engineering*, 24, pp. 1–26.

Wambach, J., Baiker, A. and Wokaun, A. (1999) 'CO_2 hydrogenation over metal/zirconia catalysts', *Physical Chemistry Chemical Physics*, 1, pp. 5071–5080.

Wan Isahak, W. N. R., Che Ramli, Z. A., Ismail, M., Mohd Jahim, J. and Yarmo, M. A. (2015) 'Recovery and purification of crude glycerol from vegetable oil transesterification', *Separation & Purification Reviews*, 44, pp. 250–267.

Wang, W. and Gong, J. (2011) 'Methanation of carbon dioxide: An overview', *Frontiers of Chemical Engineering in China*, 5, pp. 2–10.

Wang, W., Wang, S., Ma, X. and Gong, J. (2011) 'Recent advances in catalytic hydrogenation of carbon dioxide.', *Chemical Society Reviews*, 40, pp. 3703–27.

Wang, X., Wang, M., Song, H. and Ding, B. (2006) 'A simple sol–gel technique for preparing lanthanum oxide nanopowders', *Materials Letters*, 60, pp. 2261–2265.

Wang, Y., Liu, H., Zhang, H. and Ying, W. (2016) 'Ta_2O_5 modified Al_2O_3 as a methanol dehydration component in the single-step synthesis of dimethyl ether from

syngas', *Reaction Kinetics, Mechanisms and Catalysis*, 119, pp. 585–594.

Wijngaarden, R. I., Westerterp, K. R. and Kronberg, A. (1998) *Industrial catalysis: Optimizing catalysts and processes*. Weinheim: John Wiley & Sons.

Wilson, G., Travaly, Y., Brun, T., Knippels, H., Armstrong, K., Styring, P., Krämer, D., Saussez, G. and Bolscher, H. (2015) *A vision for smart CO_2 transformation in Europe: Using CO_2 as a resource*. Brussels.

Wolf, R. E. (2005) *What is ICP-MS? and more importantly, what can it do?*, *Crustal USGS*. Available at: https://crustal.usgs.gov/laboratories/icpms/What_is_ICPMS.pdf (Accessed: 11 November 2017)

Xiao, J., Mao, D., Guo, X. and Yu, J. (2015) 'Effect of TiO_2, ZrO_2, and TiO_2-ZrO_2 on the performance of CuO-ZnO catalyst for CO_2 hydrogenation to methanol', *Applied Surface Science*, 338, pp. 146–153.

Yadav, G. D. and Joshi, A. V. (2002) 'A green route for the acylation of resorcinol with acetic acid', *Clean Technologies and Environmental Policy*, 4, pp. 157–164.

Yang, J., Zhao, Q., Xu, H., Li, L., Dong, J. and Li, J. (2012) 'Adsorption of CO_2, CH_4 and N_2 on gas diameter grade ion-exchange small pore zeolite', *Journal of Chemical Engineering Data*, 57, pp. 3701–3709.

Yuan, J., Wang, X., Gu, C., Sun, J., Ding, W., Wei, J., Zuob, X. and Hao, C. (2017) 'Photoelectrocatalytic reduction of carbon dioxide to methanol at cuprous oxide foam cathode', *RSC Advances*, 7, pp. 24933–26939.

Zha, F., Ding, J., Chang, Y., Ding, J., Wang, J. and Ma, J. (2012) 'Cu-Zn-Al oxide cores packed by metal-doped amorphous silica-alumina membrane for catalyzing the hydrogenation of carbon dioxide to dimethyl ether', *Industrial & Engineering Chemistry Research*, 51, pp. 345–352.

Zhang, J. and He, D. (2014a) 'Surface properties of Cu/La_2O_3 and its catalytic performance in the synthesis of glycerol carbonate and monoacetin from glycerol and carbon dioxide.', *Journal of Colloid and Interface Science*, 419, pp. 31–38.

Zhang, J. and He, D. (2014b) 'Synthesis of glycerol carbonate and monoacetin from glycerol and carbon dioxide over Cu catalysts: the role of supports', *Journal of Chemical Technology & Biotechnology*, 90, pp. 1077–1085.

Zhang, X., Wang, M., Yang, A., Kong, C. and Zhai, Y. (2015) 'Effect of $SrCO_3$ additive on CuZnAl/HZSM-5 catalyst property for the direct DME synthesis', *Water, Air and Soil Pollution*, 226: 378, pp. 1–6.

Zhang, Y., Ji, X., Xie, Y. and Lu, X. (2016) 'Screening of conventional ionic liquids for carbon dioxide capture and separation', *Applied Energy*, 162, pp. 1160–1170.

Zhang, Z., Wang, Y., Wang, M., Lu, J., Zhang, C., Li, L., Jiang, J. and Wang, F. (2016) 'The cascade synthesis of α,β-unsaturated ketones via oxidative C–C coupling of ketones and primary alcohols over a ceria catalyst', *Catalysis Science & Technology*, 6, pp. 1693–1700.

Zhokh, A. A., Trypolskyi, A. I. and Strizhak, P. E. (2017) 'Effect of HZSM-5/Al_2O_3 catalyst acidity on the convesion of methanol', *Theoritical and Experimental Chemistry*, 53, pp. 276–282.

Zhou, G., Liu, H., Cui, K., Jia, A., Hu, G., Jiao, Z., Liu, Y. and Zhang, X. (2016) 'Role of surface Ni and Ce species of Ni/CeO_2 catalyst in CO_2 methanation', *Applied Surface Science*, 383, pp. 248–252.

Zhou, J., Wang, Y., Guo, X., Mao, J. and Zhang, S. (2014) 'Etherification of glycerol with isobutene on sulfonated graphene: reaction and separation', *Green Chemistry*, 16, pp. 4669–4679.

Zhou, L., Al-Zaini, E. and Adesina, A. A. (2013) 'Catalytic characteristics and parameters optimization of the glycerol acetylation over solid acid catalysts', *Fuel*, 103, pp. 617–625.

Zhou, Q., Zhang, H., Chang, F., Li, H., Pan, H., Xue, W., Hu, D.-Y. and Yang, S. (2015) 'Nano La_2O_3 as a heterogeneous catalyst for biodiesel synthesis by transesterificatiob of Jatropha curcas L. oil', *Journal of Industrial and Engineering Chemistry*, 31, pp. 385–392.

Zhu, P., Chen, Q., Yoneyama, Y. and Tsubaki, N. (2014) 'Nanoparticle modified Ni-based bimodal pore catalysts for enhanced CO_2 methanation', *Royal Society of Chemistry Advance*, 4, pp. 64617–64624.

Zuhaimi, N. A. S., Indran, V. P., Deraman, M. A., Mudrikah, N. F., Maniam, G. P., Hin, T.-Y. Y. and Rahim, M. H. A. (2015) 'Reusable gypsum based catalyst for synthesis of glycerol carbonate from glycerol and urea', *Applied Catalysis A: General*,

502, pp. 312–319.

APPENDIX I

1- Standard deviation

Reaction products were analysed using a GC equipped with MS detector using 30m CP-wax column. Diethylene glycol methyl ether has been used as the internal standard. The average of area under the peak of the internal standard was measured and the standard deviation was calculated as below and the standard deviation shown to be less than 10%.

$$S^2 = \left(\frac{\sum(x-\mu)^2}{n-1}\right)$$

$$S = \sqrt{\left(\frac{\sum(x-\mu)^2}{n-1}\right)}$$

Where:

S^2 = Sample variance

S = standard deviation

Σ = summation or total

x = sample

μ = mean value of the population

n = number of values in sample minus 1

Table 0.1. The area under the graph of the internal standard (diethylene glycol methyl ether) for the glycerol calibration.

Number of measurement	Area under the graph (a.u)
1	23.01
2	23.82
3	23.23
4	22.42
Average	23.12
Standard deviation	0.018
Percentage	1.80%

$$Average = \frac{23.01 + 23.82 + 23.23 + 22.42}{4}$$

$$Variance = \frac{((23.01 - 23.12)^2 + (23.82 - 23.12)^2 + (23.23 - 23.12)^2 + (22.42 - 23.12)^2)}{(4 - 1)}$$

$$Standard\ deviation = \sqrt{Variance}$$

2- Glycerol calibration

The stock solution for glycerol calibration was prepared by serial dilution method as shown in figure 0.1. The initial concentration of glycerol was 1.26 g/ml. The stock solution was dilute in ethanol by 20 times. Stock 1 was further dilute by mixing 1 ml of glycerol of 0.06 g/ml concentration with methanol. The stock solution for GlyC and acetins were prepared using the same method.

$$Stock\ 1 = \frac{1.26\ g}{1\ ml + 20\ ml\ ethanol + 1\ \mu L\ of\ internal\ standard}$$
$$Stock\ 1 = 0.06 \frac{g}{ml}$$

$$Stock\ 2 = \frac{0.06\ g}{1\ ml + 5\ ml\ ethanol + 1\ \mu L\ of\ internal\ standard}$$
$$Stock\ 2 = 0.01 \frac{g}{ml}$$

$$Stock\ 3 = \frac{0.06\ g}{1\ ml + 10\ ml\ ethanol + 1 \mu L\ of\ internal\ standard}$$
$$Stock\ 3 = 0.00545 \frac{g}{ml}$$

$$Stock\ 4 = \frac{0.06\ g}{1\ ml + 12\ ml\ ethanol + 1\ \mu L\ of\ internal\ standard}$$
$$Stock\ 4 = 0.004615 \frac{g}{ml}$$

$$Stock\ 5 = \frac{0.06\ g}{1\ ml + 20\ ml\ ethanol + 1\ \mu L\ of\ internal\ standard}$$
$$Stock\ 5 = 0.00285 \frac{g}{ml}$$

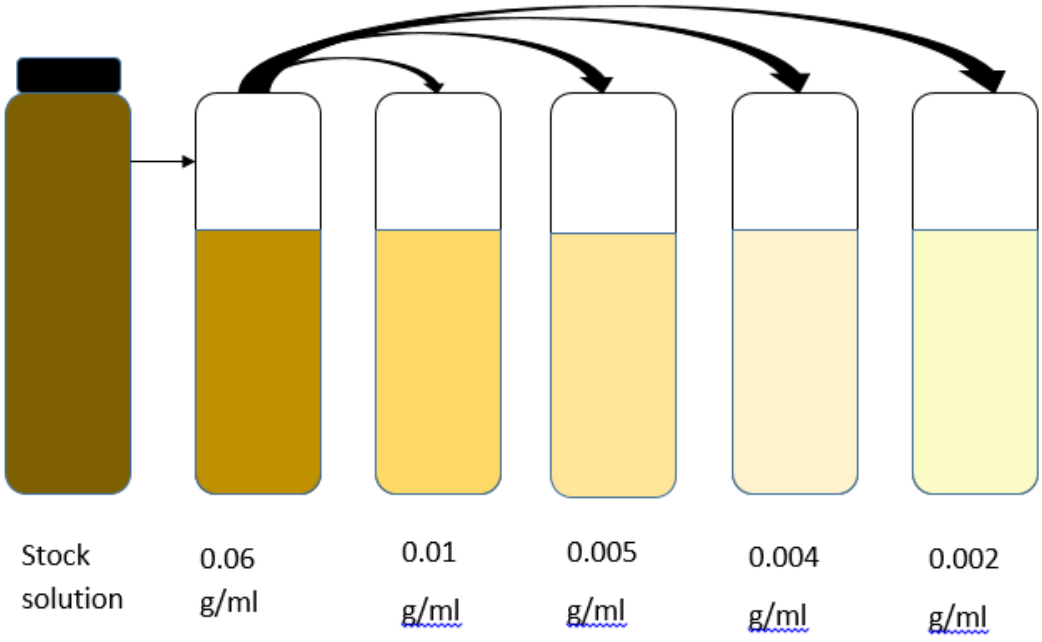

Figure 0.1. The calibration stock solution.

Table 0.2. The under the graph for glycerol calibration on GC-MS.

Concentration (g/ml)	Area under the graph (a.u)
0.06	63.58
0.01	11.58
0.00545	5.87
0.004615	5.48
0.00285	3.22

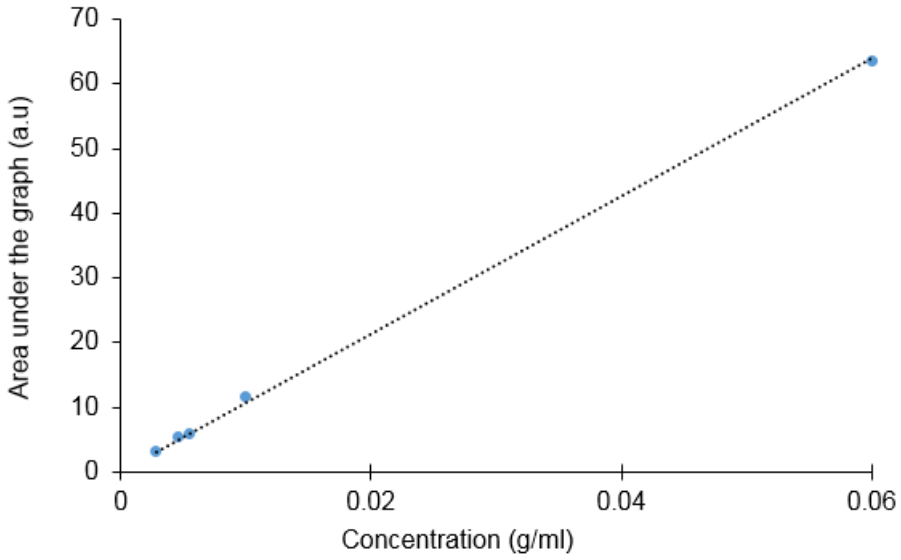

Figure 0.2. The calibration curve of the glycerol; y = 1063.3 x.

The glycerol concentration was measured as follow:

y = mx

Where

y = area of reactant or products under the peak curve

m = is the gradient of reactant or products calibration curve

x = the final reactant or products concentration.

The initial glycerol concentration for the

$$Initial\ glycerol\ concentration = \frac{y}{m}$$

$$Initial\ glycerol\ concentration = \frac{16.894}{1063.3}$$

$$Initial\ glycerol\ concentration = 0.0159\ g/ml$$

Table 0.3. The glycerol left and the GlyC fomed during the reaction of glycerol and carbon dioxide over La_2O_3-C in presence of adiponitrile

Minute	Area under the graph	Name
20.2	390	Adiponitrile
20.4	7	Glycerol
28.1	1	Glycerol carbonate

3- Glycerol conversion calculation

$$Final\ glycerol\ concentration = \frac{7.3}{1063.3}$$

$$Final\ glycerol\ concentration = 0.0069\ g/ml$$

$$Glycerol\ conversion = \frac{(0.0159 - 0.0069)}{0.0069}\ x\ 100$$

$$Glycerol\ conversion = 56\%$$

4- Glycerol carbonate selectivity

$$GlyC\ formed = \frac{1.57}{776.44\ (GlyC\ calibration\ curve)}$$

$$GlyC\ formed = 0.0020\frac{g}{ml}$$

$$GlyC\ formed = 0.0172\ mmol/ml$$

$$Glycerol\ consumed = \frac{Initial - final\ concentration\ (\frac{g}{ml})}{molar\ mass\ of\ glycerol\ (\frac{g}{mol})} x\ 1000$$

$$Glycerol\ consumed = \frac{0.0159 - 0.0069\ (\frac{g}{ml})}{92\ (\frac{g}{mol})} x\ 1000$$

$$Glycerol\ consumed = 0.0978\ mmol/ml$$

$$GlyC\ selectivity = \frac{GlyC\ formed}{Glycerol\ consumed} x\ 100$$

$$GlyC\ selectivity\ = \frac{0.0172\ (\frac{mmol}{ml})}{0.0978\ (\frac{mmol}{mol})} x\ 100$$

$$GlyC\ selectivity = 17.6\%$$

5- Glycerol carbonate yield

$$GlyC\ formed = 0.0172\ mmol/ml$$
$$Glycerol\ introduced =\ 0.0159 \frac{g}{ml}$$
$$Glycerol\ introduced = 0.1728 \frac{mmol}{ml}$$

$$GlyC\ yield = \frac{GlyC\ formed}{Glycerol\ introduced} x\ 100$$
$$GlyC\ yield = \frac{0.0172\ (\frac{mmol}{ml})}{0.1728\ (\frac{mmol}{mol})} x\ 100$$
$$GlyC\ yield = 9.95\%$$

6- Calculation of CO_2-TPD

$$PV = nRT$$

$$\frac{V}{n} = \frac{RT}{P}$$

$$\frac{V}{n} = 22414 \frac{cm^3}{mol}$$

$$CO2\ asorbed = 2.32\ cm^3$$

$$Amount\ of\ catalyst = 0.132\ g$$

$$= \frac{2.32\ cm^3}{22414\ cm^3\ mol}$$

$$= \frac{1.03506\ x\ 10^4\ mol}{0.132\ g}$$

$$= 7.8414\ x\ 10^4\ mol/g$$

$$= 0.784 \frac{mmol}{g}$$

APPENDIX II

1- Conferences

i) Direct carboxylation of glycerol with CO_2 over heterogeneous catalysts, UK Catalysis Conference, Loughborough, January 2015.

ii) Direct carboxylation of glycerol into glycerol carbonate and by-products over La_2O_3 in the presence of dehydrating agents, Smart Carbon Dioxide Transformation Final Conference, Brussel, June 2016.

iii) Direct carboxylation of glycerol into glycerol carbonate and by-products over La_2O_3 in the presence of dehydrating agents, International Conference on Carbon Dioxide Utilisation, Sheffield, September 2016.

2- Departmental seminars

i) 18-month poster presentation, 'Direct carboxylation of glycerol with CO_2 over heterogeneous catalysts', Sir Robert Hadfield Building, Department of Chemical and Biological Engineering, University of Sheffield (December 2015).

ii) 30-month departmental presentation, 'Carboxylation of crude glycerol to synthesise the glycerol carbonate over La_2O_3', Sir Robert Hadfield Building, Department of Chemical and Biological Engineering, University of Sheffield (January 2017).